AD-A061 920 BATTELLE COLUMBUS LABS OHIO F/G 11/6
SPECTRUM LOADING FATIGUE-CRACK-GROWTH PREDICTIONS AND SAFETY-FA--ETC(U)
SEP 76 D BROEK, S H SMITH N62269-76-C-0093
UNCLASSIFIED BATT-G-6320 NADC-76383-30 NL

1 OF 2
AD A061920

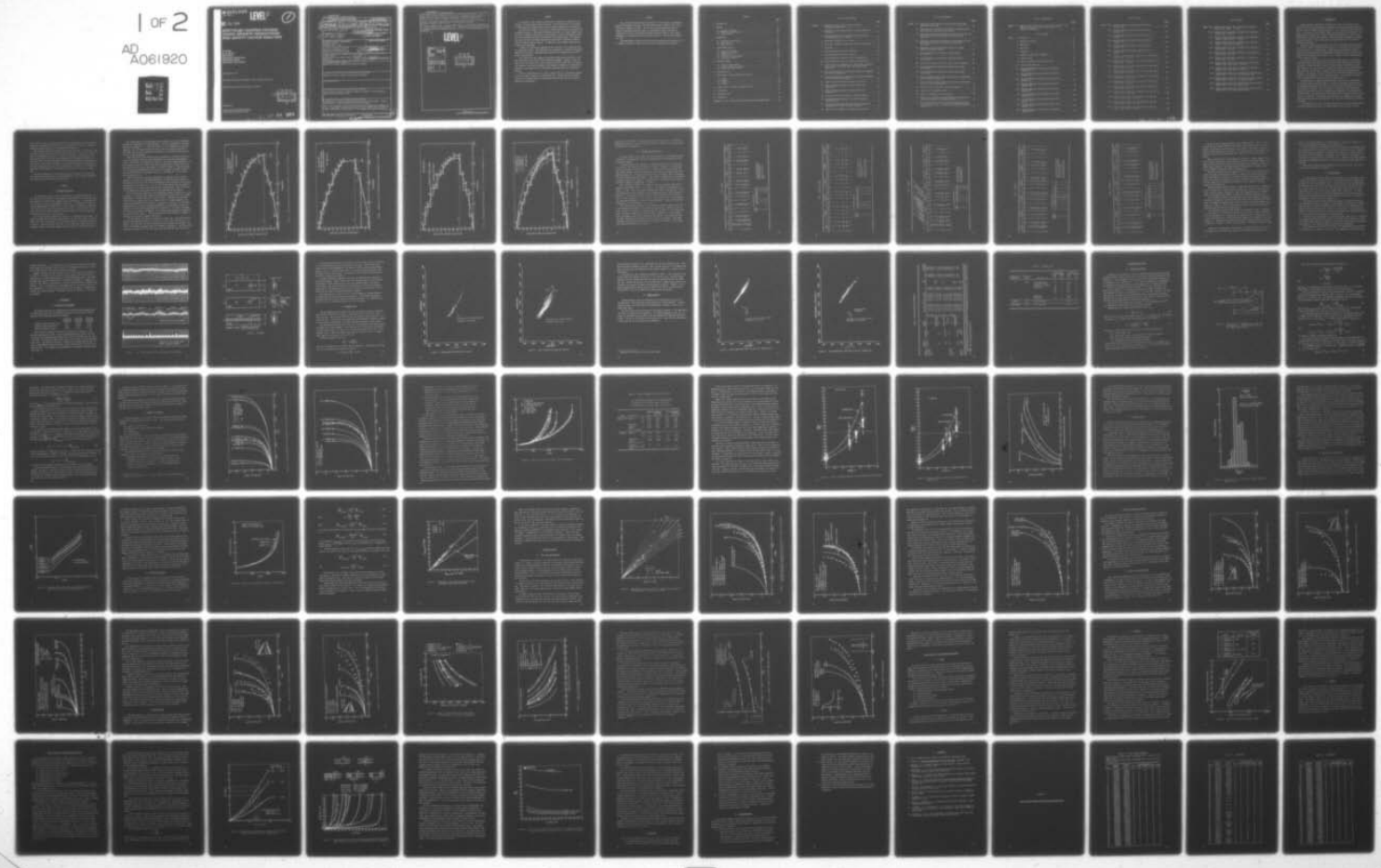

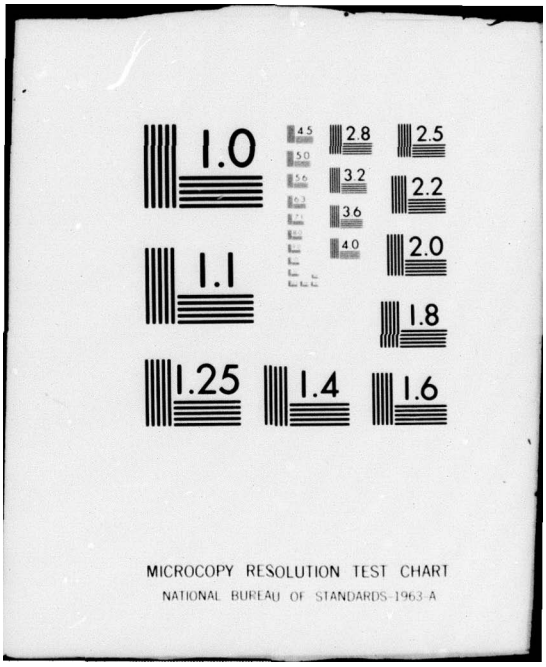
1.0
1.1
1.25
1.4
1.6
1.8
2.0
2.2
2.5
2.8
3.2
3.6
4.0
4.5
5.0
5.6
6.3
7.1
8.0
9.0
MICROCOPY RESOLUTION TEST CHART
NATIONAL BUREAU OF STANDARDS-1963-A

NADC-76383-30

LEVEL II

SPECTRUM LOADING FATIGUE-CRACK-GROWTH PREDICTIONS AND SAFETY-FACTOR ANALYSIS

D. Broek
S. H. Smith
BATTELLE
Columbus Laboratories
505 King Avenue
Columbus, Ohio 43201

24 September 1976

Final Report for Period 30 September 1975 — 24 September 1976

Prepared for

NAVAL AIR DEVELOPMENT CENTER
Warminster, Pennsylvania 18974

UNCLASSIFIED

SECURITY CLASSIFICATION OF THIS PAGE *(When Data Entered)*

(19) REPORT DOCUMENTATION PAGE

READ INSTRUCTIONS BEFORE COMPLETING FORM

(18) 1. REPORT NUMBER: NADC-76383-30	(9) Final Rept. 30 Sep 75-24 Sep 76 — 2. GOVT ACCESSION NO. — 3. RECIPIENT'S CATALOG NUMBER
(6) 4. TITLE *(and Subtitle)*: Spectrum Loading Fatigue-Crack-Growth Predictions and Safety-Factor Analysis.	5. TYPE OF REPORT & PERIOD COVERED: Final Report 9/30/75 – 9/24/76
(14) BATT	6. PERFORMING ORG. REPORT NUMBER: G-6320
(10) 7. AUTHOR(s): D. Broek and S. H. Smith	(15) 8. CONTRACT OR GRANT NUMBER(s): N62269-76-C-0093
9. PERFORMING ORGANIZATION NAME AND ADDRESS: Battelle's Columbus Laboratories, 505 King Avenue, Columbus, Ohio 43201	10. PROGRAM ELEMENT, PROJECT, TASK AREA & WORK UNIT NUMBERS
11. CONTROLLING OFFICE NAME AND ADDRESS: Naval Air Development Center, Warminster, Pennsylvania 18974 (11) 24	12. REPORT DATE: Sep[illegible], 1976 — 13. NUMBER OF PAGES: 126
14. MONITORING AGENCY NAME & ADDRESS *(if different from Controlling Office)*: DCASMA, Dayton, Defense Electronics Supply Center, Building 5, 1502 Wilmington Pike, Dayton, Ohio 45444 (12) 141 p.	15. SECURITY CLASS. *(of this report)*: Unclassified — 15a. DECLASSIFICATION/DOWNGRADING SCHEDULE

16. DISTRIBUTION STATEMENT *(of this Report)*

Approved for public release; distribution unlimited.

17. DISTRIBUTION STATEMENT *(of the abstract entered in Block 20, if different from Report)*

Approved for public release; distribution unlimited.

18. SUPPLEMENTARY NOTES

19. KEY WORDS *(Continue on reverse side if necessary and identify by block number)*

Fatigue Crack Propagation, Spectrum Loading, Retardation, Life Prediction, Damage Tolerance, Safety Factor.

20. ABSTRACT *(Continue on reverse side if necessary and identify by block number)*

The adequacy of fatigue-crack-growth predictions was investigated. Various possibilities of applying safety factors were examined.

The work was confined to service-load histories as experienced by fighter aircraft. Crack-growth analyses were made for a basic fighter spectrum and for numerous variations of that spectrum. The analyses were based on existing

over

DD FORM 1 JAN 73 1473 EDITION OF 1 NOV 65 IS OBSOLETE S/N 0102-014-6601 |

UNCLASSIFIED

SECURITY CLASSIFICATION OF THIS PAGE *(When Data Entered)*

407088

crack-growth retardation models, using the CRACKS computer program. Also, a simpler computational technique was developed. Crack-growth experiments were carried out on a 7075-T73 aluminum alloy and a Ti-6Al-4V titanium alloy.

Adequate crack-growth predictions can be made consistently with some of the techniques, however, some experiments will always be necessary.

The only satisfactory way to apply a safety factor to crack-growth predictions is to apply a factor to crack-growth life. Safety factors on initial crack size or baseline data are unacceptable because they result in varying degrees of conservatism.

LEVEL II

SUMMARY

The purpose of this research program was to evaluate the adequacy of predictions of fatigue-crack growth in service. More specifically, it was aimed at evaluating how and where safety factors should be applied in the analysis.

The work was confined to the case of service-load histories as experienced by fighter aircraft. Crack-growth analyses were made for a basic fighter spectrum and for numerous variations tf that spectrum, thereby covering more generally the conceivable service load histories for a fighter wing. The analyses were based on three available crack-growth integration (retardation) models, using the CRACKS computer program. In addition, a much simpler computational technique was developed.

A number of crack-growth experiments were carried out for comparison with the analytical results. The specimens were subjected to a variety of flight-by-flight load histories. Materials tested were 7075-T73 aluminum alloy and Ti-6Al-4V titanium alloy.

The results show that adequate analytical crack-growth predictions can be made consistently with some of the techniques available. However, since the results are very sensitive to the accuracy of the data input and to the empirical constants used, some experiments will always be necessary to establish the adequacy of the prediction for a particular spectrum shape and a particular material.

The only satisfactory way to apply a safety factor to crack-growth predictions is to apply a factor to crack-growth life. Safety factors on initial crack size or baseline data are unacceptable because they result in varying degrees of conservatism.

PREFACE

This research program has been conducted by the Structures and Mechanics Research Department, Battelle's Columbus Laboratories, Columbus, Ohio, under Contract No. N62269-76-C-0093. The contract was administered by the Air Vehicle Technology Department, Naval Air Development Center, Warminster, Pennsylvania, with Mr. Paul Kozel providing technical liaison. This report summarizes work performed during the period October 1, 1975 through September 30, 1976.

The experimental portions of this research were performed by Messrs. Lee R. Taggart and Henry J. Malik of the Structural Engineering Laboratories.

CONTENTS

		Page
1.	INTRODUCTION	9
2.	SPECTRA	10
	2.1 Exceedance Diagrams	10
	2.2 Missions and Mission Mix	16
	2.3 Load Histories	23
3.	EXPERIMENTS	24
	3.1 Materials and Specimens	24
	3.2 Baseline Data	27
	3.3 Spectrum Tests	30
4.	CRACK-GROWTH ANALYSIS	35
	4.1 Retardation Models	35
	4.2 Comparison of Models	39
	4.3 Goodness of Fit	49
	4.4 Sensitivity to Randomness	51
	4.5 Semilinear Analysis	53
5.	SPECTRUM EFFECTS	57
	5.1 Spectrum Approximation	57
	5.2 Spectrum Shape and Severity	63
	5.3 Effect of Design Stress	63
6.	GENERALIZATION	67
7.	THE ACCURACY OF CRACK-GROWTH PREDICTIONS	75
	7.1 Scope	75
	7.2 Cracks	75
	7.3 Spectra	77
	7.4 Summary	79
8.	SAFETY FACTOR IN DAMAGE-TOLERANCE ANALYSIS	80
9.	CONCLUSIONS	86
10.	RECOMMENDATIONS	87
11.	REFERENCES	89
APPENDIX A.	BASIC FIGHTER SPECTRUM AND FATIGUE-CRACK-GROWTH DATA	90

LIST OF ILLUSTRATIONS

			Page
FIGURE	1.	Comparison of Basic Spectrum With Spectrum A (Staircase Approximation)	12
	2.	Comparison of Basic Spectrum With Truncated Spectrum A (12 Levels)	13
	3.	Coarse Approximation of Spectrum A By 11 Levels And Fine Approximation By 17 Levels	14
	4.	Comparison of Spectra A, B, C, And D	15
	5.	Strip Chart Records Of Basic Spectrum And Of Spectrum B	25
	6.	Specimens	26
	7.	Crack-Growth-Rate Curve For Ti-6Al-4V	28
	8.	Crack-Growth-Rate Curve For 7075-T73	29
	9.	Crack-Growth-Rate Curve For 7075-T73 (Forman Plot)	31
	10.	Crack-Growth-Rate Curve For Ti-6Al-4V (Forman Plot)	32
	11.	Yield Zone Due To Overload (r_{po}), Crack Size At Overload (a_o), Current Yield Zone (r_{pi}), And Current Crack Size (a_i)	36
	12.	Various Procedures For Crack-Growth Calculation Compared For 7075-T73, Spectrum B	40
	13.	Various Procedures For Crack-Growth Calculation Compared For Ti-6Al-4V, Basic Spectrum	41
	14.	Effect Of Ground-Air-Ground Cycles In Spectrum B	43
	15.	Effect Of Wheeler Exponent On Crack-Growth Life Predictions	46
	16.	Effect Of Wheeler Exponent On Crack-Growth Life Predictions	47
	17.	Sensitivity Of Various Spectra To Wheeler Exponent	48
	18.	Histogram Of Rates Between Best Wheeler Prediction And Test Result	50
	19.	Predicted Crack-Growth Rates With Various Models And Baseline Data For 7075-T73 Under Spectrum B	52
	20.	Effect Of Load Sequence On Predicted Crack Growth	54

LIST OF ILLUSTRATIONS

			Page
FIGURE	21.	Comparison Of Best Wheeler Predictions With Approximate Semilinear Predictions	56
	22.	Comparison Of Test Data With Best Wheeler Calculations And With Approximate Semilinear Calculations	58
	23.	Comparison Of Wheeler Calculations With Test Results For The Basic Spectrum And Three Versions Of Spectrum A In 7075-T73	59
	24.	Comparison Of Wheeler Calculation With Test Results For The Basic Spectrum And Various Versions of Spectrum A In Ti-6Al-4V	60
	25.	Comparison Of Basic Spectrum With Spectrum A On The Basis Of Semilinear Analysis	62
	26.	Crack Propagation As Affected By Spectrum Shape In 7075-T73	64
	27.	Crack Propagation As Affected By Spectrum Severity In 7075-T73	65
	28.	Crack-Growth Predictions For The Case Of A Gust Spectrum. .	66
	29.	Crack Propagation As Affected By Design Stress Level In Ti-6Al-4V	68
	30.	Crack Propagation As Affected By Design Stress Level In 7075-T73	69
	31.	Effect Of Design Stress (Limit Load Stress) On Crack-Growth Life (Ti-6Al-4V, Spectrum B)	70
	32.	Effect Of Design Stress (Limit Load Stress) On Crack-Growth Life (7075-T73 Al, Spectrum B)	71
	33.	Cracks At Holes In 7075-T73 Under Basic Spectrum	73
	34.	Crack Growth In Stiffened Panels	74
	35.	Effect Of Clipping For Various Spectra	78
	36.	Effect Of K_c On Predicted Crack-Growth Life Calculated By Semilinear Analysis Using Forman Equation	82
	37.	Crack Growth From .02 And .05 Inch Initial Flaw Sizes For Various Configurations, Calculated With Semilinear Analysis (Spectrum A)	83

LIST OF ILLUSTRATIONS

			Page
FIGURE	38.	Ratio Of Crack Growth Lives From .02 And .05 Inch Initial Flaws To Failure For Various Configurations As A Function Of Thickness	85

LIST OF TABLES

TABLE	1.	Spectrum A	17
	2.	Spectrum A (Coarse)	18
	3.	Spectrum B	19
	4.	Spectrum C	20
	5.	Spectrum D	21
	6.	Baseline Crack-Growth Information	33
	7.	Spectrum Tests	34
	8.	Ratio of Predicted Life Over Test Life	44
	A-1.	Basic Fighter Spectrum	91
	A-2.	Constant-Amplitude Fatigue-Crack-Growth Data – Specimen AL-1	96
	A-3.	Constant-Amplitude Fatigue-Crack-Growth Data – Specimen AL-2	97
	A-4.	Constant-Amplitude Fatigue-Crack-Growth Data – Specimen AL-3	98
	A-5.	Constant-Amplitude Fatigue-Crack-Growth Data – Specimen AL-4	99
	A-6.	Constant-Amplitude Fatigue-Crack-Growth Data – Specimen AL-5	100
	A-7.	Constant-Amplitude Fatigue-Crack-Growth Data – Specimen AL-6	101
	A-8.	Constant-Amplitude Fatigue-Crack-Growth Data – Specimen AL-7	102
	A-9.	Constant-Amplitude Fatigue-Crack-Growth Data – Specimen AL-8	103
	A-10.	Constant-Amplitude Fatigue-Crack-Growth Data – Specimen AL-9	104

LIST OF TABLES

		Page
TABLE A-11.	Constant-Amplitude Fatigue-Crack-Growth Data — Specimen A10	105
A-12.	Constant-Amplitude Fatigue-Crack-Growth Data — Specimen T-1	106
A-13.	Constant-Amplitude Fatigue-Crack-Growth Data — Specimen T-2	107
A-14.	Constant-Amplitude Fatigue-Crack-Growth Data — Specimen T-3	108
A-15.	Constant-Amplitude Fatigue-Crack-Growth Data — Specimen T-4	109
A-16.	Constant-Amplitude Fatigue-Crack-Growth Data — Specimen T-5	110
A-17.	Fatigue Crack Growth Data, Specimen AL-22 Spectrum B, Limit Stress = 27.0 ksi	111
A-18.	Fatigue Crack Growth Data, Specimen AL-18 Spectrum B, Limit Stress = 30.0 ksi	112
A-19.	Fatigue Crack Growth Data, Specimen AL-11 Spectrum B, Limit Stress = 33.6 ksi	113
A-20.	Fatigue Crack Growth Data, Specimen AL-19 Spectrum B, Limit Stress = 37.0 ksi	114
A-21.	Fatigue Crack Growth Data, Specimen Ti-11 Spectrum B, Limit Stress = 55.0 ksi	115
A-22.	Fatigue Crack Growth Data, Specimen Ti-8 Spectrum B, Limit Stress = 60.0 ksi	116
A-23.	Fatigue Crack Growth Data, Specimen Ti-9 Spectrum B, Limit Stress = 65.0 ksi	117
A-24.	Fatigue Crack Growth Data, Specimen Ti-10 Spectrum B, Limit Stress = 70.0 ksi	118
A-25.	Fatigue Crack Growth Data, Specimen AL-12 Spectrum Basic, Limit Stress = 33.6 ksi	119
A-26.	Fatigue Crack Growth Data, Specimen AL-14 Spectrum Basic, Limit Stress = 33.6 ksi	120
A-27.	Fatigue Crack Growth Data, Specimen Ti-6 Spectrum Basic, Limit Stress = 65.0 ksi	121

LIST OF TABLES

		Page
TABLE A-28.	Fatigue Crack Growth Data, Specimen Ti-7 Spectrum Basic, Limit Stress = 65.0 ksi	122
A-29.	Fatigue Crack Growth Data, Specimen A1-15 Spectrum A, Limit Stress = 33.6 ksi	123
A-30.	Fatigue Crack Growth Data, Specimen A1-27 Spectrum A (Coarse), Limit Stress = 33.6 ksi	124
A-31.	Fatigue Crack Growth Data, Specimen Ti-13 Spectrum A (Coarse), Limit Stress = 65.0 ksi	125
A-32.	Fatigue Crack Growth Data, Specimen A1-24 Spectrum D, Limit Stress = 33.6 ksi	126
A-33.	Fatigue Crack Growth Data, Specimen Ti-12 Spectrum D, Limit Stress = 65.0 ksi	127
A-34.	Fatigue Crack Growth Data, Specimen A-7 Spectrum C, Limit Stress = 33.6 ksi	128
A-35.	Fatigue Crack Growth Data, Specimen A1-26 Spectrum B (Without GAG), Limit Stress = 33.6 ksi	129
A-36.	Fatigue Crack Growth Data, Specimen Ti-14 Spectrum B (Without GAG), Limit Stress = 65.0 ksi	130
A-37.	Fatigue Crack Growth Data, Specimen A1-17 Spectrum Basic, Limit Stress = 33.6 ksi 0.5 Inch Diameter Hole	131
A-38.	Fatigue Crack Growth Data, Specimen A1-29 Spectrum Basic, Limit Stress = 33 ksi 0.5 Inch Diameter Hole	132
A-39.	Fatigue Crack Growth Data, Specimen A1-20 Spectrum Basic, Limit Stress = 33.6 ksi Stiffened Panel	133
A-40.	Fatigue Crack Growth Data, Specimen A1-21 Spectrum Basic, Limit Stress = 33.6 ksi Stiffened Panel	134

1. INTRODUCTION

Damage-Tolerance assessment of airplane structures has long been based almost entirely on data derived from experiments. Recent developments now provide the tools for damage-tolerance analysis. This has prompted the issuance by the U. S. Air Force of MIL-A-83444, Damage Tolerance Design Requirements. Thus, damage-tolerance analysis has become a necessary ingredient of aircraft structural design. However, many questions remain regarding the adequacy of damage-tolerance analysis. Some of these questions were addressed in the research program reported here.

Basically, damage tolerance means that (real or assumed) preexisting flaws do not grow, within a certain defined period, to a size that would cause loss of the aircraft at a specified load. Damage-tolerance assessment involves analysis of (1) fatigue and environmentally assisted growth of an initial flaw under the anticipated service loading and (2) residual strength characteristics of the cracked structure.

In principle, present-day fracture mechanics and modern stress-analysis techniques permit the prediction of residual strength characteristics of many structures. Though the basic tools for fatigue-crack-growth prediction were also available, the techniques for dealing with random or quasi-random service-load histories did not exist. Recently, some semiempirical techniques were proposed. The adequacy of these techniques for crack-growth predictions is the subject of investigation in this research program. In particular, the magnitude of required safety factors is a major consideration.

Safety factors in damage-tolerance analysis may be tacitly introduced by (1) assuming large preexisting flaws, (2) using conservative baseline data, or (3) showing crack-growth lives that cover more than one lifetime (or more than one inspection interval). Any of these tacit assumptions could confuse the results and preclude the correct assessment of the degree of conservatism in the predictions. An evaluation of these hidden safety factors was made in this study. In particular, this program has shown that the assumption of a large preexisting flaw may be ultraconservative in some cases and barely conservative in others.

Crack-growth predictions will gain credibility if the use of hidden safety factors is abandoned in favor of a general safety factor on life. Such a

safety factor as part of damage-tolerance design requirements will assign equal degrees of conservatism to various crack configurations. The use of different preexisting flaw sizes does not accomplish this objective.

The work was confined to fighter service load histories. In Section 2, the baseline spectrum and its variations will be discussed. Subsequently, Section 3 gives the experimental details. The analysis procedures, their results, and their sensitivity to data input and assumptions are discussed in Section 4. Section 5 deals with spectrum effects and the required accuracy of spectrum representation. The subject of Section 6 is the generalization of the procedures and their application to real crack configurations. Sections 7 and 8 deal with the accuracy of predictions, the necessary safety factors, and how to apply them.

Detailed information on the spectra that were used, and all unprocessed test results are presented in the attached Appendix. Thus, they are available for reanalysis with forthcoming new techniques.

2. SPECTRA

2.1 Exceedance Diagrams

The load spectrum used in this investigation was a fighter spectrum. It was received from the Naval Air Development Center (NADC) in the form of a basic load sequence of 72,000 cycles comprising 6,000 flight hours. A tabulation of this sequence is given in the Appendix, Table A-1. It consisted of blocks of cycles representing 20 flight hours as a basic block. In addition, there were four other blocks of cycles that occurred once every 200 hours (after every 10 basic blocks), once every 1,000 hours (every 50 basic blocks), and once every 6,000 hours (at the end of the sequence).

The 20-hour block consisted of a sequence of 32 different load ranges. The number of cycles per load range varied between 1 and 57, all cycles of a given range occurring as one group. The total cycle content of the 20-hour block was 213 cycles. The extra blocks after 200, 1,000, 3,000, and 6,000 hours were of a similar nature, but the load ranges and cycle content of each were different.

The load maxima of this load sequence were counted, and a load exceedance diagram was established for 100 flight hours. This is represented by the solid data points in Figure 1. It will be referred to in the following as the basic spectrum. The curve drawn through the data points is denoted as Spectrum A. This means that the basic spectrum and Spectrum A are identical from the point of view of load exceedance.

Other spectra and load sequences were established on the basis of Figure 1. In the first place, Spectrum A was approximated by a staircase approximation using 17 load levels, as indicated in Figure 1. Since the lowest maximum in the basic spectrum was .37 of limit load (see data point 1200 in Figure 1) a truncated version of Spectrum A was devised, as shown in Figure 2. The load levels for the staircase approximation are the same as in Figure 1; however, levels 11 and 12 were omitted by truncating at level 10, and levels 14, 15, 16, and 17 were all taken at zero.

Apart from the fine staircase approximation of Spectrum A by 17 levels (Figure 1), a coarse staircase approximation of 11 levels was made (Figure 3). The load levels used for this coarse approximation were the same as for the fine approximation, but levels 3, 5, 7, 9, 12, and 15 were omitted and the number of exceedances for the other levels were adjusted appropriately. This can be seen in the comparison of the coarse with the fine approximation in Figure 3.

Three variations of Spectrum A were generated, denoted as Spectra B, C, and D (Figure 4). Spectra B and C have the same maximum as Spectrum A, but a higher (Spectrum B) or a lower (Spectrum C) cycle content. Spectrum D has the same cycle content as Spectrum A, but it contains loads of a higher magnitude, although the maximum load is the same as in Spectrum A. Spectra B, C, and D were approximated by a 17-level staircase approximation, using exactly the same 17 levels as used for the fine approximation of Spectrum A. Of course, the number of cycles at each level is different. The staircase approximations of Spectra B and C are shown in Figure 4. The one for Spectrum D was omitted for reasons of clarity, but is given in tabular form later.

All load levels are given as a fraction of limit load. The stress at limit load for all spectra was taken at 33.6 ksi for 7075-T73 and at 65 ksi for Ti-6Al-4V. On this basis, the stress levels for all the spectra are defined. The effect of variation in design stress was studied for Spectrum B. The limit load stresses were taken as 27, 30, 33.6, and 37 ksi for 7075-T73, and 55, 60, 65,

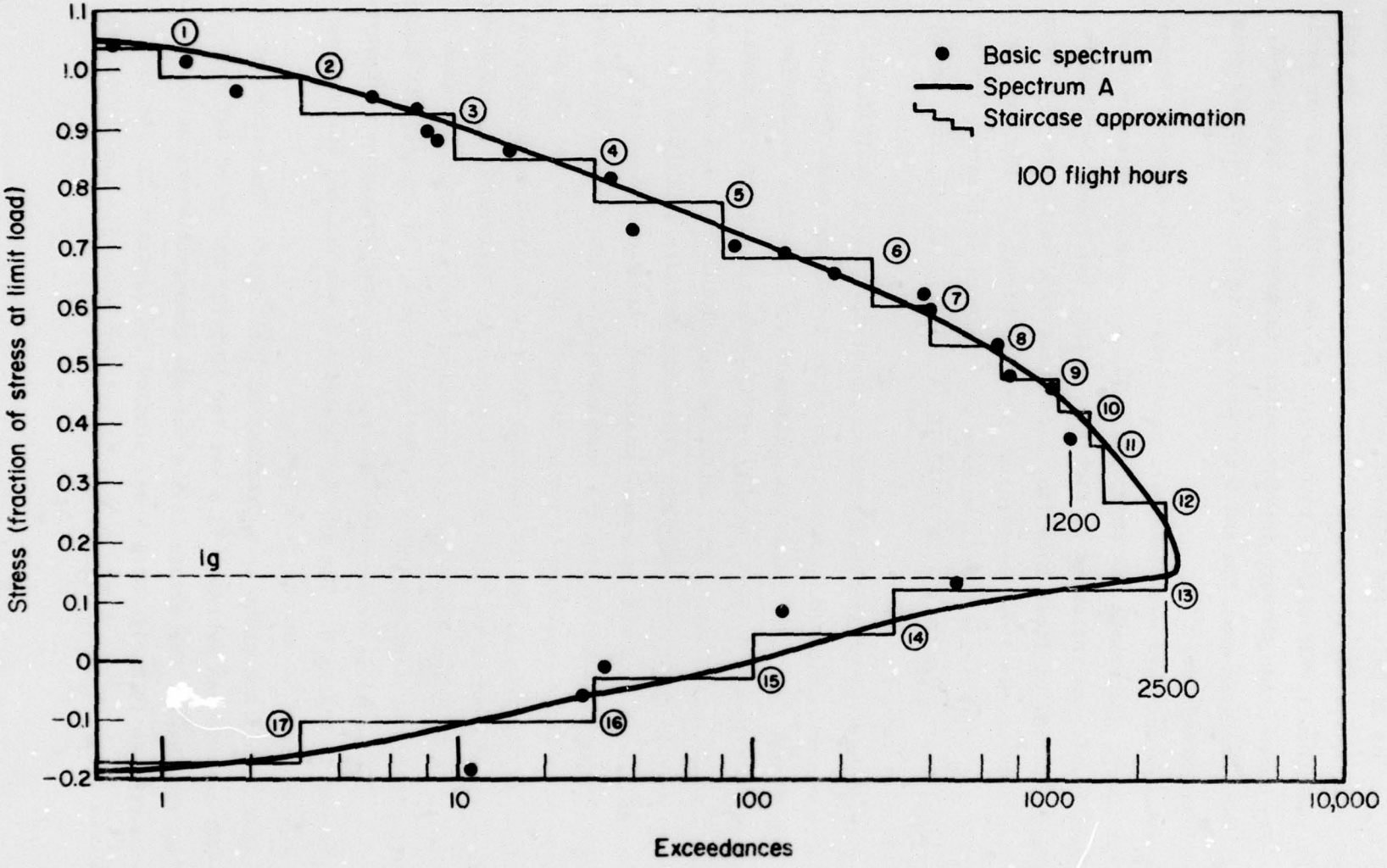

FIGURE 1. COMPARISON OF BASIC SPECTRUM WITH SPECTRUM A (STAIRCASE APPROXIMATION)

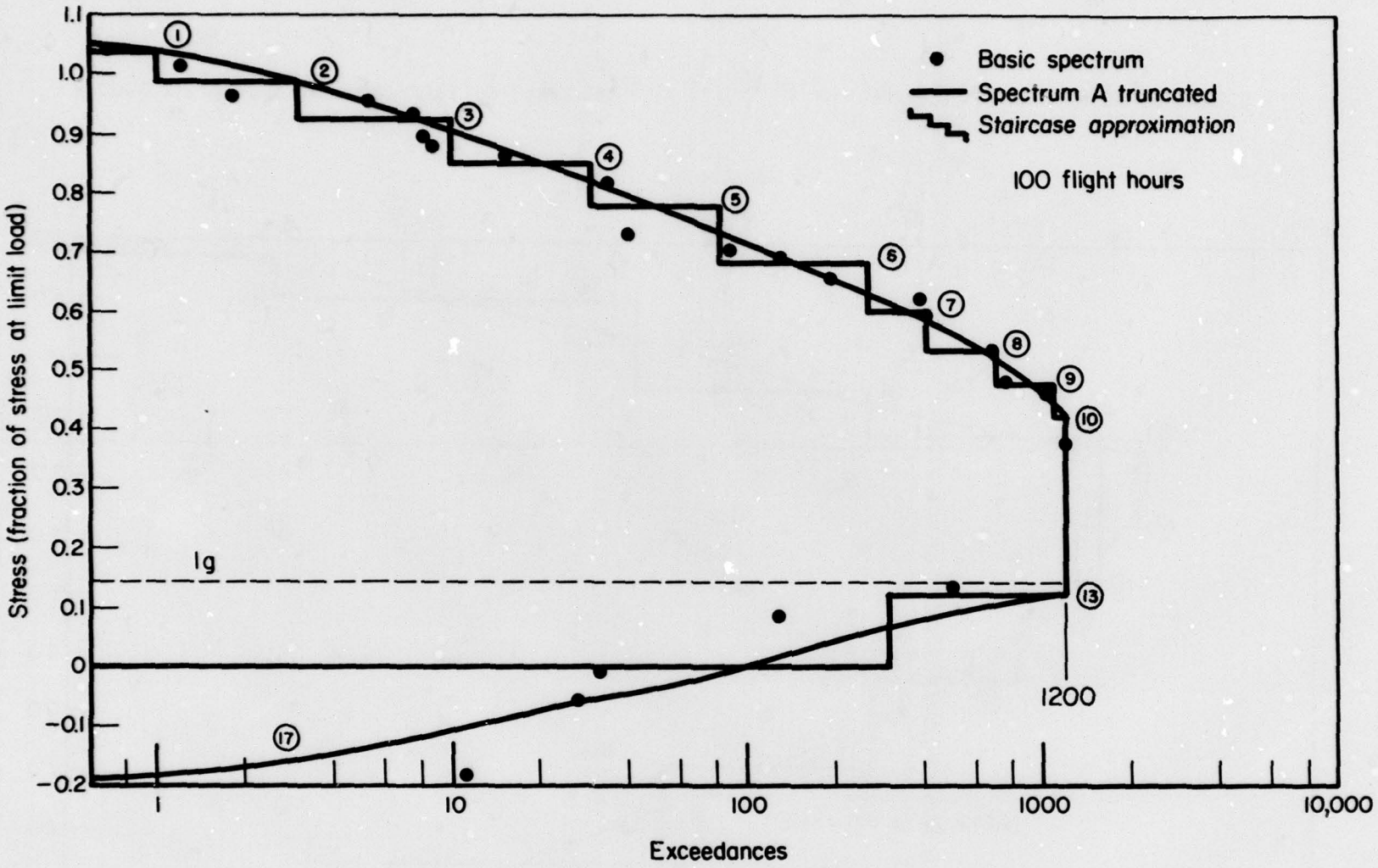

FIGURE 2. COMPARISON OF BASIC SPECTRUM WITH TRUNCATED SPECTRUM A (12 LEVELS)

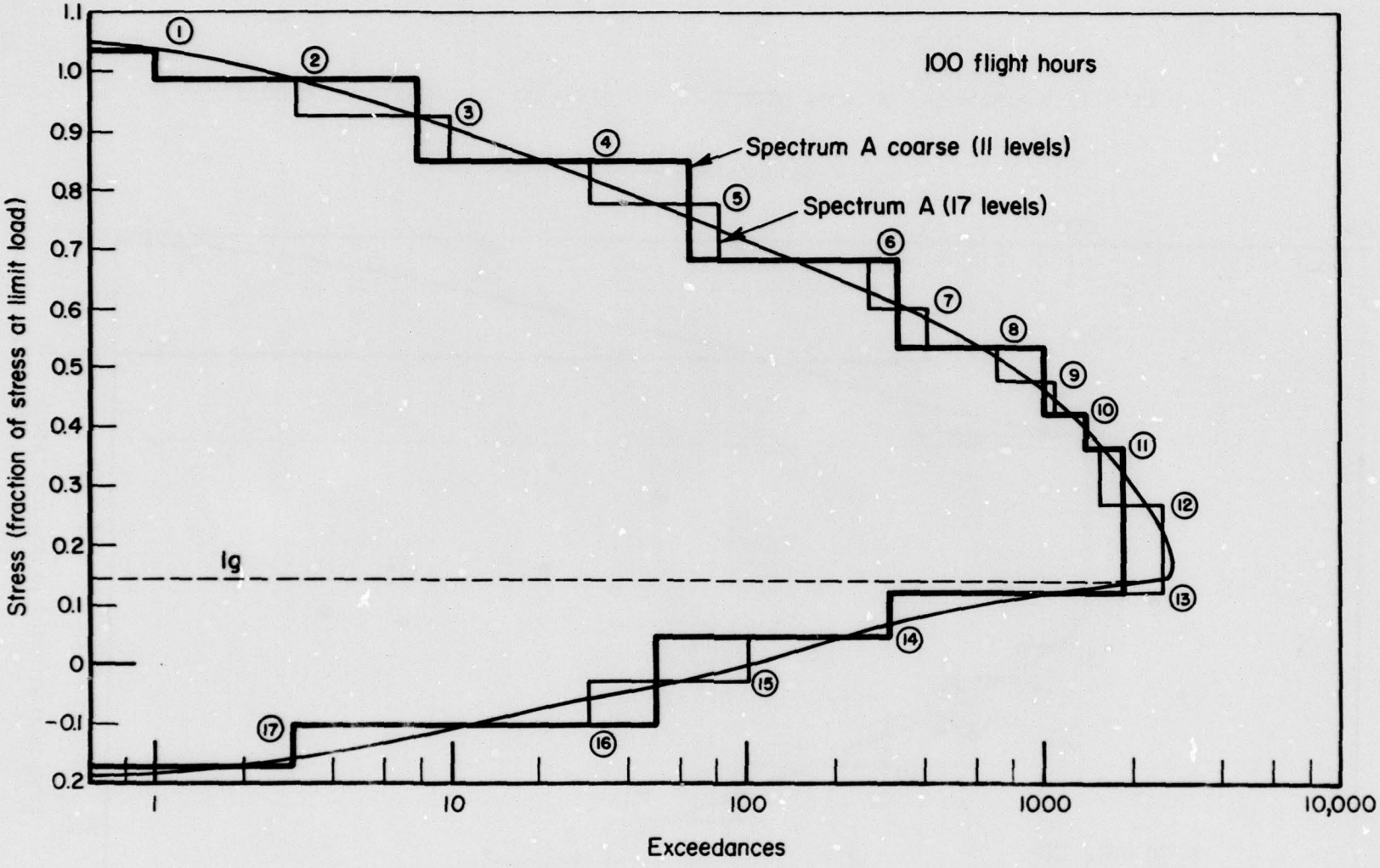

FIGURE 3. COARSE APPROXIMATION OF SPECTRUM A BY 11 LEVELS AND FINE APPROXIMATION BY 17 LEVELS

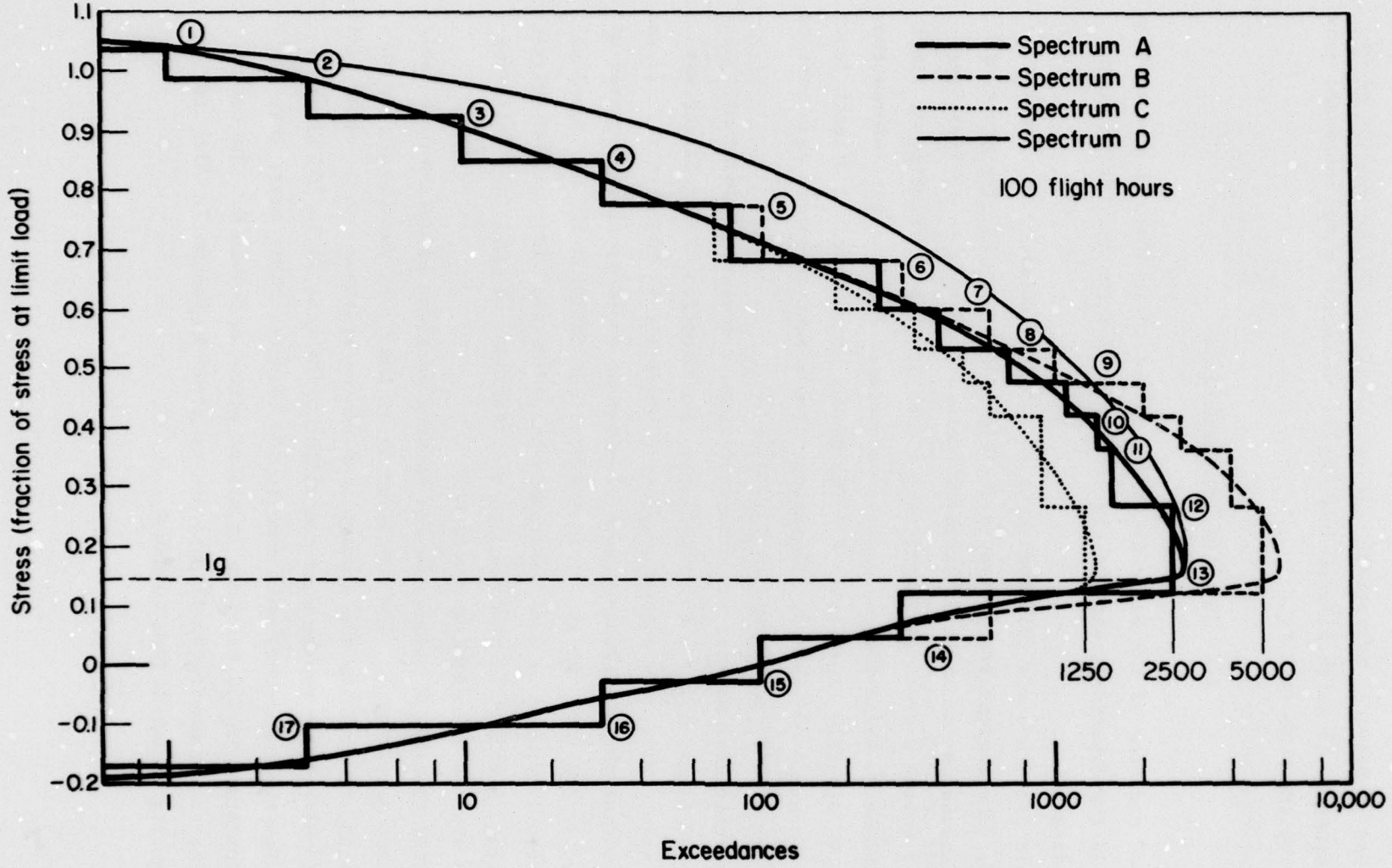

FIGURE 4. COMPARISON OF SPECTRA A, B, C, AND D

and 70 ksi for Ti-6Al-4V. Essentially, these variations can be considered as additional spectra, in which all the load levels in Figure 4 are increased proportionally by the same factor.

2.2 Missions and Mission Mix

The load sequence of the basic spectrum, discussed in the previous section (tabulated in the Appendix), was the starting point for the derivation of the exceedance diagrams.

A simple procedure was followed to establish mission mixes for Spectra A, B, C, and D. The results are presented in Tables 1 through 5. The procedure will be discussed on the basis of Table 3. Column 1 of this table lists the load levels; Column 2 gives the magnitude of each level as a fraction of limit load; and Column 3, the number of exceedances of each level. This information can be derived directly from Figure 4. The number of occurrences of each level is given in Column 4 of Table 3. It follows from a subtraction of each pair of successive numbers of exceedances in Column 3.

The occurrences represent the number of times a given load level will be reached in 100 flight hours. For simplicity, the duration of one flight was taken at 1 hour. Thus, the numbers represent the loads in 100 flights. It was then assumed that three different types of missions would be flown, denoted as Missions I, II, and III. Mission I is the severest, Mission III the least severe. Mission I appears in four versions: heavy (Mission Ia), medium (Mission Ib), and light (Missions Ic or Id). The arbitrariness of these and following assumptions will be discussed in Section 5.

The cycle content of Mission Ia was assumed as given in Column 5 of Table 3 (occurrences per flight). Since Mission Ia is the heavy version of the severest mission, it contains the highest load of the spectrum – 1.04 times limit load. Obviously, there can be only one flight of Mission Ia in 100 flights, since the highest load occurs only once in 100 flights. This means that all the loads contained in all Missions Ia are as given in Column 6. The cycles remaining for the remaining 99 flights are as given in Column 7. They follow from subtracting Column 6 from Column 4.

TABLE 1. SPECTRUM A

	Total			Mission Ia 1X			Mission Ib 3X			Mission Ic 6X			Mission Id 30X			Mission II 50X			Mission III 10X		
Level	% LL	Exc.	Occ.	Occ.	1X	Rest	Occ.	3X	Rest	Occ.	6X	Rest	Occ.	30X	Rest	Occ.	50X	Rest	Occ.	10X	Rest
1	1.04	1	1	1	1	--	--	--	--	--	--	--	--	--	--	--	--	--	--	--	--
2	0.98	3	2	2	2	--	--	--	--	--	--	--	--	--	--	--	--	--	--	--	--
3	0.92	10	7	1	1	6	2	6	--	--	--	--	--	--	--	--	--	--	--	--	--
4	0.84	30	20	2	2	18	2	6	12	2	12	--	--	--	--	--	--	--	--	--	--
5	0.77	80	50	2	2	48	2	6	42	2	12	30	1	30	--	--	--	--	--	--	--
6	0.63	260	180	2	2	178	4	12	166	6	36	130	1	30	100	2	100	--	--	--	--
7	0.60	400	140	2	2	138	2	6	132	2	12	120	2	60	60	1	50	10	1	10	--
8	0.53	700	300	4	4	296	4	12	284	4	24	260	5	150	110	2	100	10	1	10	--
9	0.47	1100	400	4	4	396	4	12	384	4	24	360	6	180	180	3	150	30	3	30	--
10	0.41	1400	300	10	10	290	10	30	260	5	30	230	--	--	230	4	200	30	3	30	--
11	0.36	1500	100	10	10	90	10	30	60	10	60	--	--	--	--	--	--	--	--	--	--
12	0.26	2500	1000	30	30	970	30	90	880	30	180	700	10	300	400	6	300	100	10	100	--
13	0.12	2500	2200	60	60	2140	60	180	1960	60	360	1600	*25*	*750*	*850*	*14*	*700*	*150*	15	150	--
14	0.05	300	200	2	2	198	2	6	192	2	12	180	--	--	180	3	150	30	3	30	--
15	-0.03	100	70	5	5	65	5	15	50	0	0	50	--	--	50	1	50	--	--	--	--
16	-0.10	30	27	3	3	24	2	6	18	3	18	--	--	--	--	--	--	--	--	--	--
17	-0.18	3	3	0	0	3	1	3	--	--	--	--	--	--	--	--	--	--	--	--	--

100 Flights Sequence

Block Sequence	Sequence of Flights in Block
C	III, Id, Id, 5 times II, Ic, Id
C	Ic,
B	Ib,
C	Ic,
C	Ic,
A	Ia,
B	Ib,
C	Ic,
B	Ib,
C	Ic,

Level 10 (max) combined with Levels 14, 15, 16, 17 (min)
Level 13 (min) combined with all other levels (max).

Levels are the same as in Table 3.

TABLE 2. SPECTRUM A (COARSE)

	Total		Mission Ia 1X				Mission Ib 3X				Mission Ic 6X				Mission II 50X				Mission III 40X			
Level	Exc.	Occ.	Occ.	Exc.	X1	Rest	Occ.	Exc.	X3	Rest	Occ.	Exc.	X6	Rest	Occ.	Exc.	50X	Rest	Occ.	Exc.	40X	Rest
1	1	1	1	1	1	--	--	--	--	--	--	--	--	--	--	--	--	--	--	--	--	--
2	8	7	1	2	1	6	2	2	6	--	--	--	--	--	--	--	--	--	--	--	--	--
3																						
4	70	62	5	7	5	57	5	7	15	42	7	7	42	--	--	--	--	--	--	--	--	--
5																						
6	340	270	5	12	5	265	5	12	15	250	5	12	30	220	2	2	100	120	3	3	120	--
7																						
8	1000	660	6	18	6	654	6	18	18	636	6	18	36	600	8	10	400	200	5	8	200	--
9																						
10	1300	300	11	29	11	289	11	29	33	256	6	24	36	220	2	12	100	120	3	11	120	--
11	1800	500	12	41	12	488	12	41	36	452	12	36	72	380	2	14	100	280	7	18	280	--
12																						
13	1800	1500	30	41	30	1470	30	41	90	1380	30	36	180	1200	12	14	600	600	15	18	600	--
14	300	250	6	11	6	244	6	11	18	226	1	6	6	220	2	2	100	120	3	3	120	--
15																						
16	50	47	5	5	5	42	4	5	12	30	5	5	30	--	--	--	--	--	--	--	--	--
17	3	3	--	--	--	3	1	1	3	--	--	--	--	--	--	--	--	--	--	--	--	--

100 Flights Sequence

Block Sequence	Sequence of Flights in Block
C	III, Ic, III, 5 times II, III, III
B	Ib,
C	Ic,
C	Ic,
A	Ia,
C	Ic,
B	Ib
C	Ic
C	Ic
B	Ib

Level 10 (max) combined with Levels 14, 16, 17 (min).
Level 13 (min) combined with all other levels.

Levels are the same as for other spectra (see Table 3).

TABLE 3. SPECTRUM B

	Total			Mission Ia 1X			Mission Ib 3X			Mission Ic 6X			Mission Id 30X			Mission II 50X			Mission III 10X		
Level	% LL	Exc.	Occ.	Occ.	1X	Rest	Occ.	3X	Rest	Occ.	6X	Rest	Occ.	30X	Rest	Occ.	50X	Rest	Occ.	10X	Rest
1	2	3	4	5	6	7	8	9	10	11	12	13	14	15	16	17	18	19	20	21	22
1	1.04	1	1	1	1	--	--	--	--	--	--	--	--	--	--	--	--	--	--	---	--
2	0.98	3	2	2	2	--	--	--	--	--	--	--	--	--	--	--	--	--	--	--	--
3	0.92	10	7	1	1	6	2	6	--	--	--	--	--	--	--	--	--	--	--	--	--
4	0.84	30	20	2	2	18	2	6	12	2	12	--	--	--	--	--	--	--	--	--	--
5	0.77	100	70	2	2	68	2	6	62	2	12	50	0	0	50	1	50	--	--	--	--
6	0.68	300	200	2	2	198	4	12	186	6	36	150	5	150	--	0	0	--	--	--	--
7	0.60	600	300	2	2	298	2	6	292	2	12	280	2	60	220	4	200	20	2	20	--
8	0.53	1000	400	4	4	396	4	12	384	4	24	360	5	150	210	4	200	10	1	10	--
9	0.47	2000	1000	4	4	996	4	12	984	4	24	960	11	330	630	12	600	30	3	30	--
10	0.41	2600	600	10	10	590	10	30	560	5	30	530	8	240	290	5	250	40	4	40	--
11	0.36	4000	1400	10	10	1390	10	30	1300	10	60	1300	20	600	700	12	600	100	10	100	--
12	0.26	5000	1000	30	30	970	30	90	880	30	180	700	10	300	400	6	300	100	10	100	--
13	0.12	5000	4400	60	60	4340	60	180	4160	60	360	3800	53	1590	2210	39	1950	260	26	260	--
14	0.05	600	500	2	2	498	2	6	492	2	12	480	8	240	240	4	200	40	4	40	--
15	-0.03	100	70	5	5	65	5	15	50	0	0	50	0	0	50	1	50	--	--	--	--
16	-0.10	30	28	3	3	24	2	6	18	3	18	--	--	--	--	--	--	--	--	--	--
17	-0.18	3	3	0	0	3	1	3	--	--	--	--	--	--	--	--	--	--	--	--	--

100 Flights Sequence

Block Sequence	Sequence of Flights in Block
C	III, Id, Id, 5 times II, Ic, Id
C	Ic,
B	Ib,
C	Ic,
C	Ic,
A	Ia,
B	Ib,
C	Ic,
B	Ib,
C	Ic,

Level 10 (max) combined with Levels 14, 15, 16, 17 (min).

Level 13 (min) combined with all other levels (max).

TABLE 4. SPECTRUM C

	Total		Mission Ia 1X				Mission Ib 3X				Mission Ic 6X				Mission II 20X				Mission IV 70X			
Level	Exc.	Occ.	Occ.	Exc.	X1	Rest	Occ.	Exc.	X3	Rest	Occ.	Exc.	X3	Rest	Occ.	Exc.	X2	Rest	Occ.	Exc.	X70	Rest
1	1	1	1	1	1	--	--	--	--	--	--	--	--	--	--	--	--	--	--	--	--	--
2	3	2	2	3	2	--	--	--	--	--	--	--	--	--	--	--	--	--	--	--	--	--
3	10	7	1	4	1	6	2	2	6	--	--	--	--	--	--	--	--	--	--	--	--	--
4	30	20	2	6	2	18	2	4	6	12	2	2	12	--	--	--	--	--	--	--	--	--
5	70	40	2	8	2	38	2	6	6	32	2	4	12	20	1	1	20	--	--	--	--	--
6	180	110	2	10	2	108	2	8	6	102	2	6	12	90	1	2	20	70	1	1	70	--
7	330	150	2	12	2	148	2	10	6	142	2	8	12	130	3	5	60	70	1	2	70	--
8	490	160	2	14	2	158	2	12	6	152	2	10	12	140	--	5	--	140	2	4	14	--
9	600	110	2	16	2	108	2	14	6	102	2	12	12	90	1	6	20	70	1	5	70	--
10	900	300	10	26	10	290	10	24	30	260	10	22	60	200	3	9	60	140	2	7	140	--
11	900	--	--	26	--	--	--	24	--	--	--	26	--	--	--	9	--	--	--	7	--	--
12	1250	350	4	30	4	346	4	28	12	334	4	26	24	310	5	14	100	210	3	10	210	--
13	1250	950	20	30	20	930	18	28	54	876	16	26	96	780	11	14	220	560	8	10	560	--
14	300	200	2	10	2	198	2	10	6	192	2	10	12	180	2	3	40	140	2	2	140	--
15	100	70	5	8	5	65	5	8	15	50	5	8	30	20	1	1	20	--	--	--	--	--
16	30	27	3	3	3	24	2	3	6	18	3	3	18	--	--	--	--	--	--	--	--	--
17	3	3	--	--	--	3	1	1	3	--	--	--	--	--	--	--	--	--	--	--	--	--

100 Flights Sequence

Block Sequence	Sequence of Flights in Block
C	III, III, III, II, Ic, II, III, III, III, III
B	Ib,
C	Ic,
C	Ic,
A	Ia,
C	Ic,
B	Ib,
C	Ic,
C	Ic,
B	Ib,

Level 10 (max) combined with Levels 14, 15, 16, 17 (min). Level 13 (min) combined with all other levels (max).

Levels are the same as for other spectra (see Table 3).

TABLE 5. SPECTRUM D

	Total		Mission Ia 1X				Mission Ib 3X				Mission Ic 6X				Mission II 70X				Mission III 20X			
Level	Exc.	Occ.	Occ.	Exc.	X1	Rest	Occ.	Exc.	X3	Rest	Occ.	Exc.	X6	Rest	Occ.	Exc.	X	Rest	Occ.	Exc.	X	Rest
1	1	1	1	1	1	--	--	--	--	--	--	--	--	--	--	--	--	--	--	--	--	--
2	27	26	2	3	2	24	2	2	6	18	3	3	18	--	--	--	--	--	--	--	--	--
3	74	47	2	5	2	45	5	7	15	30	5	8	30	--	--	--	--	--	--	--	--	--
4	150	76	3	8	3	73	1	8	3	70	--	8	--	70	1	1	70	--	--	--	--	--
5	290	140	3	11	3	137	3	11	9	128	3	11	18	110	1	2	70	40	2	2	40	--
6	540	250	4	15	4	246	4	15	12	234	4	15	24	210	3	5	210	--	--	2	--	--
7	800	260	5	20	5	255	5	20	15	240	5	20	30	210	1	6	70	140	7	9	140	--
8	1100	300	4	24	4	296	4	24	12	284	4	24	24	260	2	8	140	120	6	15	120	--
9	1400	300	4	28	4	296	4	28	12	284	4	28	24	260	2	10	140	120	6	21	120	--
10	1800	400	12	40	12	388	12	40	36	352	12	40	72	280	2	12	140	140	7	28	140	--
11	2100	300	4	44	4	296	4	44	12	284	4	44	24	260	2	14	140	120	6	34	120	--
12	2500	400	4	48	4	396	4	48	12	384	4	48	24	360	4	18	140	120	4	38	120	--
13	2500	2100	36	48	36	2064	36	48	108	1956	36	48	216	1740	16	18	1120	620	31	38	620	--
14	400	250	4	12	4	246	4	12	12	234	4	12	24	210	1	2	70	140	7	7	140	--
15	150	90	2	8	3	88	2	8	6	82	2	8	12	70	1	1	70	--	--	--	--	--
16	60	40	4	6	4	36	4	6	12	24	4	6	24	--	--	--	--	--	--	--	--	--
17	20	20	2	2	2	18	2	2	6	12	2	2	12	--	--	--	--	--	--	--	--	--

100 Flights Sequence

Block Sequence	Sequence of Flights in Block
C	II, II, II, III, Ic, III, II, II, II, II
B	Ib,
C	Ic,
C	Ic,
A	Ia,
C	Ic,
B	Ib.
C	Ic,
C	Ic,
B	Ib,

Level 10 (max) combined with Levels 14, 15, 16, 17 (min)
Level 13 (min) combined with all other levels (max).

Levels are the same as for other spectra (see Table 3).

Mission Ib is the medium version of the severest mission. Hence, it will contain the next highest available load level. Since levels 1 and 2 are exhausted, the highest load of Mission Ib is of level 3. The load occurrences of Mission Ib were assigned as in Column 8. The cycle content is essentially the same as for Mission Ia (same mission type) apart from those at the highest levels.

Level 3 occurs twice in each Mission Ib (Column 8). There remained 6 cycles of level 3 (Column 7); hence, Mission Ib can occur only three times. This means that the total cycle content of all Missions Ib is as given in Column 9 (three times Column 8). The occurrences for the remaining 96 flights are as given in Column 10 (subtract Column 9 from Column 7).

Mission Ic contains the next highest level and its cycle content is essentially the same as for Missions Ia and Ib. Level 4 occurs twice (Column 11). Since there remain 12 occurrences of level 4, Mission Ic occurs six times. Thus, the content of all Missions Ic is as in Column 12 (six times Column 11), and the cycles for the remaining 90 flights are as in Column 13 (subtract Column 12 from Column 10).

Similar procedures were followed to devise Missions Id and II. Mission Id occurs 30 times and it exhausts level 6 (Column 16). Mission II occurring 50 times, exhausts level 5 (Column 19). Thus, the remaining cycles in Column 19 occur in the remaining 10 flights, automatically leaving 10 Mission III's.

The procedures followed for the positive excursions (above 1g, represented by levels 1 through 12) are essentially the same as for the negative excursions. Since the number of exceedances for levels 12 and 13 is the same (Figure 4 and Column 3 in Table 3), care was taken that the number of positive and negative excursions was the same for a given mission.

The procedure resulted in 100 flights of six different types – 40 Mission I's (1 of type Ia, 3 of type Ib, 6 of type Ic, and 30 of type Id), 50 Mission II's and 10 Mission III's. Obviously, the smallest block of flights that still contains all missions is a block of 10 with 4 Mission I's, 5 Mission II's, and 1 Mission III. The sequence of flights within this 10-flight block was taken as 1 times III, 2 times I, 5 times II, and 2 times I. This block is shown in Table 3.

There are four missions I in each block. The second pair was always a pair of Mission Id's. The first pair consisted of Id paired with either Ia, Ib,

or Ic. A block with Mission Ia is called block A, a block with Mission Ib is block B, and a block with Mission Ic is called block C.

The total sequence of 100 flights consists of 10 blocks of 10 flights each. Since there are three mission Id's in each block, Mission Id occurs 30 times in the total sequence as required. Since Mission Ia occurs once, there should be one block A in the 100 flights. Similarly, there should be three block B's (3 Mission Ib's) and six block C's (six Mission C's). Therefore, the block sequence was taken as CCBCCABCBC (see Table 3). The entire sequence of 100 flights was repeated.

Very similar procedures were followed for the other spectra. They can be reconstructed from Tables 1 through 5.

2.3 Load Histories

The load sequence within a flight still remained to be established. First, a load cycle needed to be defined, i.e., the various positive and negative excursions had to be combined into cycles. This was done in the following manner. All positive excursions (except the ones to level 10) were started from level 13, to form ranges 13-1, 13-2, etc. The excursions to level 10 were started from levels 14, 15, 16, and 17 to give ranges 14-10, 15-10, etc. (In anticipation of this procedure, the staircase approximation of the spectra was prepared so that the number of occurrences of level 10 was equal to the number of exceedances of level 14 [Tables 1 through 5].)

The resulting cycles in each flight were ordered low-high-low (assuming that the highest loads occur during the attack phase in the middle of a flight). The excursions to level 10 (following levels 12 and 11) at the beginning of a flight were started from 14, 15, 16, and 17, in this order. The excursions to level 10 (preceding 11 and 12) at the end of the flight were started from levels 17, 16, 15, and 14 (in this order) if they occurred.

Each flight was terminated by a ground-air-ground (GAG) cycle. It consisted of a negative excursion to level 15 and a touch down cycle to level 14. Since each flight starts and ends at level 13, the complete GAG operation consisted of 13-15-14-15-13. The effect of omitting the GAG was investigated.

The sequencing of cycles within a flight, the combinations of load levels, and the GAG were the same for all spectra. The combination of load levels was

not made arbitrarily. It was selected in such a way that the exceedance diagram of the ranges for Spectrum A was the same as the exceedance diagram for ranges of the stress history used to derive the basic spectrum.

Examples of the strip-chart records of the stress histories are presented in Figure 5. Although the basic spectrum contains many more levels than the other spectra, it shows large patches of constant-amplitude cycles. The flight-by-flight load history of Spectrum B is also shown in Figure 5. Although the number of load levels is much smaller, it shows a subtle and more realistic load sequence. Yet, it is defined in a much simpler way for the purposes of tests and computations: it only requires a definition of 3 missions, a definition of a block, and a block sequence. Strip-chart records of Spectra A, C, and D are very similar.

3. EXPERIMENTS

3.1 Materials and Specimens

The material used for the experiments were Ti-6Al-4V mill-annealed plate 0.25-inch thick, and 7075-T73 aluminum alloy plates 0.25-inch and 0.50-inch thick with the following mechanical properties:

	Ti-6Al-4V, 0.25 inch	7075-T73, 0.25 inch	7075-T73, 0.50 inch
Ultimate tensile strength, ksi	137.0	71.113	71.113
Tensile yield strength, ksi	128.7	60.383	60.383
Fracture toughness, ksi/in.	120.0	67.70	67.70.

Three types of specimens were used, as illustrated in Figure 6. Each specimen contained two cracks. Center-cracked panels (Type a) were used for the generation of baseline crack-growth data and for the majority of the spectrum tests. Two Type b specimens were used to obtain data on a crack emanating from a hole: one specimen contained a through-the-thickness crack at each of two 0.2-inch-diameter holes; the other a corner crack at each of two 0.5-inch-diameter holes. Two specimens were provided with a stringer of the same material (Type c).

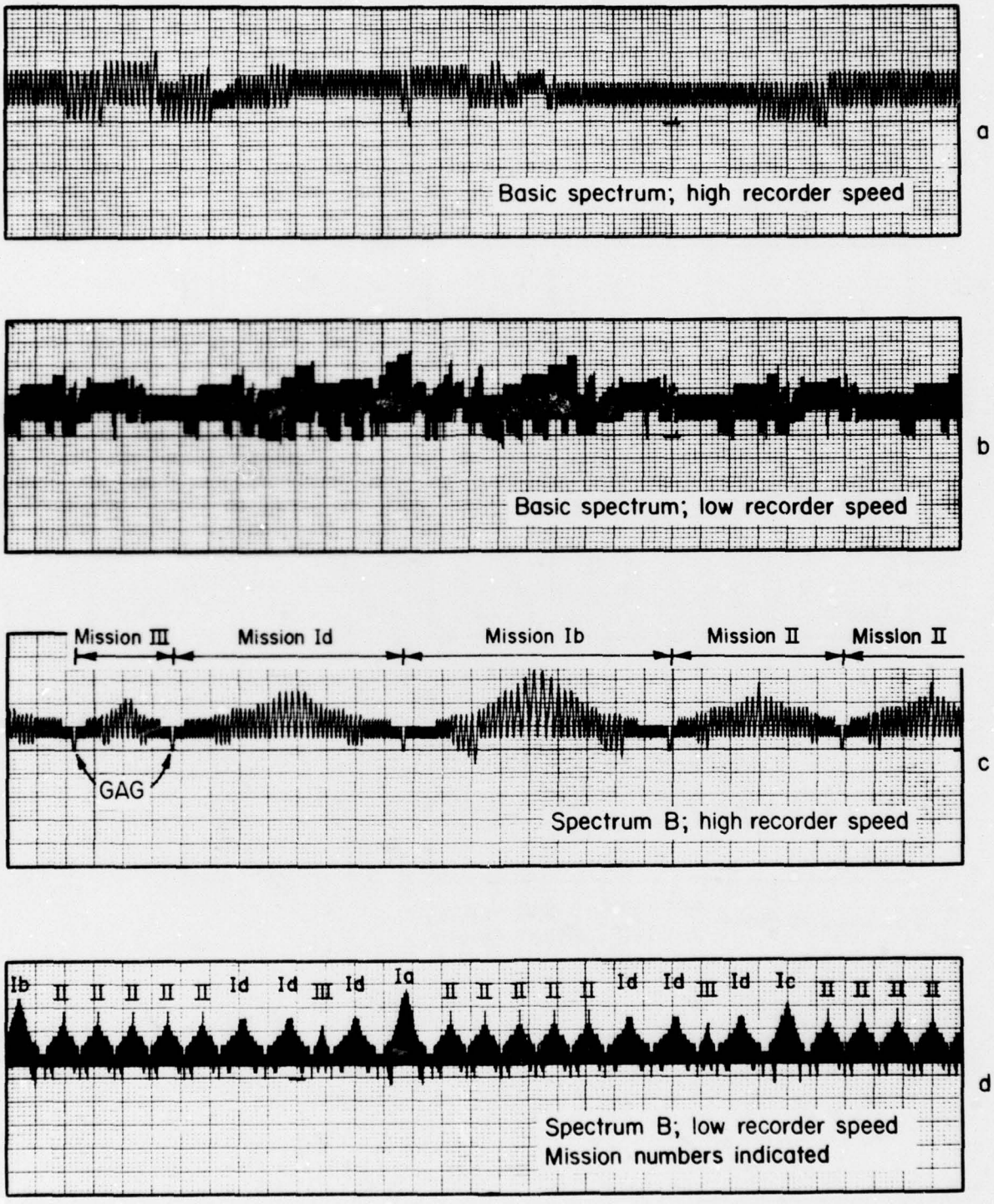

FIGURE 5. STRIP CHART RECORDS OF BASIC SPECTRUM AND OF SPECTRUM B

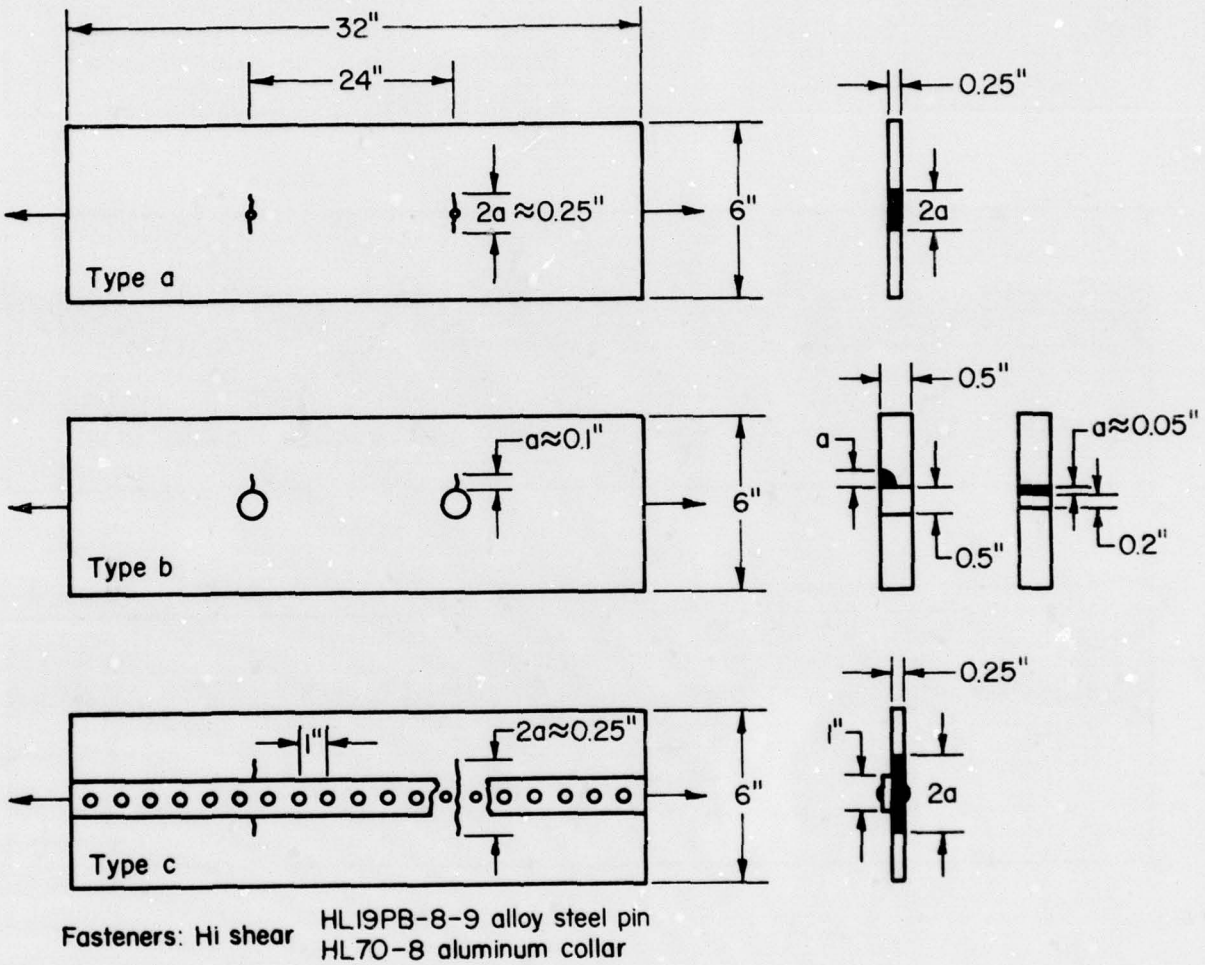

FIGURE 6. SPECIMENS

All center-cracked specimens contained 0.25-inch starter notches, consisting of a 0.4-inch-diameter hole with two jeweler's saw cuts. These notches were found to start cracks immediately. The cracks at holes were also started from a jeweler's saw cut. They were precracked to the desired crack dimensions; then the spectrum tests were started. The specimens with stringers were precracked before the stringers were mounted.

In order to prevent compressive buckling, the specimens were supported by antibuckling guides. These consisted of a 0.5-inch-steel plate at each side of the specimen, bolted together just outside the specimen edges. They were a little shorter than the free length of the specimens (to allow for compressive deformation of the specimen) lined with felt to prevent load transfer, and contained two port holes to enable crack-growth readings.

The experiments were carried out in an electrohydraulic fatigue machine of 130,000 pounds capacity with an on-line computer. Crack-growth measurements were made visually, using a 30-power traveling microscope. The temperature was kept at 70 $\pm$ 3 F, the relative humidity was 55 $\pm$ 5 percent.

3.2 Baseline Data

Constant-amplitude crack-growth data were generated using Type a specimens. The 0.25-inch 7075-T73 was tested at stress ratios of R = -0.15, 0.0, 0.15, 0.30, and 0.50. The 0.50-inch 7075-T73 and the Ti-6A1-4V were tested at R = 0.0, 0.30, and 0.50. In addition, some experiments were performed in which the region of the crack was sprayed with a saltwater solution containing 3 percent NaCl.

All unprocessed baseline data (crack size versus number of cycles) are given in tabular form in the Appendix. The data were used to derive the crack-growth rate per cycle, da/dN, as a function of the stress-intensity range, ΔK. As an example, Figure 7 shows the growth-rate curve for Ti-6A1-4V at R = 0. Figure 8 shows the effect of stress ratio for 7075-T73.

Forman's equations of the type

$$\frac{da}{dN} = C \frac{(\Delta K)^n}{(1-R)K_c - \Delta K} \qquad (1)$$

were fitted through each set of data (one per specimen). Subsequently, all data sets for one material were lumped in a plot of

$$\left\{(1-R)K_c - \Delta K\right\} \frac{da}{dN} = C\ (\Delta K)^n \quad , \qquad (2)$$

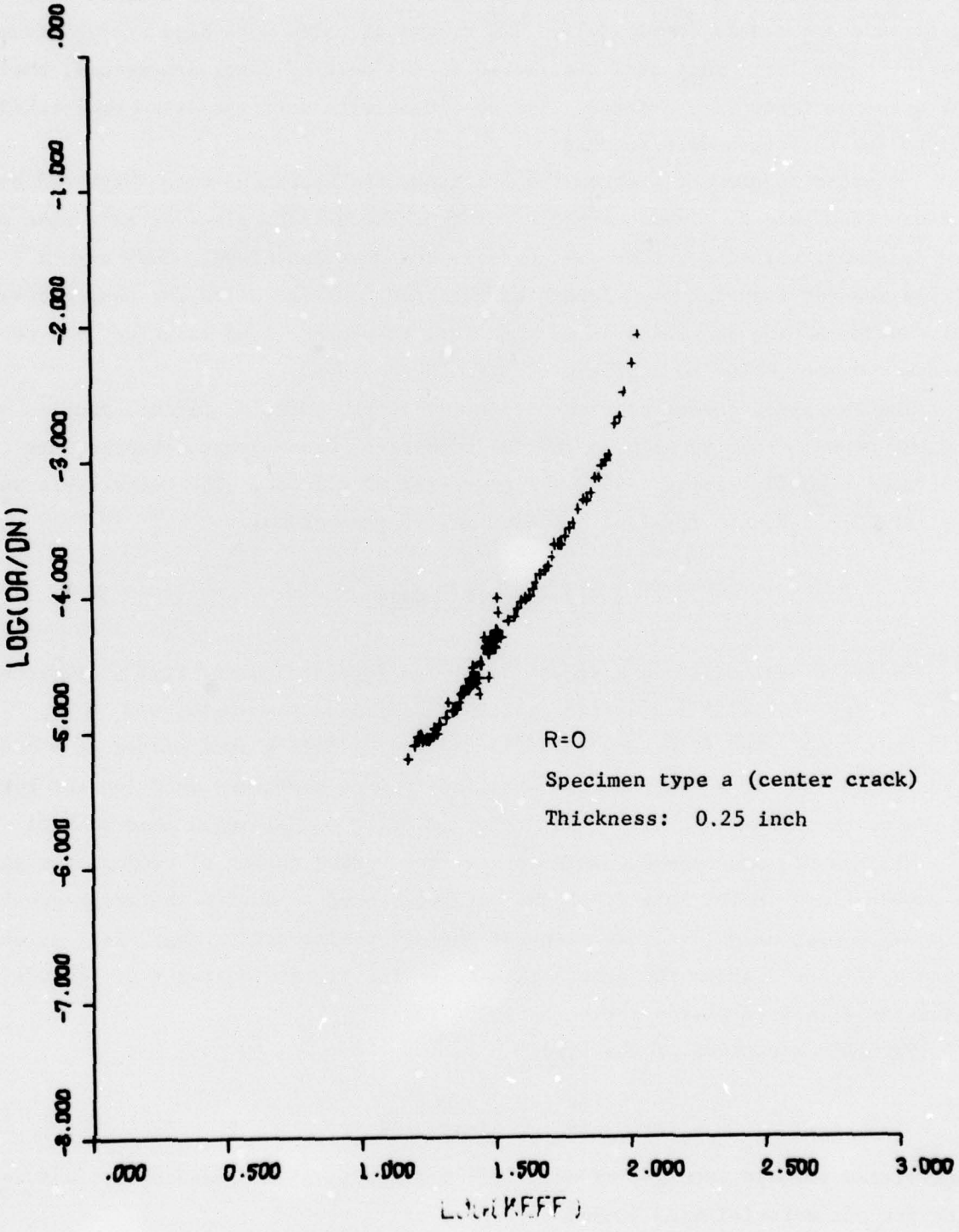

FIGURE 7. CRACK-GROWTH-RATE CURVE FOR Ti-6A1-4V

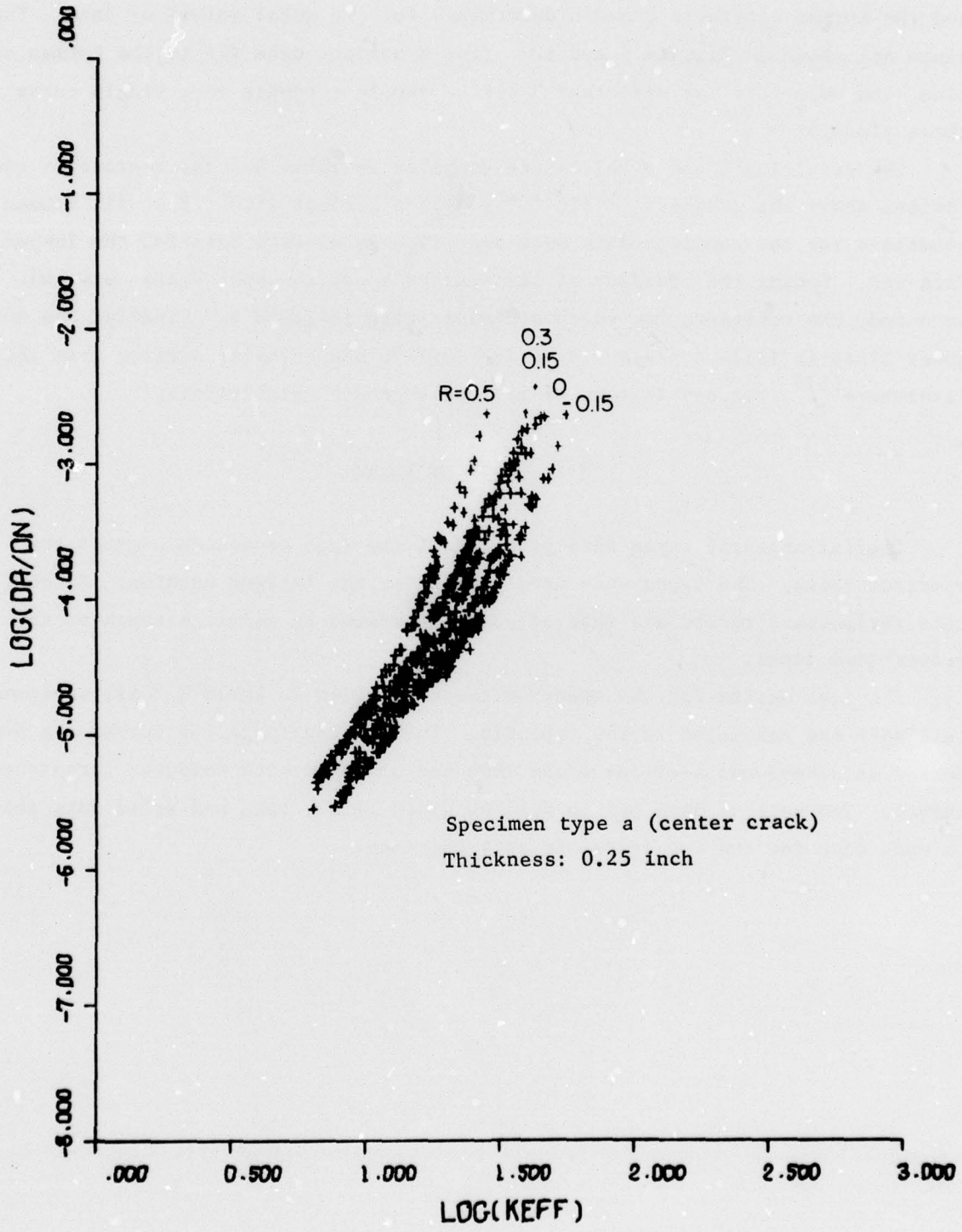

FIGURE 8. CRACK-GROWTH-RATE CURVE FOR 7075-T73

and the Forman constants C and n determined for the total volume of data. These plots are shown in Figures 9 and 10. (For a perfect data fit to the Forman equation, the data sets for different R-ratios should condense to a single curve in these plots.)

The resulting C and n values are compiled in Table 6. The regression coefficient shows the goodness of fit ($r^2 = 1$ is a perfect fit). Best-fit Forman equations for the complete data sets are given as average data for the lumped data set. Taking the boundary of the scatter band, an upper bound curve was constructed, the constants for which are also given in Table 6. Finally, the two lower lines in Table 6 present data for 7075-T6 and 2024-T3, derived from the literature[1]*, for use in some of the crack-growth calculations.

3.3 Spectrum Tests

Digital magnetic tapes were produced of the load sequences used in the spectrum tests. The tapes were used to monitor the fatigue machine. A continuous strip-chart record was made of each experiment to permit a check on the proper load input.

The test matrix for the spectrum tests is given in Table 7. All unprocessed test data are tabulated in the Appendix. The crack-propagation curves are presented in subsequent sections where they are compared with computed (predicted) curves. Two sets of data points will be given (i.e., open and solid data points) in each case for the two cracks in each specimen.

---

* References are listed at the end of the report.

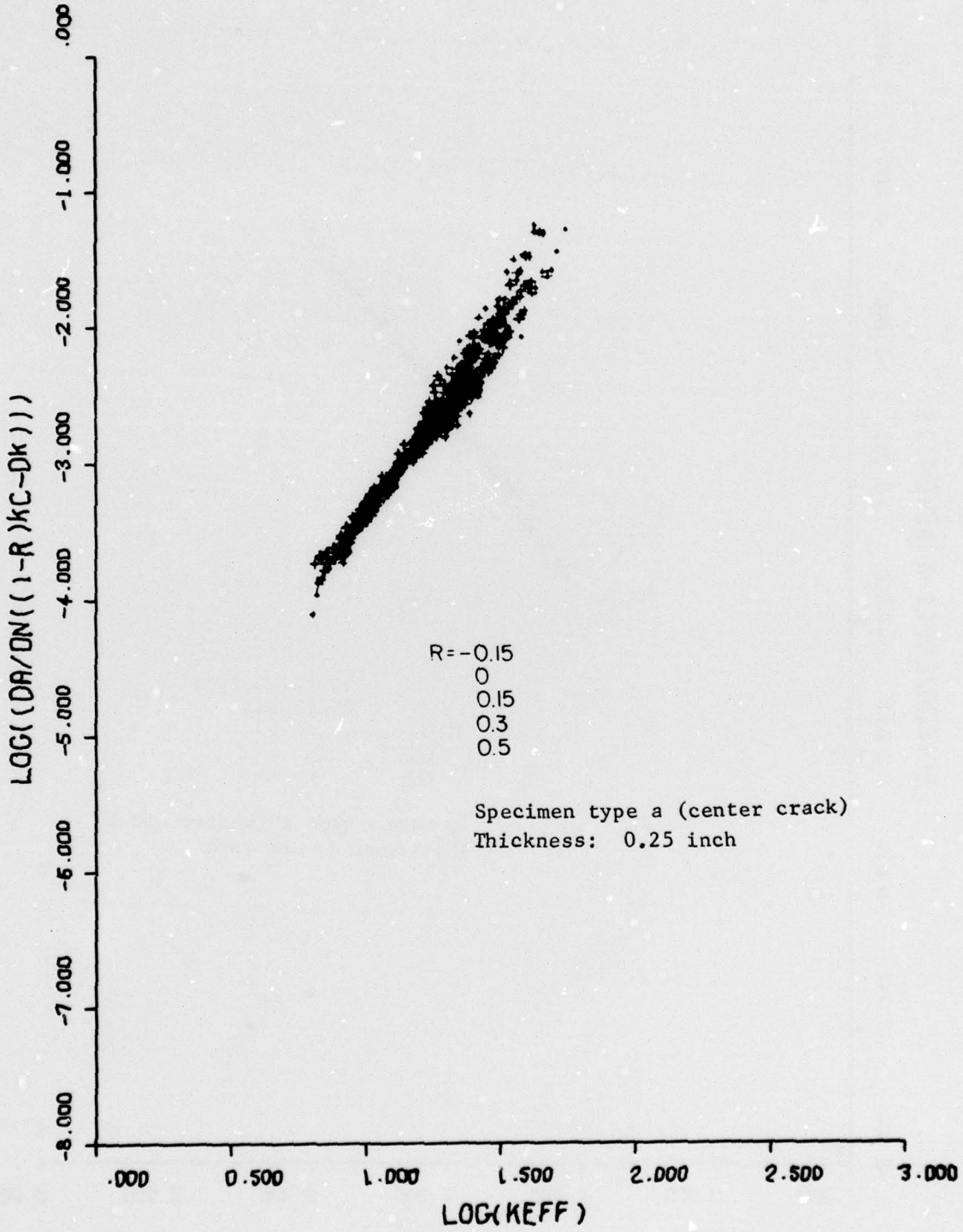

FIGURE 9. CRACK-GROWTH-RATE CURVE FOR 7075-T73 (FORMAN PLOT)

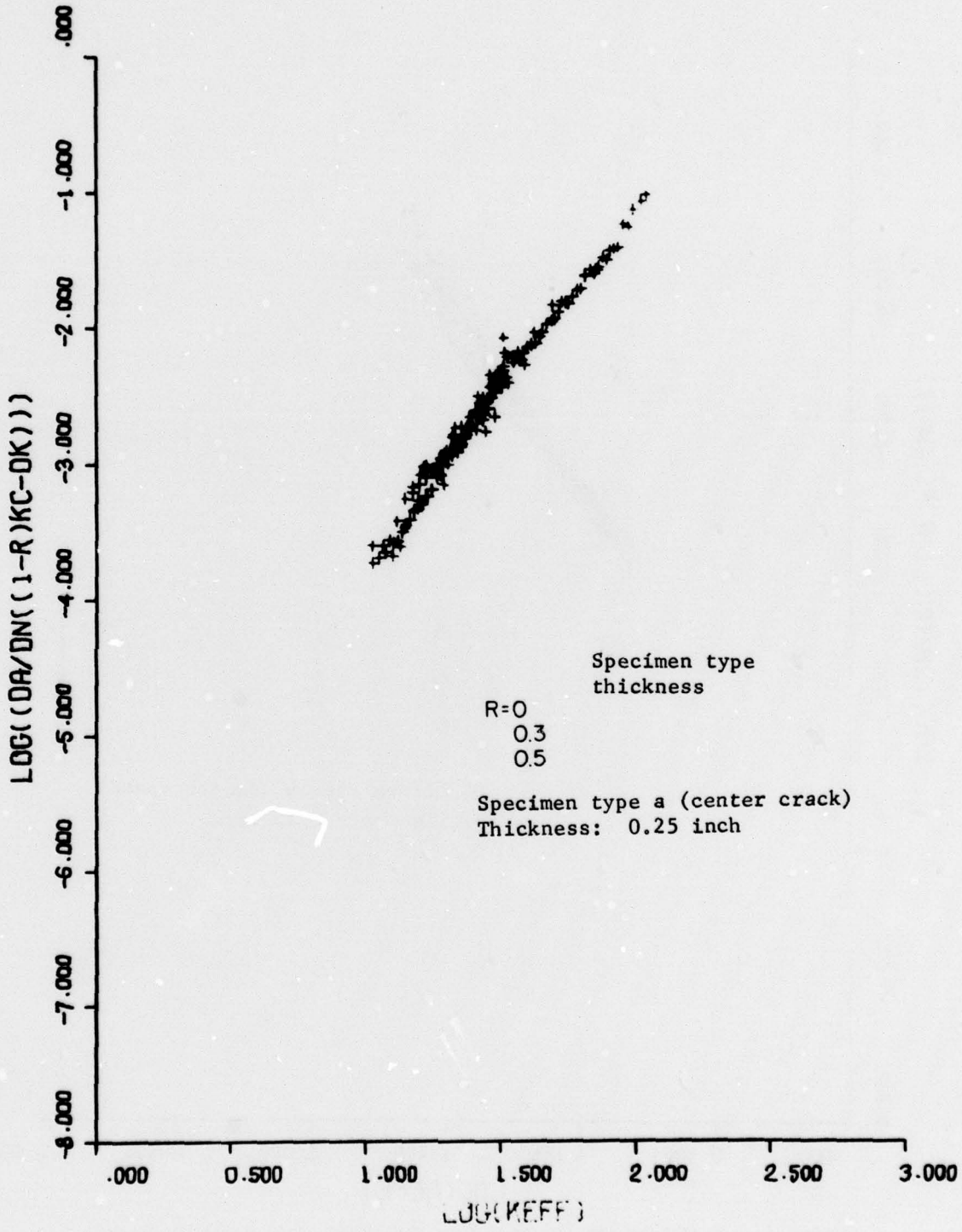

FIGURE 10. CRACK-GROWTH-RATE CURVE FOR Ti-6Al-4V (FORMAN PLOT)

TABLE 6. BASELINE CRACK-GROWTH INFORMATION

Material	Thickness, (in.)	Condition	Specimen Number	R	C: ΔK in ksi(a)	C: ΔK in psi(a)	n	K_c, ksi	R^a	Standard Deviation
7075-T73	0.25	Air	1	0.15	4.1×10^{-7}	5.0×10^{-13}	2.97		0.98	0.08
σ_{ys} = 60.5			2	0.0	4.4×10^{-7}	8.1×10^{-13}	2.91		0.96	0.13
ksi			3	0.3	9.5×10^{-7}	7.6×10^{-12}	2.70		0.99	0.06
			4	-0.15	9.3×10^{-7}	1.7×10^{-11}	2.58		0.98	0.07
			5	0.5	2.2×10^{-7}	3.4×10^{-14}	3.27		0.98	0.07
			Average Lumped(b)		7.6×10^{-7}	4.9×10^{-12}	2.73	67.7	0.96	0.12
			Upper Bound(b)		5.1×10^{-7}	5.1×10^{-13}	3.00	67.7		
	0.5	Air	6	0.0	3.4×10^{-7}	3.9×10^{-13}	2.98		0.93	0.14
			7	0.3	9.8×10^{-7}	8.9×10^{-12}	2.68		0.97	0.07
			8	0.5	1.7×10^{-7}	1.3×10^{-14}	3.37		0.98	0.09
			Average Lumped(b)		4.8×10^{-7}	7.8×10^{-13}	2.93	67.7	0.94	0.13
	0.25	Salt Water	9	0.0	2.9×10^{-5}	1.7×10^{-7}	1.74		0.90	0.08
			10	0.0	1.5×10^{-5}	4.1×10^{-8}	1.86		0.97	0.04
			Average		2.1×10^{-5}	7.8×10^{-8}	1.81		0.85	0.09
Ti-6Al-4V	0.25	Air	1	0.0	7.4×10^{-7}	2.7×10^{-11}	2.48		0.98	0.07
σ_{ys} = 130			2	0.3	4.3×10^{-7}	4.2×10^{-12}	2.67		0.98	0.07
ksi			3	0.5	4.1×10^{-7}	6.5×10^{-12}	2.60		0.95	0.09
			Average Lumped(b)		4.1×10^{-7}	4.9×10^{-12}	2.64	120	0.98	0.08
			Upper Bound(b)		7.8×10^{-7}	2.0×10^{-11}	2.53	120		
	0.25	Salt Water	4	0	4.4×10^{-7}	5.4×10^{-12}	2.97		0.91	0.13
			5	0	3.5×10^{-5}	1.4×10^{-6}	1.47		0.73	0.09
7075-T6	0.08	Air(b)			9.8×10^{-7}	7.8×10^{-12}	2.70	78		
2024-T3	0.08	Air(b)			7.4×10^{-8}	8.3×10^{-16}	3.65	130		

(a) Constants derived from da/dN plots are usually for the case that K and ΔK are expressed in ksi. CRACKS uses K and ΔK in psi, which means that C has to be divided by $10^{3(n-1)}$. The table gives values for C if ΔK is in ksi and for C if ΔK is psi.

(b) Cases used for crack-growth computations.

TABLE 7. SPECTRUM TESTS

Specimen Type (Figure 6)	Thickness, (in.)	Spectrum Type	Ti-6Al-4V Limit Load, ksi	Ti-6Al-4V Number of Tests	7075-T73 Limit Load, ksi	7075-T73 Number of Tests
a	0.25	Basic spectrum	65	2	33.6	2
		Spectrum A (fine)			33.6	1
		Spectrum A (coarse)	65	1	33.6	1
		Spectrum B	55	1	27	1
			60	1	30	1
			65	1	33.6	1
			70	1	37	1
		Spectrum C			33.6	1
		Spectrum D	65	1	33.6	1
b (Hole)	0.5	Basic Spectrum			33.6	2
c (Stiffener)	0.25	Basic Spectrum			28.8	2

4. CRACK-GROWTH ANALYSIS

4.1 Retardation Models

A fatigue cycle preceded by a load of higher magnitude produces less crack propagation than it does in the absence of the higher preload (assuming the same crack size). This phenomenon, called retardation, is extensively described in the literature (e.g., Reference 2). It is usually attributed to a combination of compressive residual stresses and crack closure due to residual stresses.

At least five models have been proposed[3-7] to treat retardation in a quantitative fashion. It is beyond the scope of this report to discuss all these models (for details, see References 2, 8, 9, and 10). Suffice it to state that none of the models have a solid physical bases, and that most are semi-empirical in the sense that they contain one or more constants that have to be derived from variable-amplitude crack-growth experiments.

The two best known models are by Wheeler[3] and by Willenborg, et al[4]. The essentials of these models will be briefly presented.

Wheeler defines a crack-growth reduction factor, C_p,

$$\frac{da}{dN} = C_p \, f(\Delta K) \quad , \tag{3}$$

where $f(\Delta K)$ is the usual crack-growth function, e.g., Equation (1). The retardation factor, C_p, is given in the following equation (see Figure 11):

$$C_p = \left(\frac{r_{pi}}{a_p + r_{po} - a_i}\right)^m = \left(\frac{r_{pi}}{s - a_i}\right)^m \quad , \tag{4}$$

where r_{pi} = current plastic zone in the ith cycle under consideration
a_i = current crack size
r_{po} = size of the plastic zone generated by a previous overload
a_o = crack size at which that overload occurred
m = empirical constant (retardation exponent).

At any given crack size, a_i, only that previous overload is of importance for which $s = a_o + r_{po}$ (Figure 11) is the largest, i.e., its plastic zone extends beyond the plastic zone of all previous overloads.

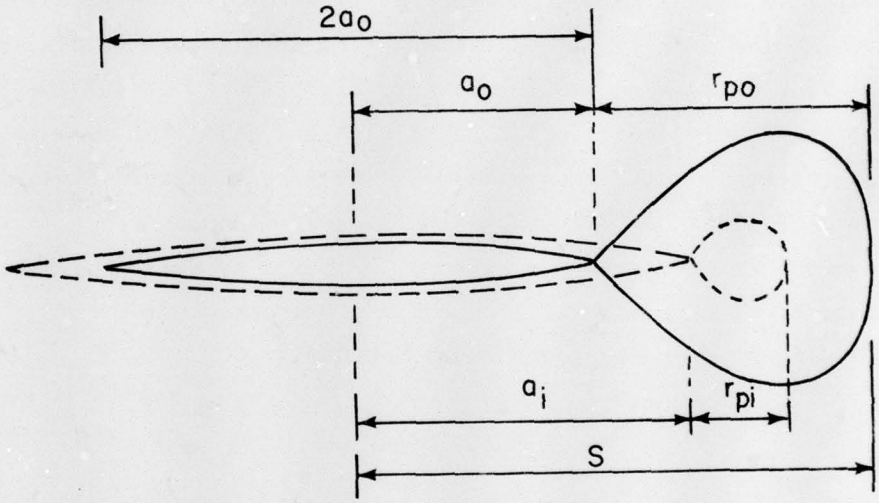

FIGURE 11. YIELD ZONE DUE TO OVERLOAD (r_{po}), CRACK SIZE AT OVERLOAD (a_o), CURRENT YIELD ZONE (r_{pi}), AND CURRENT CRACK SIZE (a_i)

The size of the plastic zone according to Reference 2 is

$$r_{pi} = \frac{K^2_{max,i}}{\alpha\sigma^2_{ys}} = \frac{(1-R)^2(\Delta K)^2_i}{\alpha\sigma^2_{ys}}$$

$$r_{po} = \frac{K^2_{max,o}}{\alpha\sigma^2_{ys}} \qquad (5)$$

with

$$K = \beta\sigma\sqrt{\pi a} \quad ,$$

where K_{max} is the maximum stress intensity in a given cycle, $\alpha = 2\pi$ for plane stress, and $\alpha = 6\pi$ for plane strain, and β is the geometry factor.

There is retardation as long as the current plastic zone size is contained within a previously generated plastic zone. If $r_{pi} >= s - a_i$, the reduction factor, C_p, is equal to one. The retarded crack-growth rate can be determined from the baseline (constant amplitude) crack-growth rate as

$$\left(\frac{da}{dN}\right)_{retarded} = C_p \left(\frac{da}{dN}\right)_{linear} \quad , \qquad (6)$$

where $(da/dN)_{linear}$ follows from an equation like Equation (1) in which the proper values of $\Delta\sigma_i$ and a_i are used for ΔK_i in the ith cycle.

The Willenborg model also relates retardation to the overload plastic zone It makes use of an effective stress-intensity factor, the maximum stress intensity in the ith cycle $\left[K_{max,i} = (1-R)\Delta K_i\right]$, being reduced to $K_{max,eff}$ as:

$$K_{max,eff} = K_{max,i} - \phi\left\{K_{max,o}\sqrt{1 - \frac{a_i - a_o}{r_{po}}} - K_{max,i}\right\} \quad ;$$

also, (7)

$$K_{min,eff} = K_{min,i} - \phi\left\{K_{max,o}\sqrt{1 - \frac{a_i - a_o}{r_{po}}} - K_{max,i}\right\} \quad ,$$

in which the symbols are defined by Figure 11.

Since K_{max} and K_{min} are reduced by the same amount, the overload does not change ΔK but causes only a reduction of the cycle ratio, R, as long as $K_{min,eff} > 0$. When $K_{min,eff} < 0$, it is set at zero. In that case $R = 0$ and $\Delta K = K_{max,eff}$.

In the original model, ϕ is equal to one. Immediately after the overload, $a_i = a_o$ which means that

$$K_{max,eff} = 2K_{max,i} - K_{max,o} \text{ for } a_i = a_o \quad . \qquad (8)$$

Consequently, the model predicts complete retardation, i.e., zero crack-growth rate for the case that the overload is twice as high as the subsequent cycle, because that would lead to $K_{max,eff} = 0$. Therefore, Gallagher and Hughes[11] introduced the factor ϕ in Equation (7) given by

$$\phi = \frac{K_{max,i} - K_{max,th}}{K_{max,o} - K_{max,i}} \tag{9}$$

in which $K_{max,th}$ is the threshold value for fatigue-crack growth. This correction was not applied in the present work.

The two models do not account for (a) the reduction of the retardation effect by negative overloads and (b) the difference in retardation caused by single and multiple overloads. The crack-closure model by Bell and Creager[7] attempts to overcome these shortcomings. It is based on a crack-rate equation using an effective stress intensity, which is the difference between the applied stress intensity and the stress intensity for crack closure. The latter is determined semiempirically. The final equation is complex, contains many empirical constants, and is difficult to apply.

In essence, all retardation models require a cycle-by-cycle integration of crack growth. During the ith cycle at crack size a_i, a stress range $\Delta\sigma_i$ is applied. The stress intensity is $\Delta K_i = \beta\Delta\sigma_i\sqrt{\pi a_i}$. The linear crack-growth rate follows from Equation (1) as $\left(\frac{da}{dN}\right)_{linear}$. Application of one of the retardation models gives the retarded crack-growth rate $\left(\frac{da}{dN}\right)_{retarded}$. This means that the crack extends to

$$a_{i+1} = a_i + \Delta a = a_i + 1 \times \left(\frac{da}{dN}\right)_{retarded} . \tag{10}$$

Then the procedure is repeated for cycle i+1. In the event that a series of cycles of the same magnitude is applied, a somewhat simpler procedure can be followed. If the total crack growth caused by these n cycles of the same magnitude is small

$$a_{i+n} = a_i + n \times \left(\frac{da}{dN}\right)_{retarded} \tag{11}$$

or instead, the integration can be based on the Simpson rule, for example.

Several computer routines for the integration of crack growth have been developed. The use of a particular routine is largely a matter of personal choice, available facilities, and computational efficiency. When properly programmed, the success of a computer routine depends primarily upon the retardation models and very little on the integration scheme.

Probably the most versatile computer routine is CRACKS*. It has options for the three models discussed previously, for many different stress-intensity solutions, and for different crack-rate equations. CRACKS III was used for the crack-growth computations reported herein. In all cases, the Forman rate equation was applied.

Card decks were prepared for all spectra; the integration followed exactly the same cycle sequence (and flight sequence) as applied during the tests. Computations for the various cases required from 300 to 1200 seconds of computer time per curve on a CDC-6400 computer.

4.2 Comparison of Models

In the first phase of this study, about 150 crack-growth curves were calculated for the experiments with central cracks. The following cases were considered:

(a) Linear (no retardation)

(b) Wheeler with various retardation exponents

(c) Willenborg

(d) Closure model.

Most cases were done twice – once with average crack-growth data and once with upper bound data (see Table 6). The closure model was run with upper bound data only. A plane-stress plastic zone was assumed, but some cases were run with a plane-strain plastic zone. Examples of the results are presented in Figure 12 for 7075-T73 under Spectrum B, and in Figure 13 for Ti-6Al-V under the basic spectrum. Test data are also shown in these figures.

The following observations can be made from the results shown in these figures as well as from results for other spectra:

- Depending upon the model, the baseline crack-growth data and the empirical constants used in the retardation model, practically any answer can be arrived at. A linear computation can be just as far off as a Wheeler (m = 2.2) or Willenborg calculation with average data.

---

* Available through AFFDL-FBEC, Fatigue, Fracture and Reliability Group.

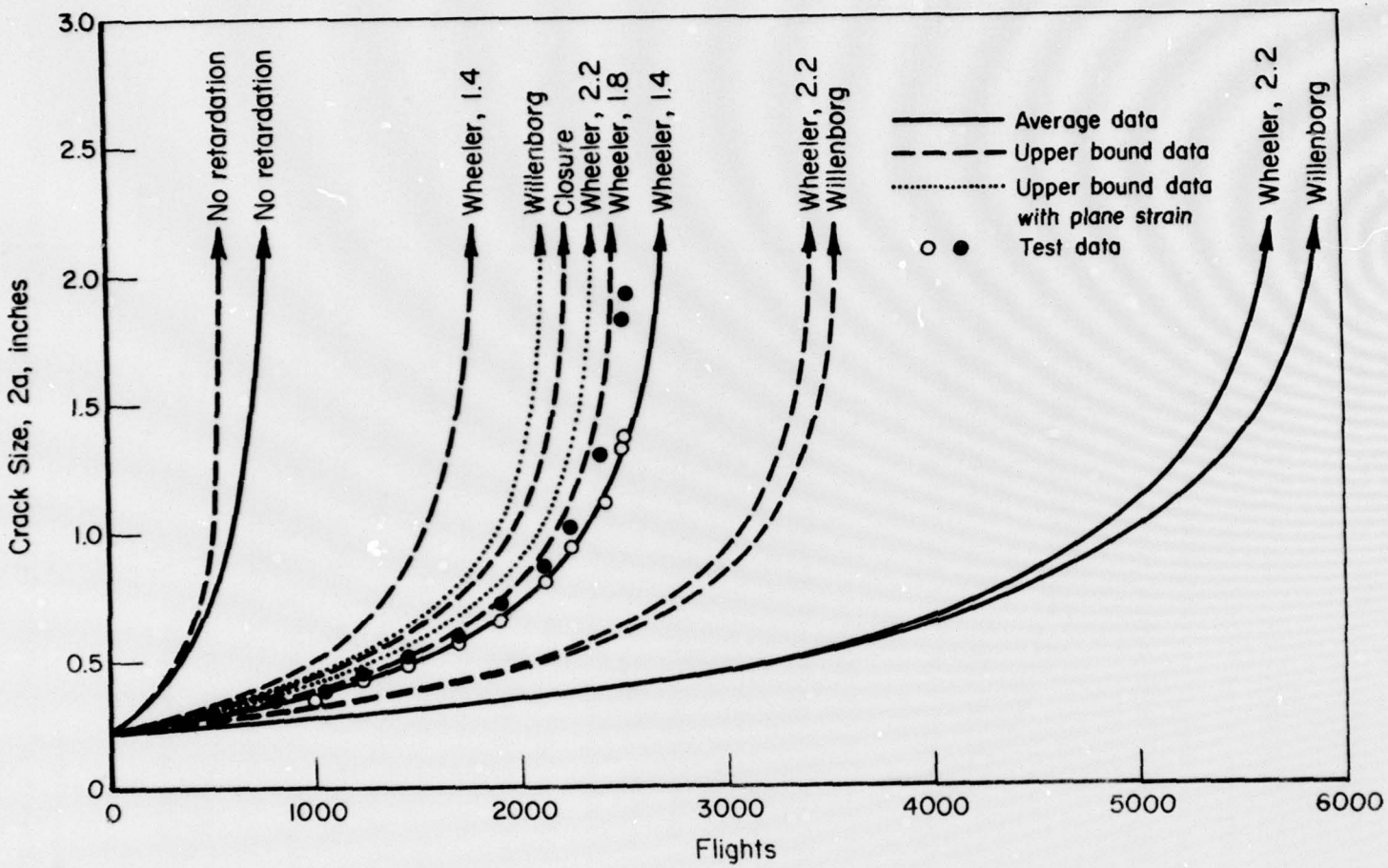

FIGURE 12. VARIOUS PROCEDURES FOR CRACK-GROWTH CALCULATION COMPARED FOR 7075-T73 SPECTRUM B

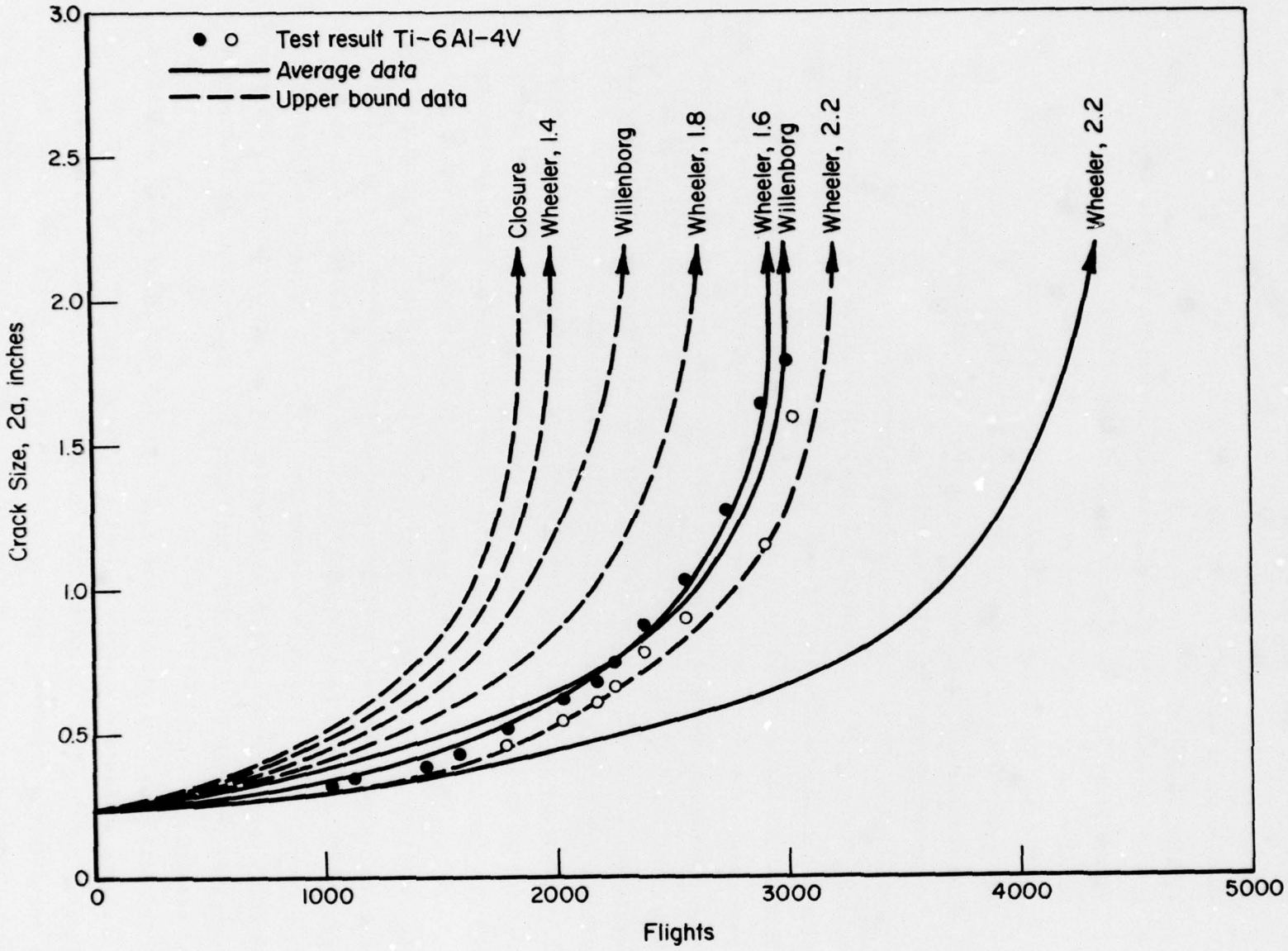

FIGURE 13. VARIOUS PROCEDURES FOR CRACK-GROWTH CALCULATION COMPARED FOR Ti-6Al-4V, BASIC SPECTRUM

- Regardless of the data used, and of other assumptions made, the Willenborg model gives approximately the same results as the Wheeler model with m = 2.0 to 2.2 for 7075-T73 and m = 1.6 to 1.9 for Ti-6Al-4V.
- Any of the models can give the correct prediction if it is adjusted properly. The Wheeler model and the closure model can be adjusted by selecting the proper values for the empirical constants. The Willenborg model cannot be adjusted, but it can give the right answer if the baseline data are adjusted (in the present case, use of the upper bound data gave the right answer for the titanium alloy).

At this point, it is interesting to check whether disregard of the effect of negative loads by the Willenborg and Wheeler models was of any consequence. Therefore, these models and the closure model were examined for the cases with and without GAG cycles. Obviously, the Wheeler and Willenborg models predict the same result for both cases. However, the closure model also gave predictions which were so close that the difference does not show in a plot. This should not be surprising for the titanium alloy since the test data show that the GAG cycles, indeed, had very little effect, (Figure 14). However, the effect was significant in the case of the aluminum alloy (Figure 14).

The question arises whether the observations listed above are consistent and independent of spectrum type or shape and independent of design stress level. To answer this question, the ratios of calculated and experimental crack-growth lives were calculated. (The crack-growth life is defined as the number of flights required to extend the crack over a certain length.) In practice, a crack-growth prediction will not always cover the same range of crack sizes. Therefore, these ratios were calculated from crack increments of 0.25 to 0.5 inch, 0.25 to 1 inch, 0.25 to 1.5 inches, and 0.25 to 2 inches. All center crack cases were included (i.e., various spectra and stress levels). The results are compiled in Table 8. (The last two entries in Table 8 will be discussed in a later section.)

The data show, indeed, that the computational results are very consistent, and that the standard deviation is small, although somewhat larger for the Willenborg model. This indicates that consistently close predictions can be made for slightly different spectrum types or slightly different stress levels, once the computation is adjusted. Of course, this adjustment for constants and crack-growth data should be based on a number of spectrum crack-growth experiments.

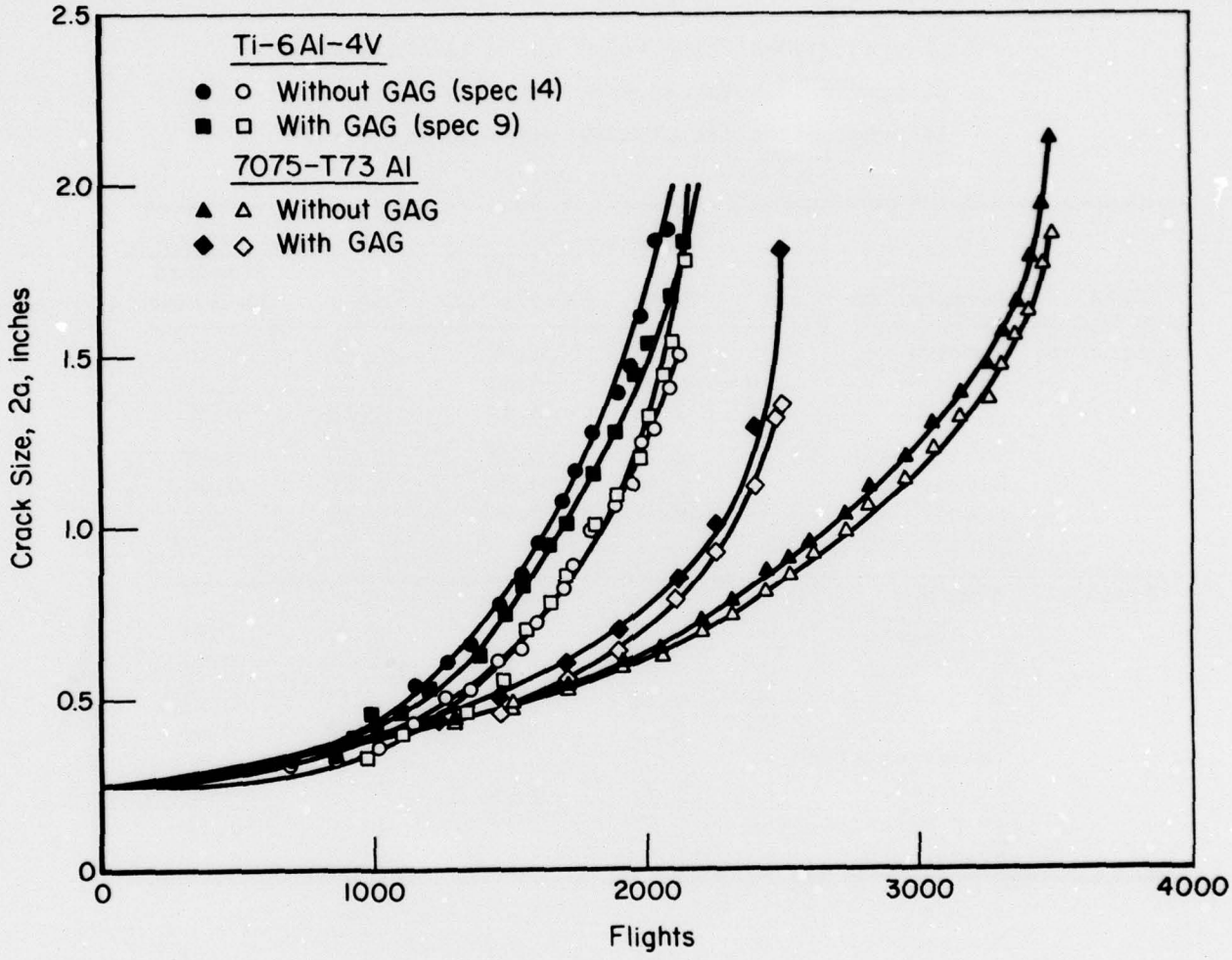

FIGURE 14. EFFECT OF GROUND-AIR-GROUND CYCLES IN SPECTRUM B

TABLE 8. RATIO OF PREDICTED LIFE OVER TEST LIFE

32 predictions for Wheeler and Willenborg cases

24 predictions for closure cases in 7075-T73

16 predictions for closure cases in Ti-6Al-4V

			Aluminum 7075-T73		Titanium 6Al-4V	
Data	Integration	m	Mean	Standard Deviation	Mean	Standard Deviation
Upper Bound	Wheeler	1.4	0.68	0.08	0.62	0.10
		1.8	0.92	0.07	0.84	0.09
		2.2	1.24	0.12	1.16	0.07
	Willenborg	--	1.19	0.18	0.95	0.13
	Closure	--	0.82	0.07	0.61	0.06
	Linear (No retardation)	--	0.24	0.06	0.22	0.07
Average	Wheeler	1.4	1.02	0.14		
		1.6			0.97	0.11
		2.2	1.88	0.23	1.52	0.13
	Willenborg	--	1.82	0.29	1.34	0.21
	Linear (No retardation)	--	0.33	0.10	0.27	0.09
	Semilinear (8 Predictions only)	1.4	1.01	0.25		
		1.6			1.04	0.18

Table 8 shows that for 7075-T73 the Willenborg model is equivalent to the Wheeler model with upper bound data and with $m \approx 2.2$ (the mean values are 1.19 and 1.24, respectively). For Ti-6Al-4V, the Willenborg model is equivalent to the Wheeler model for upper bound data with $m \approx 1.8$ (the mean values are 0.95 and 0.84, respectively).

However, the Wheeler model and the closure model are preferable to the Willenborg model because they can be adjusted to give useful predictions using average crack-growth data. The inflexibility of the Willenborg model requires adjustment by selecting arbitrary crack-growth data. Since the baseline crack-growth data comprise the only undisputable input to the predictions, the use of arbitrary data introduces an unnecessary artificiality. Moreover, if predictions would have to be made for a material with slightly different properties, there would be a problem in selecting the data. The use of some arbitrary upper bound can be the solution, but average data can be defined with less ambiguity.

Of the two adjustable models, the Wheeler model is undoubtedly the more attractive because of its ultimate simplicity. As will be shown in a subsequent section, this simplicity permits the use of far less complicated integration procedures for routine calculations. Therefore, the Wheeler model was selected as the vehicle for the second phase of this program. (It will be shown later that this does not affect the generality of the conclusions.) For this reason, the Wheeler computations made in the first phase of the program will be considered in more detail.

The ratio of predicted and experimental crack-growth life is plotted as a function of the retardation exponent in Figure 15 for 7075-T73 and in Figure 16 for Ti-6Al-4V. These figures reinforce the conclusion arrived at from Table 8 that, with average data, $m = 1.4$ gives the best fit for 7075-T73 and $m = 1.6$ for Ti-6Al-4V. The generality of these curves is still subject to doubt. Therefore, the same plots were made for the various spectra individually and some examples are shown in Figure 17.

It can be concluded from Figure 17 that some spectra show a different dependence. This means that the data points for a particular spectrum may tend to fall consistently in the lower (or upper) part of the scatter bands in Figures 15 and 16. However, deletion of Spectrum D from the population in Table 8 reduces the standard deviation for $m = 1.4$ (7075-T73) only from 0.14 to 0.13.

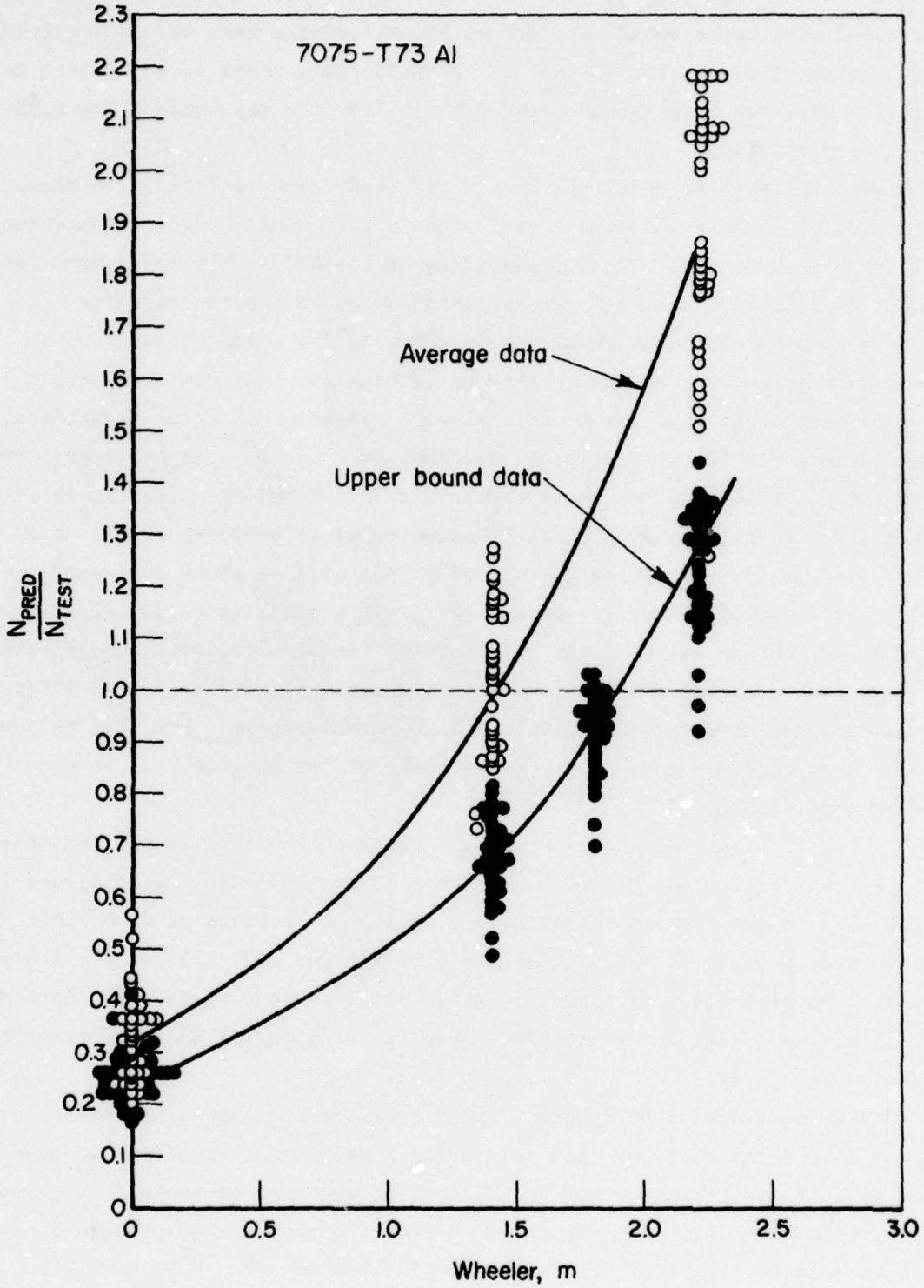

FIGURE 15. EFFECT OF WHEELER EXPONENT ON CRACK-GROWTH LIFE PREDICTIONS

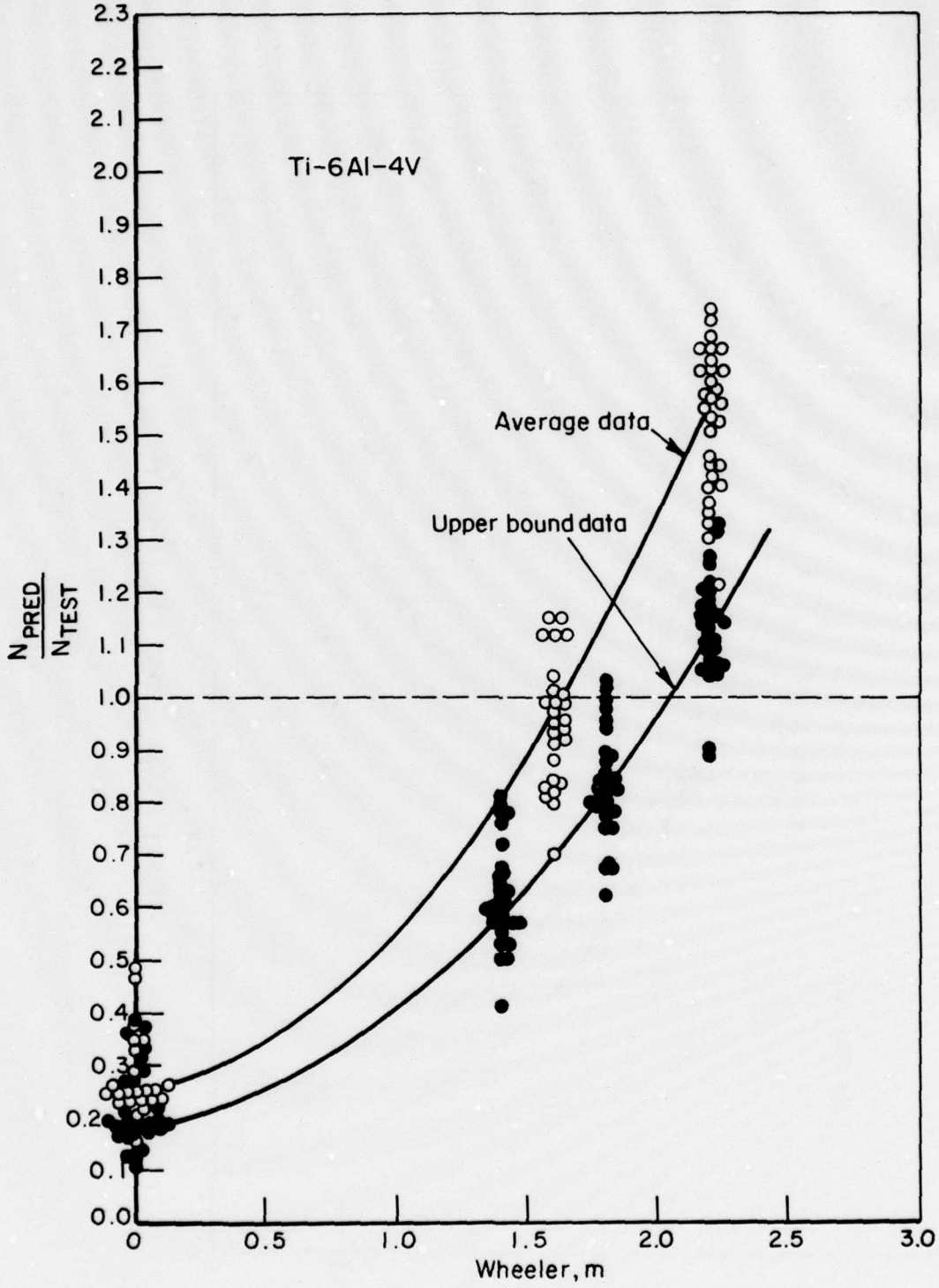

FIGURE 16. EFFECT OF WHEELER EXPONENT ON CRACK-GROWTH LIFE PREDICTIONS

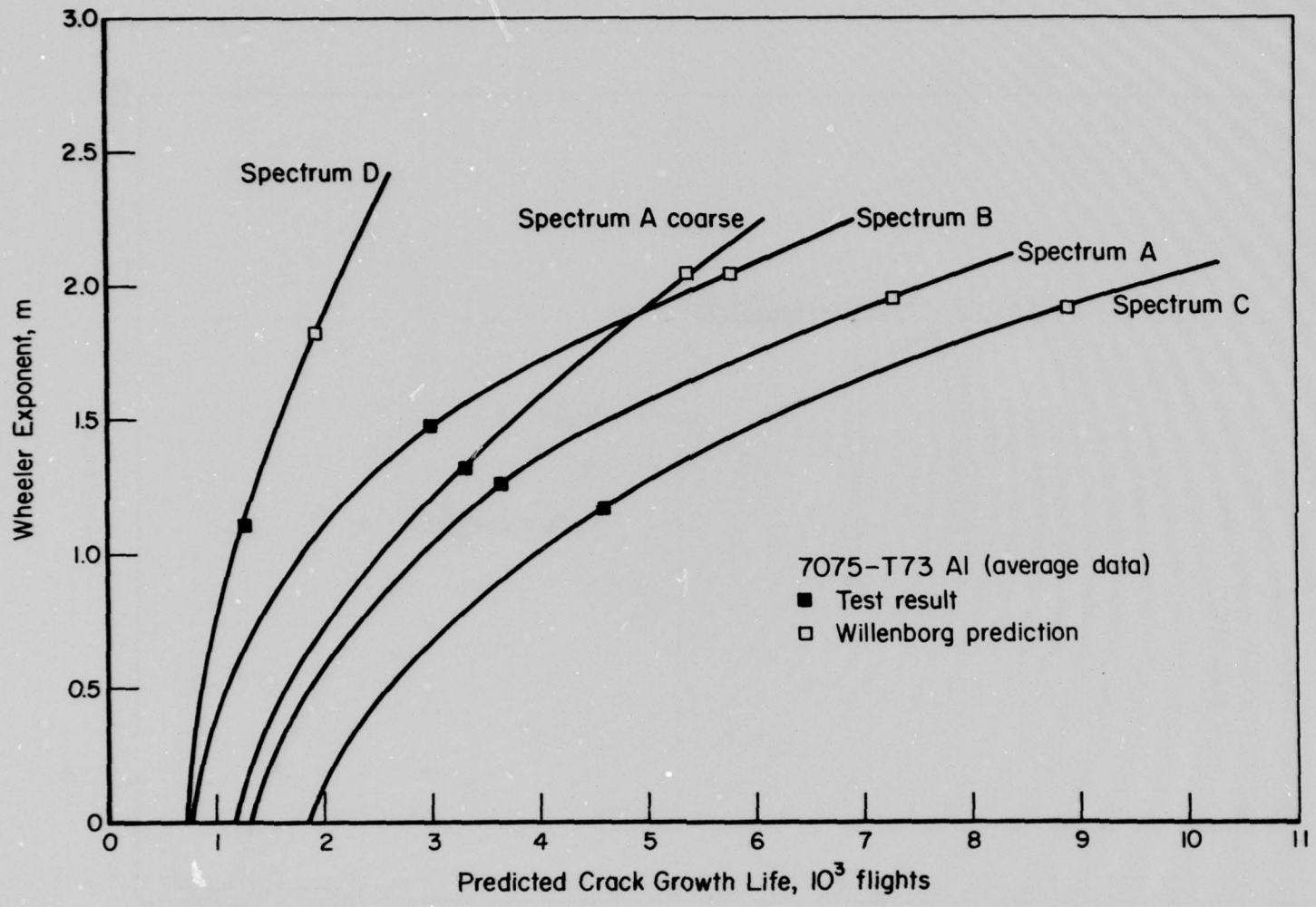

FIGURE 17. SENSITIVITY OF VARIOUS SPECTRA TO WHEELER EXPONENT

It is concluded that the values m = 1.4 and 1.6 for the present spectra and the present materials are the most appropriate. Obviously, this cannot be generalized to other spectra and other materials; but for such cases, m-values can be determined giving equally satisfactory results. This point of view will be supported in subsequent sections.

When all Wheeler predictions are considered for both the aluminum and the titanium alloy at the given values of m, the distribution shown in Figure 18 is obtained. The mean value is practically equal to 1, the standard deviation is 0.13. These values should be kept in mind when judging the computed curves, presented in the following sections, which are all based on m = 1.4 for 7075-T73 and m = 1.6 for Ti-6Al-4V.

4.3 Goodness of Fit

Before conclusions are drawn about the adequacy of crack-growth predictions, the criteria of reliable predictions should be established. Is it adequate to show that a predicted crack-growth life is close to the test life? Or is it sufficient to show a few computed curves close to an experimental curve?

In practical cases, the crack-growth increments for which predictions are required may vary greatly. Sometimes the regime between 0.02 and 0.2 inch may be of interest; in other cases, it is the regime of 0.2 to 2 inches. Also, the shape of the crack-growth curve varies largely due to a different dependence of K on crack size (compare, for example, a center crack with increasing K to a crack emanating from a loaded hole with decreasing, then increasing, K). Prediction of the correct crack-growth life would be inadequate if the predicted curve of incremental growth to cracks of intermediate size differed greatly from the experimental curve.

Consider the predicted crack-growth curves in Figures 12 and 13. At first glance, one can take parts of the predicted curves, shift them to the experimental curve, and get a close correlation. Does this mean that calculations made for a different crack-growth interval, or for a different initial crack size, would lead to different conclusions as to the applicability of the retardation models or the values of the empirical constants? A partial answer to this question is given in Table 8 and Figures 15, 16, and 18. The data for four different crack-growth intervals indicate that the relative accuracy is independent of the interval. If the interval from 0.25 to 0.5 inch is predicted within 10 percent, then the

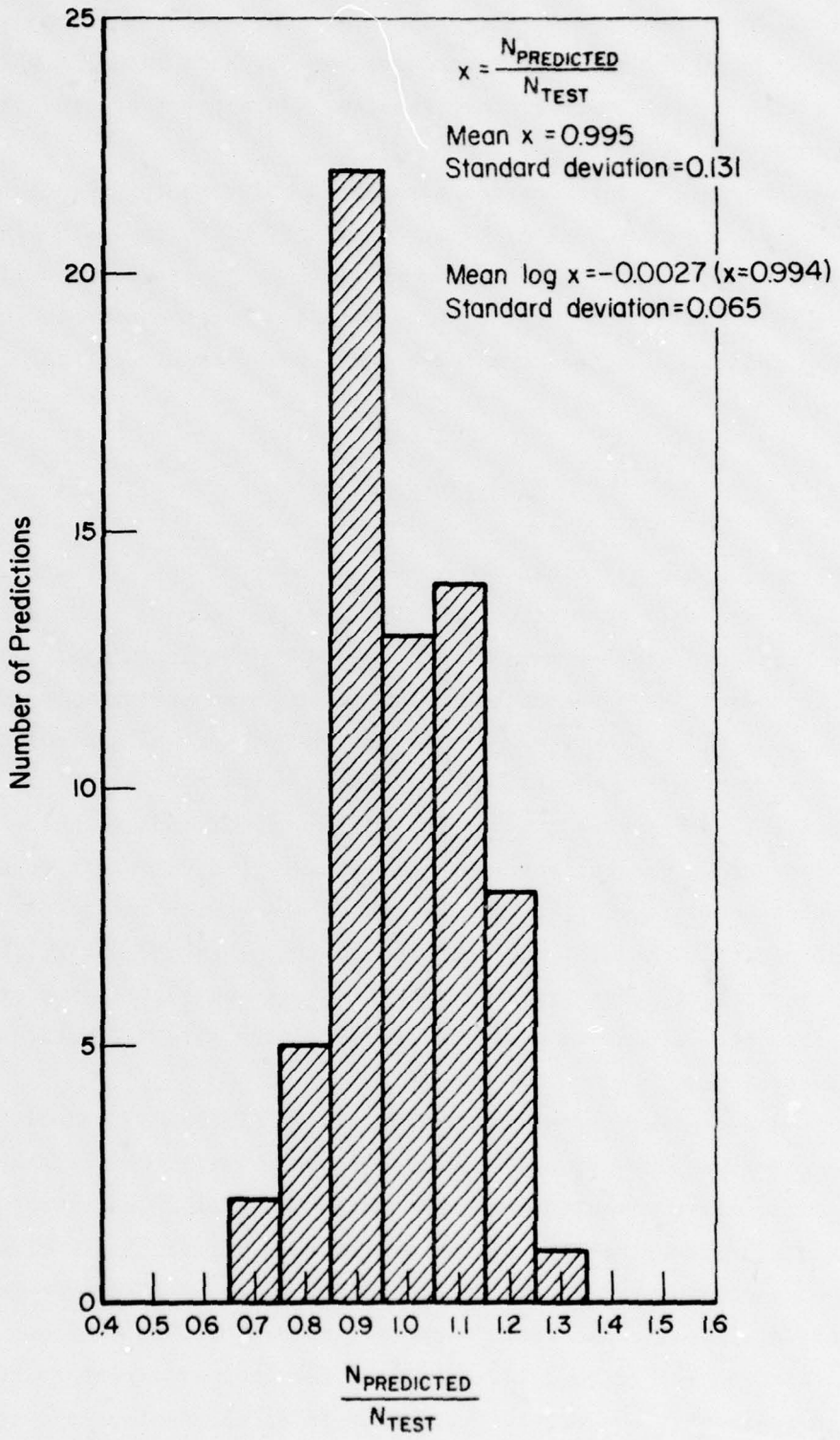

FIGURE 18. HISTOGRAM OF RATES BETWEEN BEST WHEELER PREDICTION AND TEST RESULT

interval from 0.25 to 2 inches is predicted within 10 percent. If the 10 percent deviation is on the same side in both cases, (then this implies that) the interval from 0.5 to 2 inches is also predicted within 10 percent.

More information can be obtained if the various curves are differentiated. This was done for several cases and some results are shown in Figure 19 in terms of the crack-growth rate per flight, da/dF. Since these are the same cases as in Figure 12, it can be determined that the experimental data follow the Wheeler curve for m = 1.4 and average data. The fact that these curves are almost parallel on this logarithmic plot illustrates that the growth rates differ by a constant factor, irrespective of crack size.

The above result is not surprising. Under spectrum loading without large batches of constant-amplitude cycles, the retardation effect is repetitive and approximately constant. Thus, such loading will retard crack growth by the same factor, irrespective of crack size (see Equations (4) through (7)). Of course, this would not be so for nearly constant-amplitude loading with occasional overloads, nor for block program loading with large block sizes. In such cases, retardation effects vary with crack size. If a computation would be somewhat off, the overloads would occur at a different crack size than in the test and, thus, would have a different retardation effect. With sufficiently refined spectrum loading, the overloads occur often enough to have a ubiquitous effect.

Hence, it can be concluded from this discussion and from Figure 19 that the relative accuracy of a given computation is independent of the crack-growth interval. This means that the computed and experimental crack-growth curves are generally of the same shape. *If this is not the case*, the K-formulation used for the computation was erroneous.

4.4 Sensitivity to Randomness

The arguments used in the previous section also lead to the conclusion that the sequence of cycles in individual flights (or small blocks of flights) will not greatly affect the result. This conclusion holds as long as the total amount of crack growth within the block is small compared to the instantaneous crack size. The reason behind this conclusion is that retardation factors are determined only by the largest previous plastic zone size. In other words – if the highest load levels occur often enough, crack growth will be nearly independent

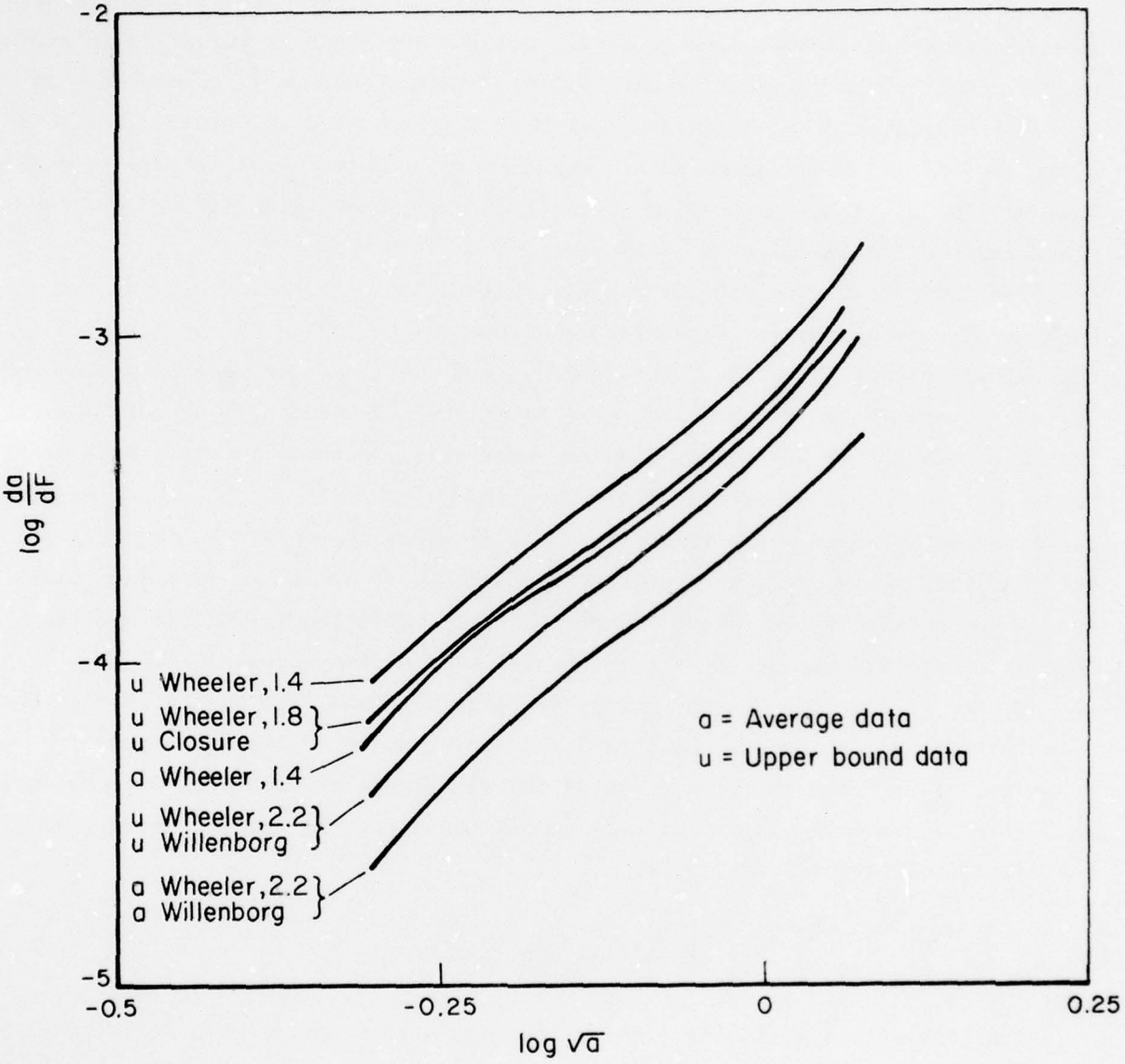

FIGURE 19. PREDICTED CRACK-GROWTH RATES WITH VARIOUS MODELS AND BASELINE DATA FOR 7075-T73 UNDER SPECTRUM B

of the load sequence. This was shown experimentally by several investigators. For example, Schijve[12] showed that random loading gives essentially the same result as a low-high-low order of loads within a flight. Only large-block program loading gives results with no bearing to service loading.

Figure 20 shows the sensitivity of computational results to block size. This case is the same as the one shown in Figure 12. The curve labeled "ordered mix" is the original curve using the exact test sequence. In order to obtain the 100 flight low-high-low block, all load cycles for 100 flights as given in Table 3 were combined into one large 100 flight low-high-low block. The random mix was obtained simply by shuffling the deck of punched cards with the load information.

Obviously, use of the 100-flight block would still be permissible for the computations. The total crack-growth life is only 5 percent less than for the original ordered mix; this percentage is entirely within the general accuracy of the predictions (standard deviation, 14 percent). Crack growth in 100 flights was about 5 to 10 percent of the instantaneous crack size throughout the larger part of the crack-growth curve, i.e., at any given crack size the next 100 flights extended the crack by about 5 to 10 percent.

This conclusion permits setting a bound to the qualitative statements made above. Apparently, it is possible to obtain reasonable results with block sizes that cause crack increments of the order of 5 percent. This means that similar step sizes can be used in the computations. It also means that the frequency of occurrence of the highest load levels should be such that they appear in each block of this size, or during every 5 percent increment in crack size.

4.5 Semilinear Analysis

The simplicity of the Wheeler model and the discussion about relative accuracy and permissible block size open possibilities for extremely simplified crack-growth computations. These can be used for quick, rough assessments of crack-growth behavior. If the block size is small enough, the instantaneous crack size, a_i, will be approximately equal to a_o, the crack size at which the overload occurred. This means that Equations (3) through (6) reduce to

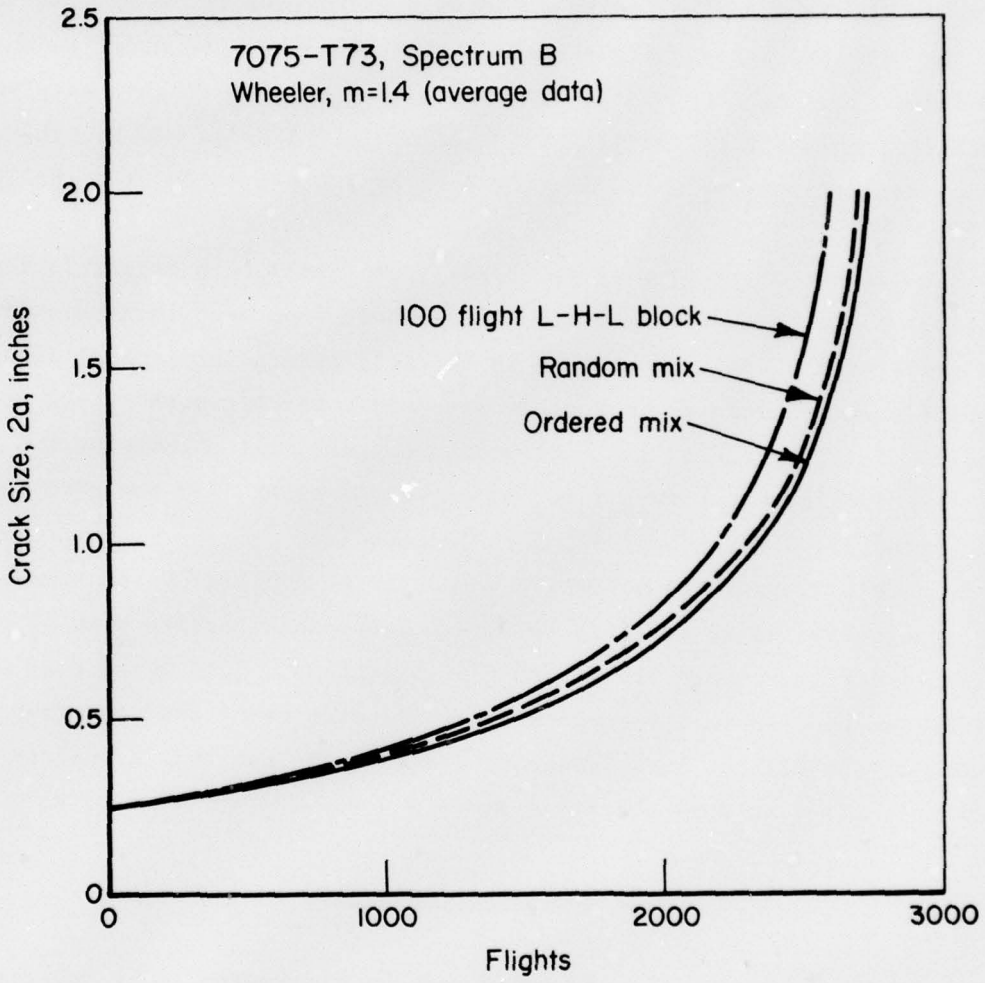

FIGURE 20. EFFECT OF LOAD SEQUENCE ON PREDICTED CRACK GROWTH

$$\left(\frac{da}{dN}\right)_{retarded} = \left(\frac{r_{pi}}{r_{po}}\right)^{m} \left(\frac{da}{dN}\right)_{linear} \quad ; \tag{12}$$

also,
$$r_p = \frac{K^2_{max}}{\alpha\sigma^2_{ys}} = \frac{\pi\sigma^2_{max}a}{\alpha\sigma^2_{ys}} \quad , \tag{13}$$

thus:
$$\left(\frac{da}{dN}\right)_{retarded} = \left(\frac{\sigma_{max,i}}{\sigma_{max,o}}\right)^{2m} \left(\frac{da}{dN}\right)_{linear} \quad . \tag{14}$$

If a block of 100 flights is considered, then the equation should be simplified to

$$\left(\frac{da}{dF}\right)_{retarded} = \left(\frac{\sigma_{max,eff}}{\sigma_{max,o}}\right)^{2m} \left(\frac{da}{dF}\right)_{linear} \quad . \tag{15}$$

In this equation, $\sigma_{max,eff}$ is an effective stress descriptive of the spectrum, whereas $\sigma_{max,o}$ is the highest load occurring in 100 flights (or in whatever the block size is).

It was determined by trial and error that $\sigma_{max,eff}$ should be taken as the rms value of all cycles in the block, but the exponent should be m instead of 2m. Then

$$\left(\frac{da}{dF}\right)_{retarded} = \left(\frac{\sigma_{rms}}{\sigma_{max}}\right)^{m} \left(\frac{da}{dF}\right)_{linear} \tag{16}$$

and
$$N_{retarded} = \left(\frac{\sigma_{max}}{\sigma_{rms}}\right)^{m} N_{linear} \quad . \tag{17}$$

The procedure is to calculate crack growth over 100 flights by a linear calculation. The number of flights required for this crack extension is determined from Equation (17). The value of m should be obtained from an actual Wheeler calculation combined with some experiments.

Computations were made with Equation (12) for both 7075-T73 and Ti-6Al-4V with various values of m in Figure 21. The results are compared with the actual Wheeler calculations for the same cases. As in the foregoing, four different crack increments were considered. In most cases, the Wheeler result was almost exactly reproduced.

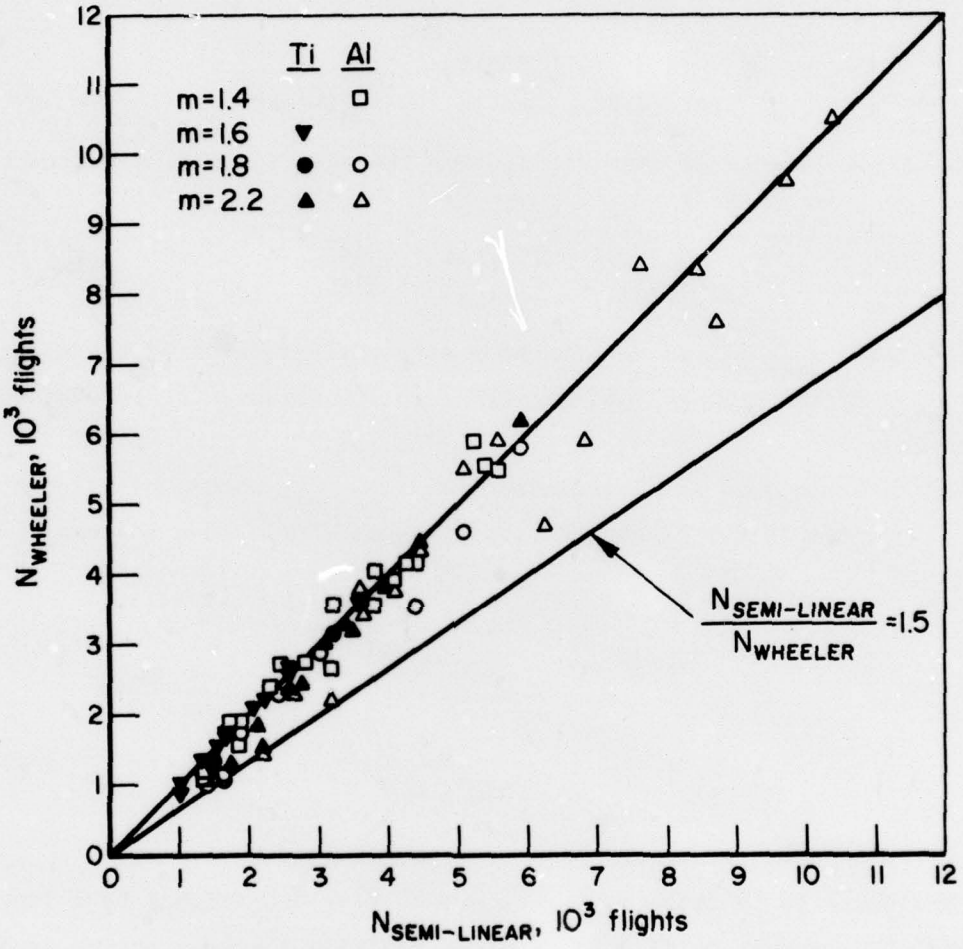

FIGURE 21. COMPARISON OF BEST WHEELER PREDICTIONS WITH APPROXIMATE SEMILINEAR PREDICTIONS

Figure 22 and Table 8 show a comparison of these semilinear computations with test results. The actual Wheeler calculations are also included. Only the cases of m = 1.4 for 7075-T73 and of m ≈ 1.6 for Ti-6Al-4V are considered. It turns out that the semilinear calculations are generally within 30 percent of the test life, with two exceptions. The Wheeler results are generally within 20 percent of the test life, with one exception.

If the linear summation is not made complex by the use of numerical integration procedures, the N_{linear} in Equation (12) can easily be calculated on the basis of a Forman equation with a programmable pocket calculator. With steps of 100 flights, a computation of a curve requires 15 minutes. Since full blown integration programs involve large expenditures for computer time, this simple procedure is very attractive for quick routine assessments of crack growth. This semilinear computation was used for some of the analyses discussed in subsequent sections.

5. SPECTRUM EFFECTS

5.1 *Spectrum Approximation*

As pointed out in Section 2, the basic spectrum is identical to Spectrum A (Figure 1). However, the basic spectrum stress history contained many more load levels than the approximation of Spectrum A (consisting of 17 levels), but the latter's stress history was more refined. Other versions of Spectrum A were also considered namely, a coarse approximation by 11 levels, and a truncated version (Figures 2 and 3). Test results and computed crack-growth curves comparing these spectra are presented in Figure 23 for 7075-T73 and in Figure 24 for Ti-6Al-4V.

The results confirm the reasoning in the previous section. Since Spectrum A is almost identical to the basic spectrum, the computed results are very similar. (Attention is called to the relatively small scatter in the data for the basic spectrum.) The coarse approximation of Spectrum A gives somewhat faster growth rates.

As might be expected after the adjustment of the model, the calculated curves follow the test data very closely. The fine version of Spectrum A, its truncated version, and the basic spectrum give nearly identical results, indicating that the introduction of the lower load levels did not change the life

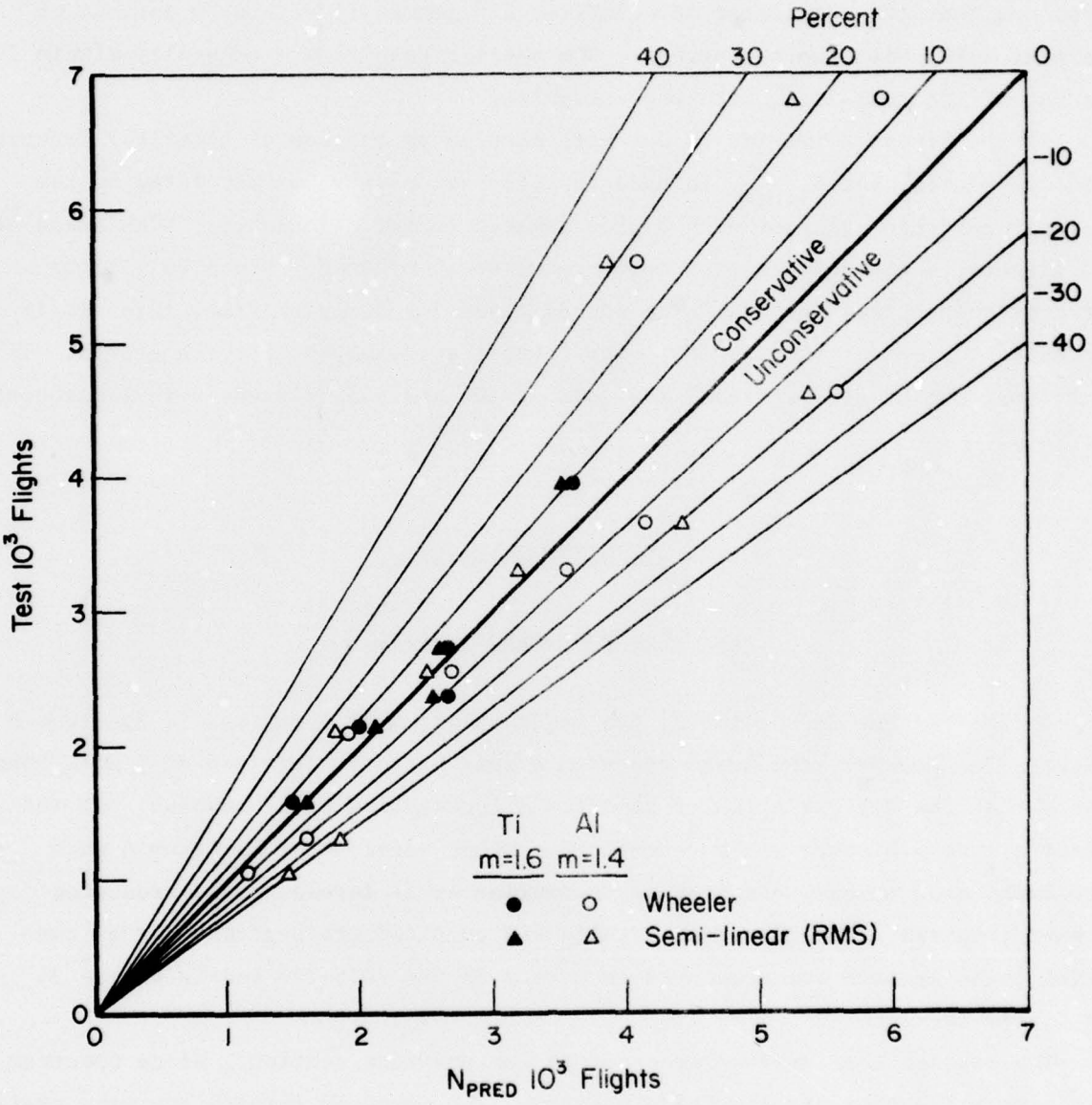

FIGURE 22. COMPARISON OF TEST DATA WITH BEST WHEELER CALCULATIONS AND WITH APPROXIMATE SEMILINEAR CALCULATIONS

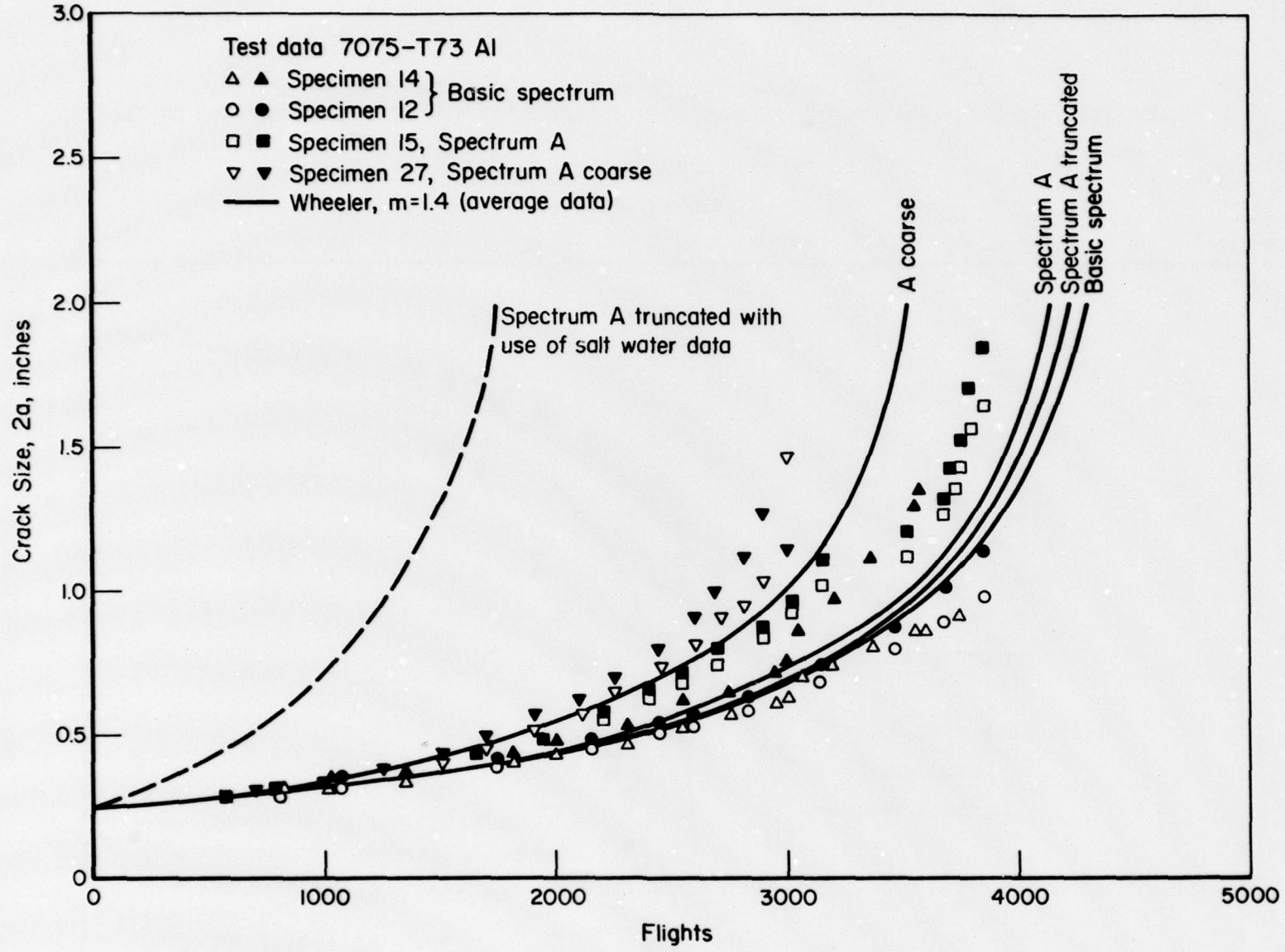

FIGURE 23. COMPARISON OF WHEELER CALCULATIONS WITH TEST RESULTS FOR THE BASIC SPECTRUM AND THREE VERSIONS OF SPECTRUM A IN 7075-T73

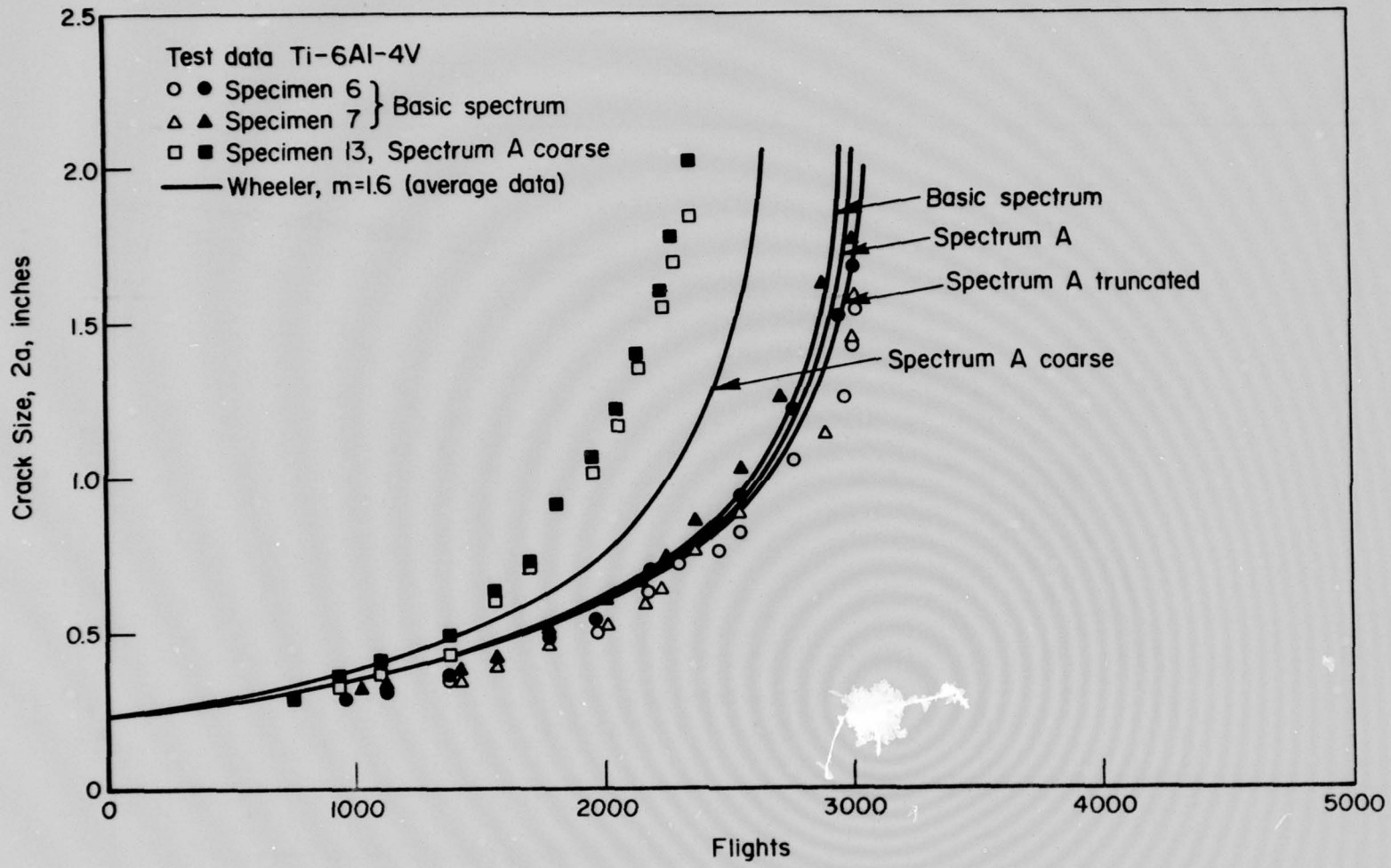

FIGURE 24. COMPARISON OF WHEELER CALCULATION WITH TEST RESULTS FOR THE BASIC SPECTRUM AND VARIOUS VERSIONS OF SPECTRUM A IN Ti-6Al-4V

(as expressed in flight hours). Apparently, the retardation behavior is somewhat affected by the coarse approximation of the spectrum. This is reflected both in the test data and the calculated curves. Even so, the difference is only in the order of 20 percent – well within the limits of accuracy one would expect for crack-growth information.

Figure 25 shows the semilinear analysis for the same cases as in Figure 23; it demonstrates the usefulness of this simple computational scheme for quick, routine calculations.

For comparison, the curve for truncated Spectrum A was also calculated on the basis of the saltwater spray data (Table 6). There appears to be a reduction of over 50 percent in crack-growth life (Figure 23). Even if an environmental factor were encountered in service, it would presumably be somewhat less influential than saltwater spray. Thus, crack growth in service would be somewhere between the curves for saltwater and air – another indication that the coarse approximation of Spectrum A may be useful in many applications.

The question then arises as to how many load levels should be selected for a staircase approximation of a spectrum. In this respect, it should be pointed out that the positive levels are the most important. Therefore, the discussion will concern only the positive levels.

The fine approximation of Spectrum A had 12 positive levels, two of which seem superfluous when compared with the truncated spectrum. The coarse version had 7 positive levels. The results of the three versions of Spectrum A were within 20 percent of each other (tests and calculations), but which of these versions is most accurate, cannot be determined. The fine version agreed most closely with the basic spectrum data; however, there is no certainty that the basic spectrum is an accurate representation of service loading.

Some data are available[10] on the effect of the number of load levels in a gust spectrum. This spectrum was approximated by 4, 5, 7, and 13 positive levels. Calculated crack-growth lives were 11,000, 37,000, 32,000, and 35,000, respectively. Apparently, the four-level approximation was too coarse, but the other cases gave nearly identical results.

This leads to the conclusion that approximations by approximately 10 levels are adequate for prediction purposes. The discussion in Section 7 will elaborate further on this conclusion.

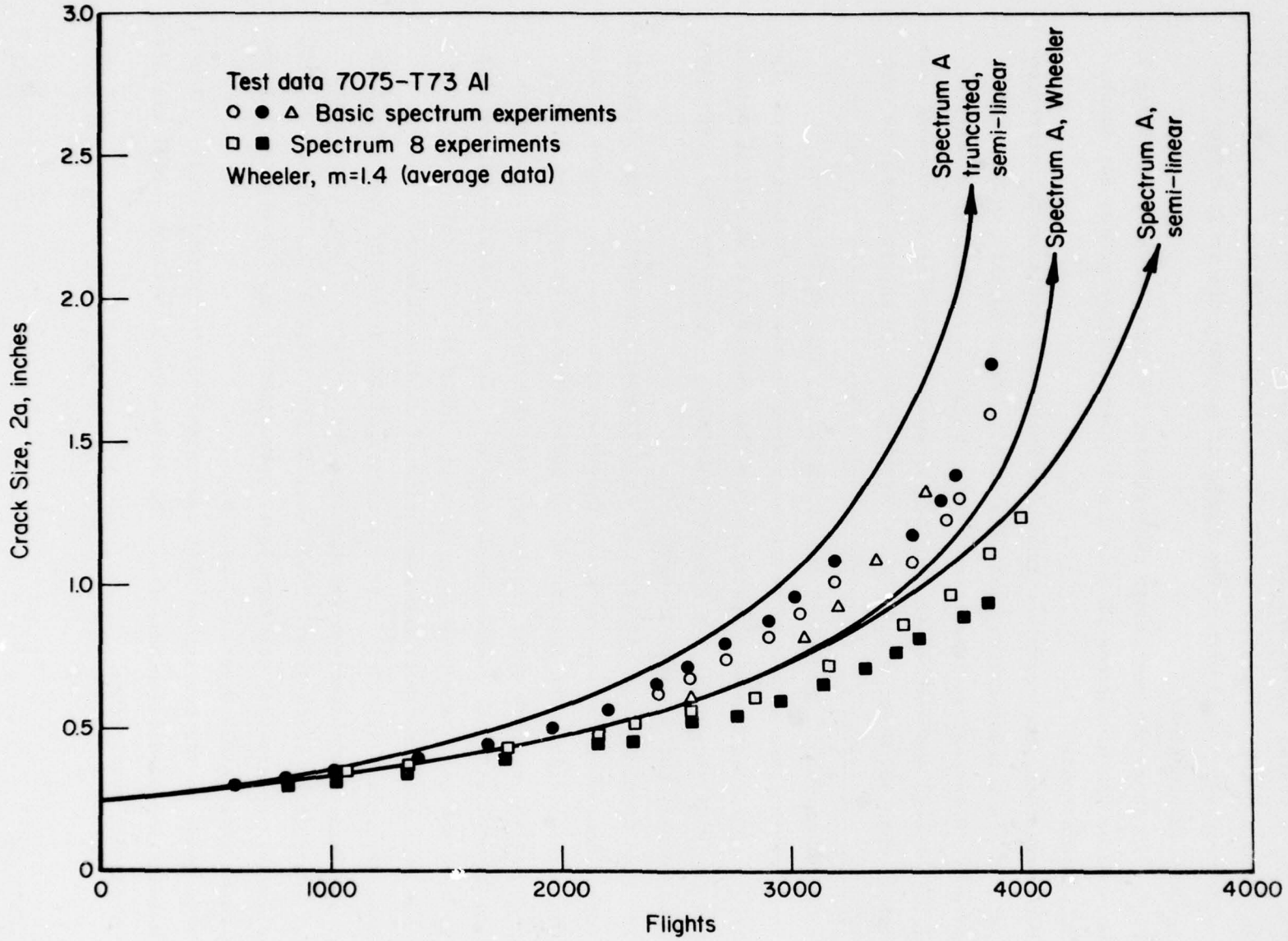

FIGURE 25. COMPARISON OF BASIC SPECTRUM WITH SPECTRUM A ON THE BASIS OF SEMILINEAR ANALYSIS

5.2 Spectrum Shape and Severity

The effects of spectrum shape and severity are demonstrated in Figures 26 and 27 for 7075-T73. The results for Ti-6Al-4V showed the same trends and are included in the statistics discussed in the previous sections.

An attempt to explain the different behaviors is considered a fruitless exercise. A comparison of computed and experimental results shows the remarkable accuracy by which the calculations reproduce the test data when the models are properly adjusted. As can be seen from Figures 21 and 22, this conclusion also holds for the semilinear analysis.

In addition, crack-growth curves were calculated for the gust spectrum data for 7075-T6 and 2024-T3 as reported by Schijve[12]. The Wheeler model was used with a retardation exponent of m = 1.4. The Willenborg model was also applied. The results are shown in Figure 28. The calculated curves are in reasonable agreement with test data for 2024-T3, but a poor correlation for 7075-T6. However, it should be noted that the test data for 7075-T6 seem to be anomalous. Apparently, it is necessary to readjust the models for such a different spectrum and different materials. (Note that in this case, the Willenborg model corresponds with Wheeler using $m \approx 1.5$ for 2024-T3.)

It is therefore concluded that the proposed computational model, adjusted on an experimental basis, can predict a wide range of variations in crack growth when slight changes are made in the spectrum, even if these would cause large changes in crack-growth behavior.

5.3 Effect of Design Stress

The stress levels associated with the various levels of the staircase approximation of the spectra were expressed as a fraction of the stress at limit load (Tables 1 through 5, Figures 1 through 4). In most of the experiments, the stress at limit load was 33.6 ksi for 7075-T73 and 65 ksi for Ti-6Al-4V. The effect on crack propagation of various design stress levels (stress at limit load) was studied on the basis of Spectrum B. Changes in stress at limit load are reflected in proportional variations in all the stress levels of the staircase approximation. Such variations would be associated with different locations in a wing and, of course, with a change in design allowables.

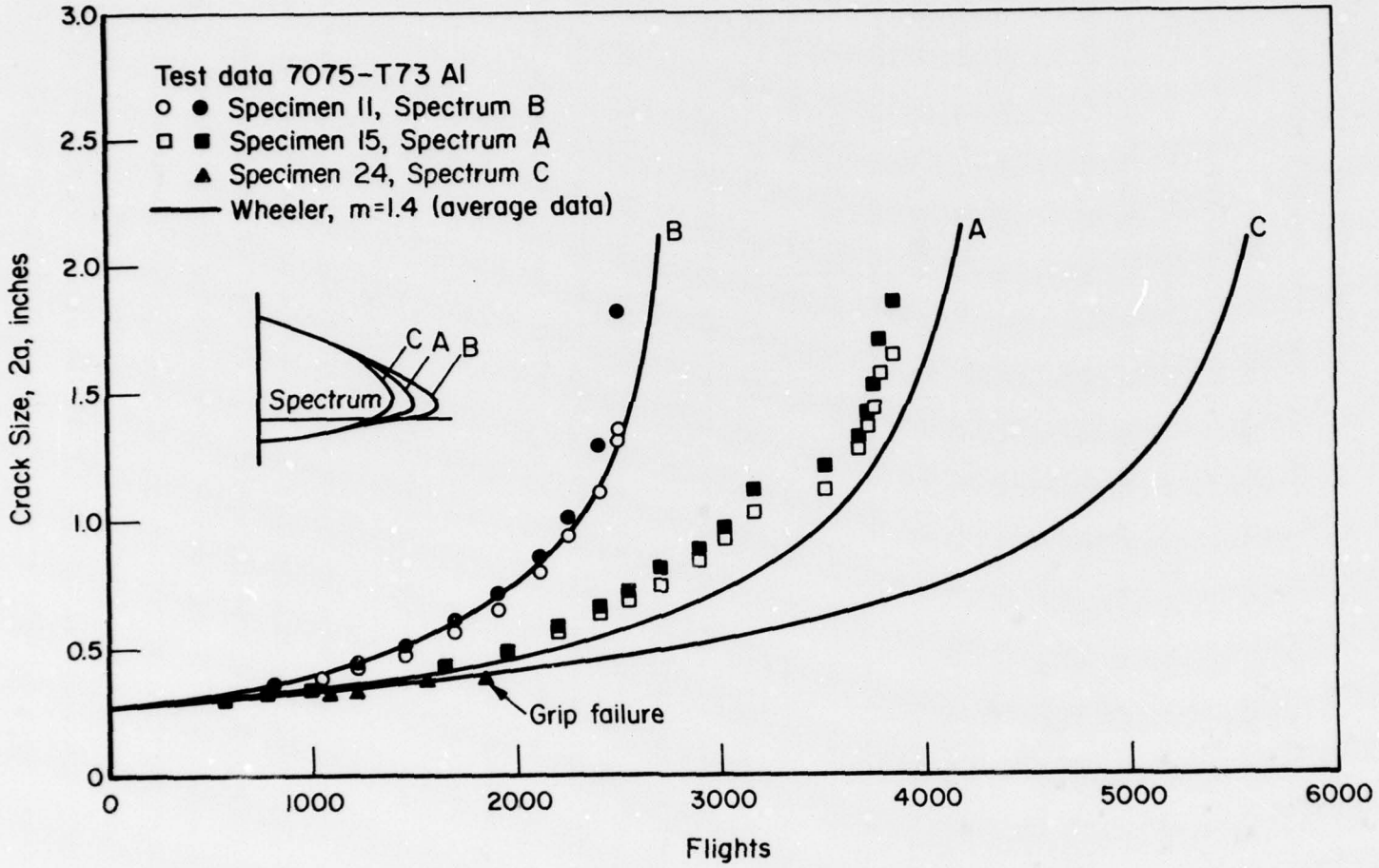

FIGURE 26. CRACK PROPOGATION AS AFFECTED BY SPECTRUM SHAPE IN 7075-T73

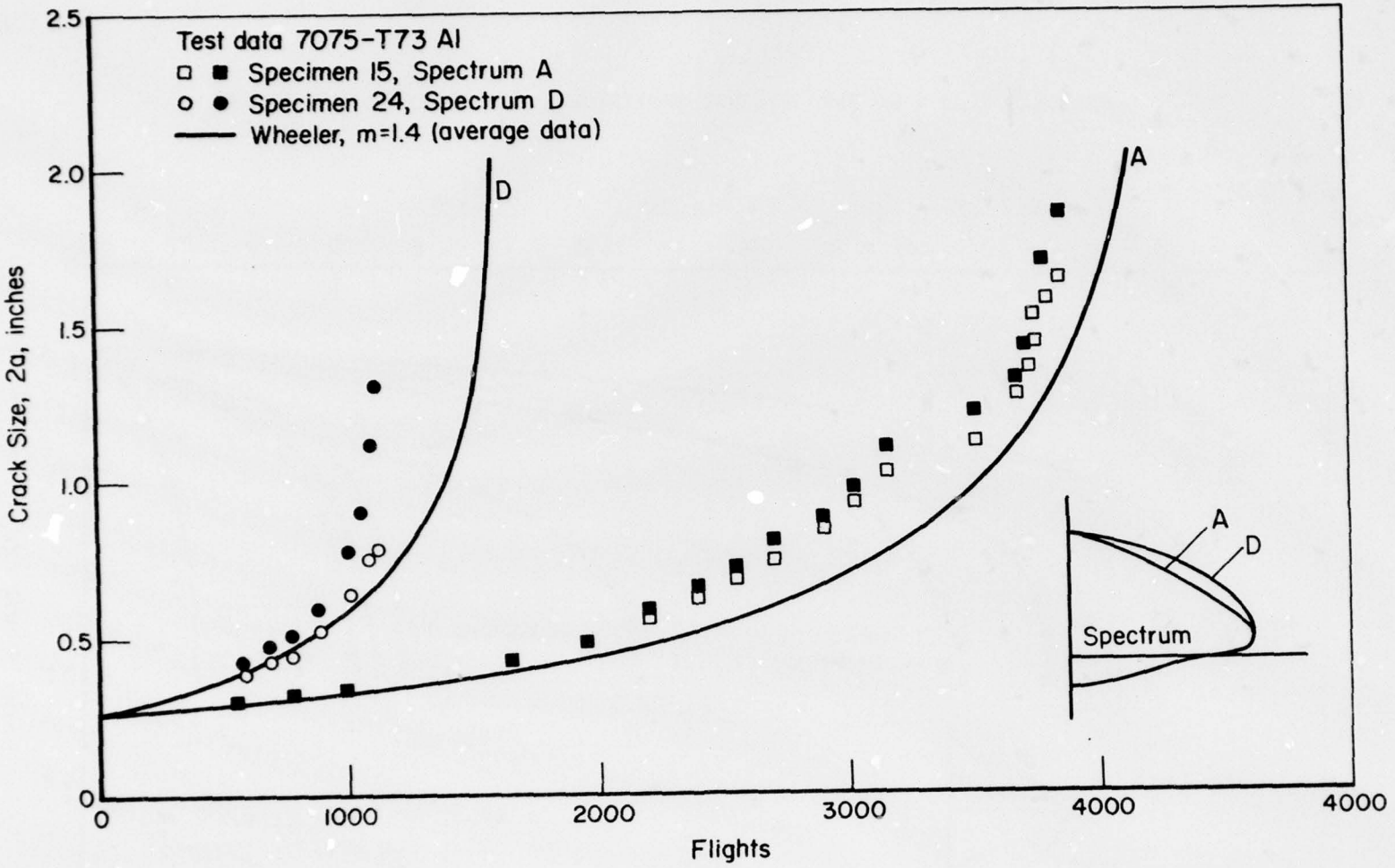

FIGURE 27. CRACK PROPAGATION AS AFFECTED BY SPECTRUM SEVERITY IN 7075-T73

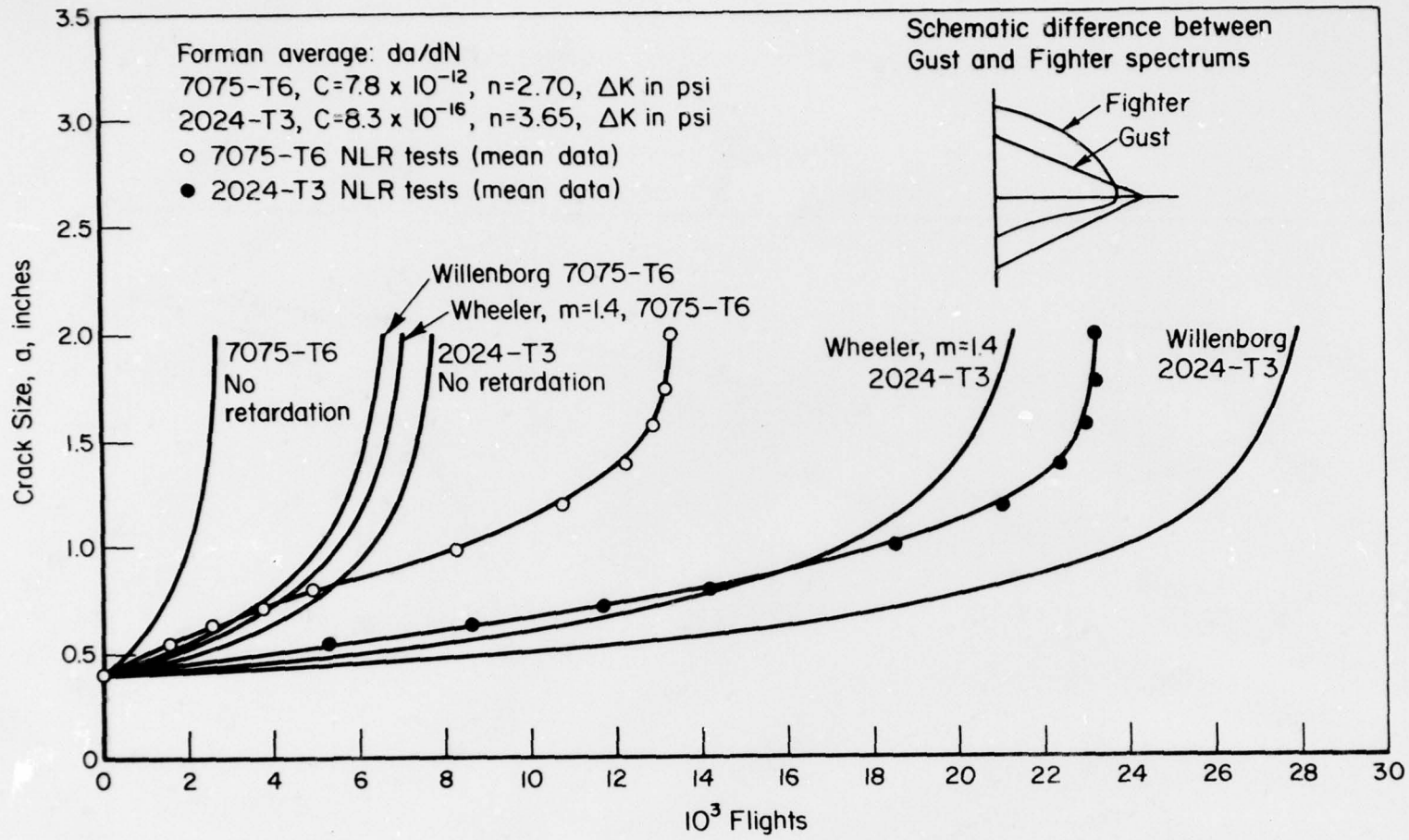

FIGURE 28. CRACK-GROWTH PREDICTIONS FOR THE CASE OF A GUST SPECTRUM

The experimental data and computational results are presented in Figure 29 for Ti-6Al-4V and in Figure 30 for 7075-T73. Again, the computations yielded a reasonably close reproduction of the test data. The results for 7075-T73 appear to be less than ideal; however, it can be seen that the results are acceptable when the crack-growth life is plotted as a function of design stress (Figures 31, and 32).

The computational data constitute a smooth curve in Figures 31 and 32. For physical reasons, one would expect the test data to fall on a smooth curve as well. This is indeed the case for Ti-6Al-4V (Figure 31), but is not true for 7075-T73 (Figure 32). Thus, the discrepancies between the computed and the experimental data may be caused by the erratic behavior of the material, rather than by the computation.

This result emphasizes the scatter in material behavior. Since the computational schemes do not take scatter into account, the calculations are not necessarily deficient if the experimental data are not always exactly reproduced. The apparent inaccuracy of a calculated crack-growth curve is largely due to variability in material behavior.

Included in Figures 31 and 32 are the results obtained with the Willenborg model and with other values of m in the Wheeler model, both for average and upper bound data. These curves give some indication of the effect to be expected from variations in material properties, since they could be visualized as the result of changing material properties.

Finally, Figure 32 also presents a curve for the basic spectrum. This curve was computed with the semilinear model. There is only one experimental data point, since 33.6 ksi was the only limit-load stress level covered by the experiments with the basic spectra. Therefore, a Wheeler curve was calculated for a stress level of 37 ksi; represented by the data point at the top of the curve. This result illustrates that semilinear analysis can be particularly useful for a quick assessment in the early design stage when sophisticated calculations are not really necessary in view of the many unknowns.

6. GENERALIZATION

Accurate prediction of crack growth in center-cracked panels does not automatically ensure reliable predictions of crack growth in complex structural geometries. Proof is required that the computational schemes can be generalized. Therefore, a few cases of structural cracks were considered in this program.

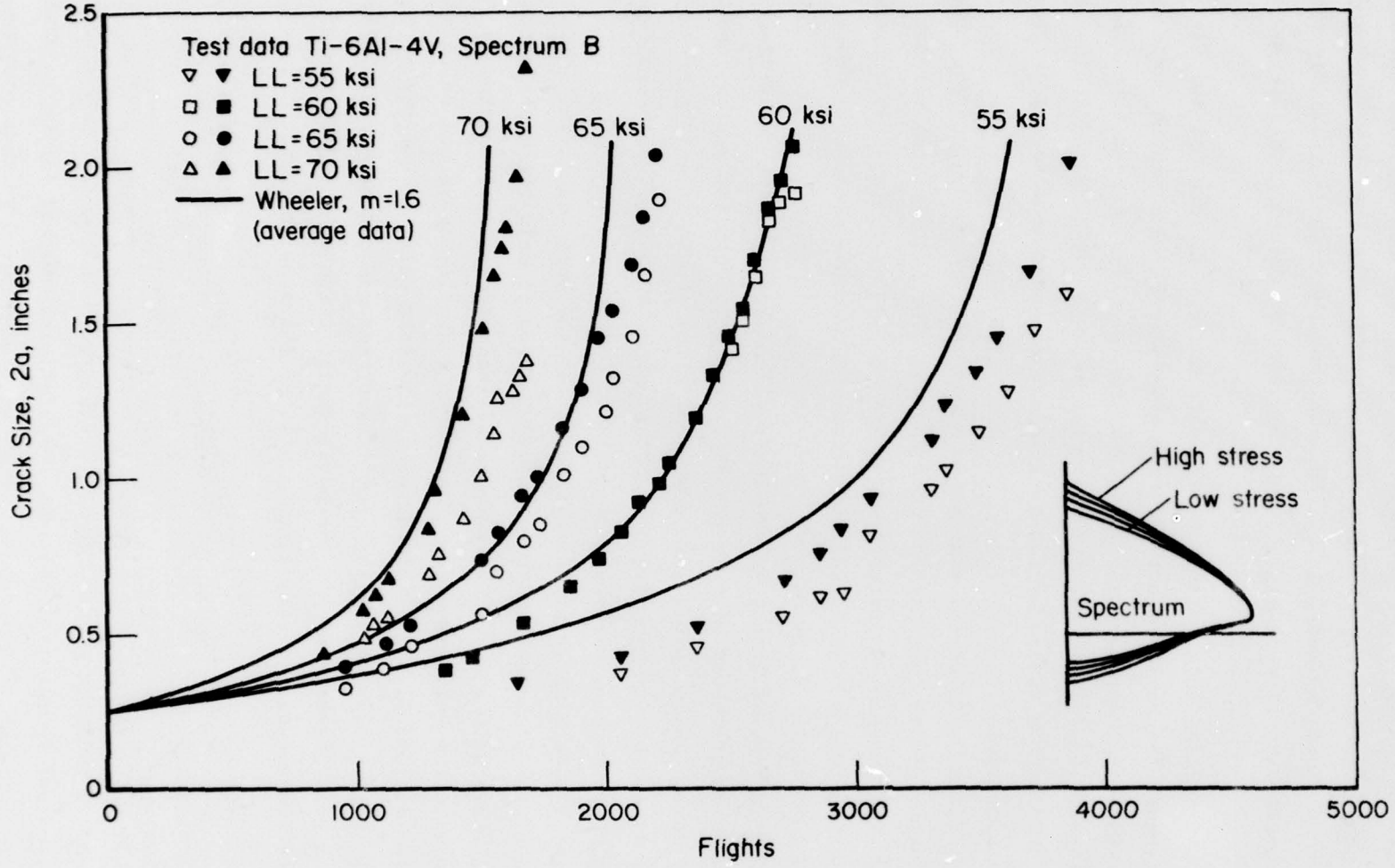

FIGURE 29. CRACK PROPAGATION AS AFFECTED BY DESIGN STRESS LEVEL IN Ti-6Al-4V

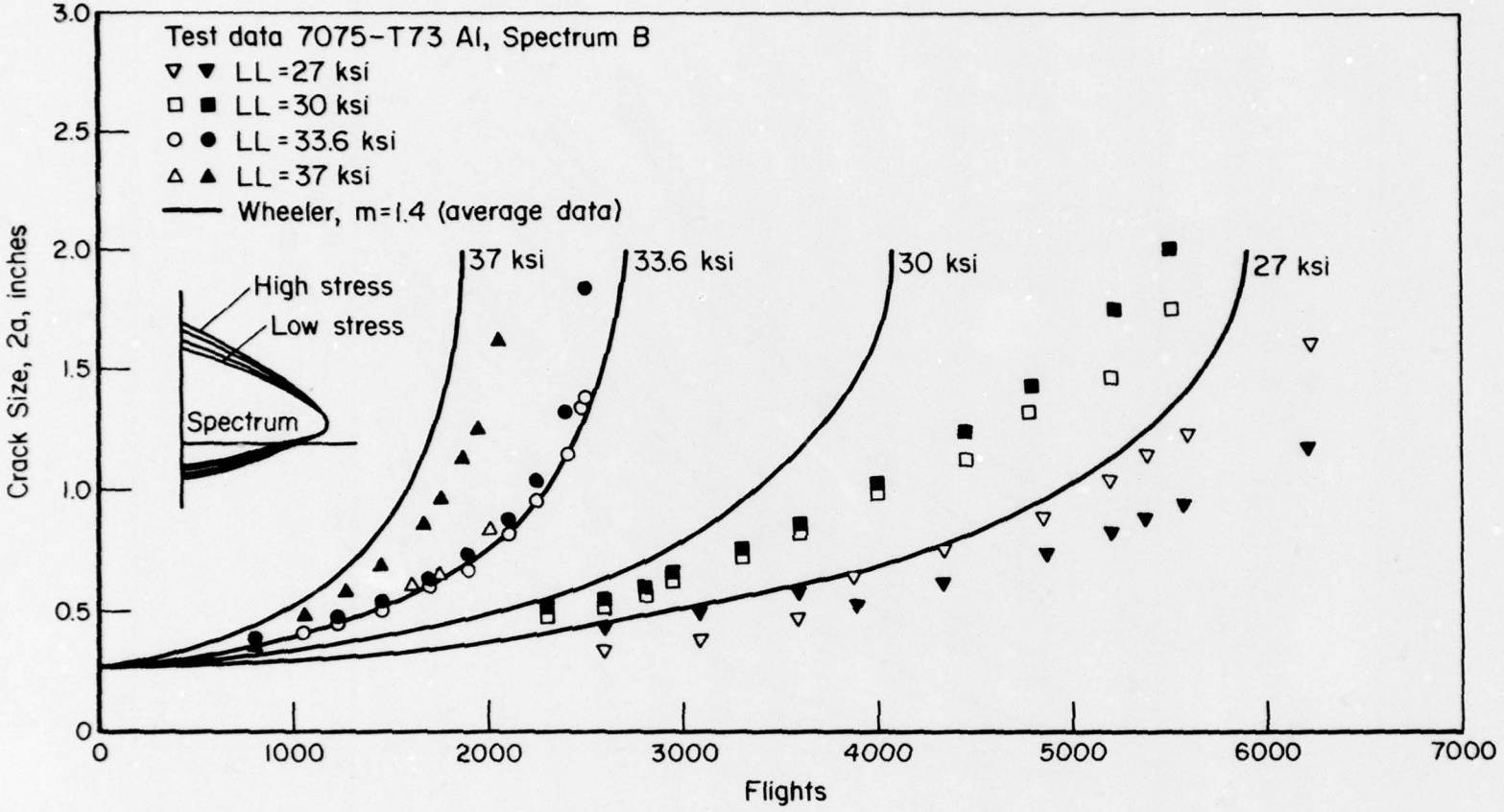

FIGURE 30. CRACK PROPAGATION AS AFFECTED BY DESIGN STRESS LEVEL IN 7075-T73

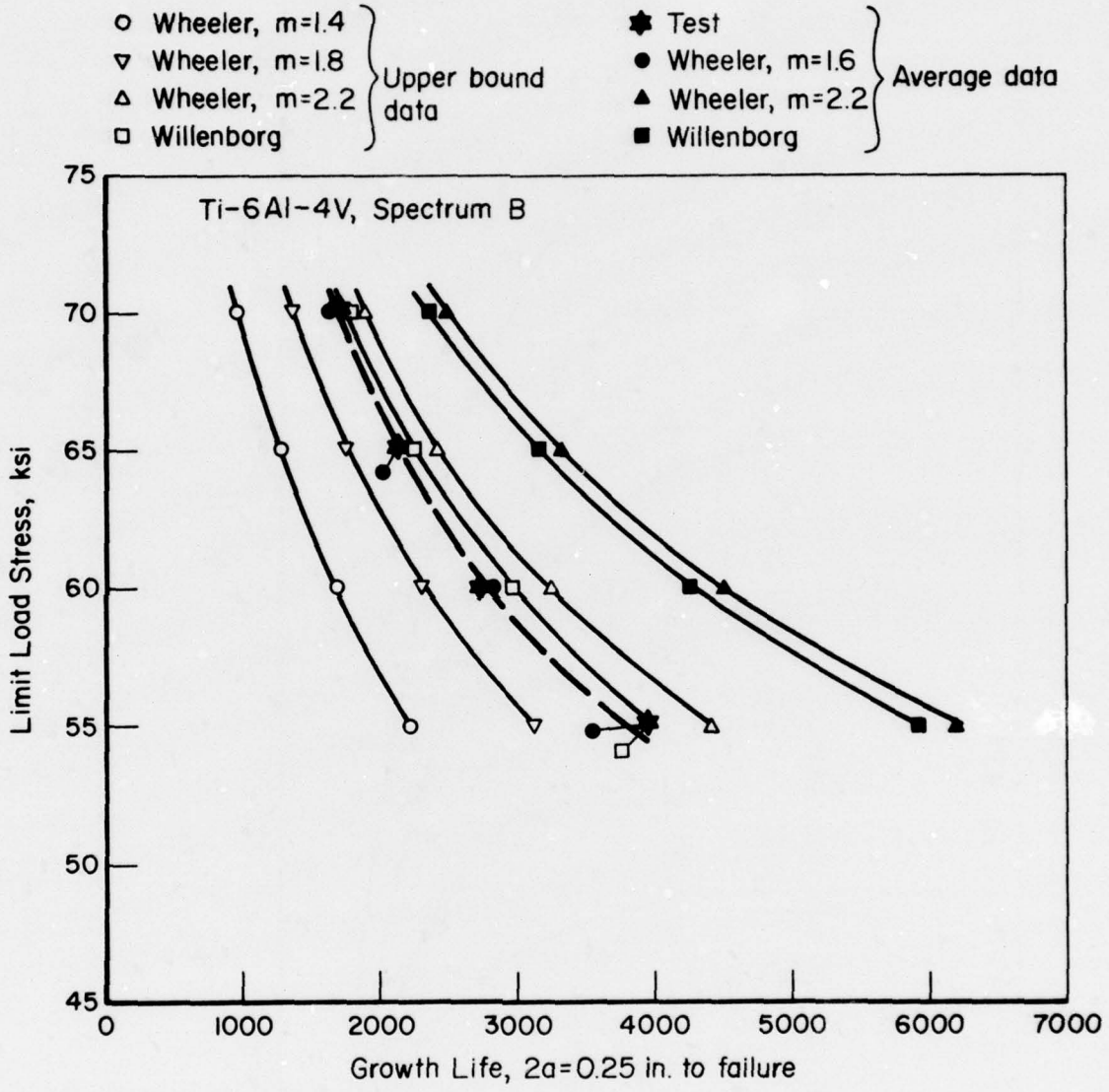

FIGURE 31. EFFECT OF DESIGN STRESS (LIMIT LOAD STRESS) ON CRACK-GROWTH LIFE (Ti-6Al-4V, SPECTRUM B)

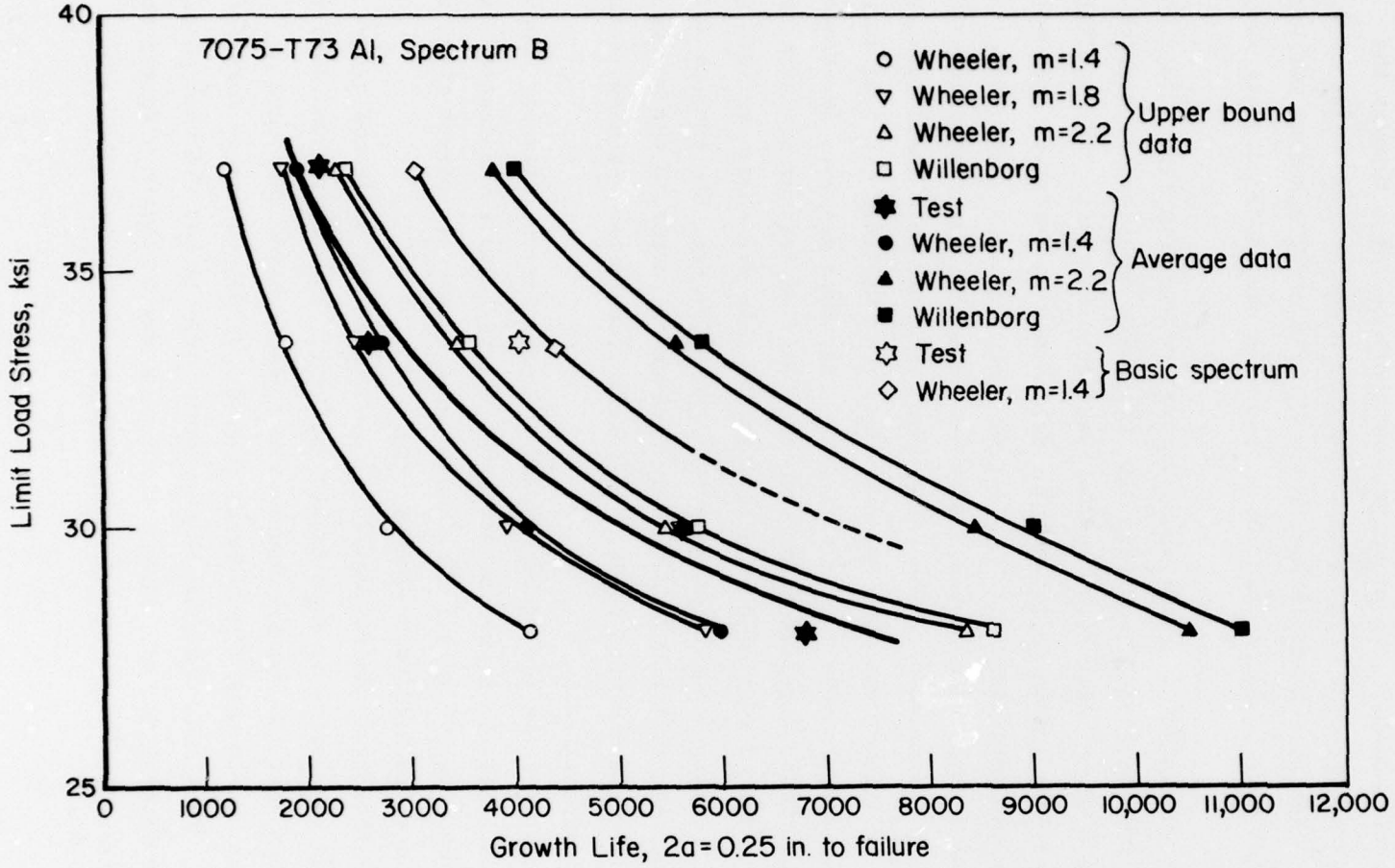

FIGURE 32. EFFECT OF DESIGN STRESS (LIMIT LOAD STRESS) ON CRACK-GROWTH LIFE (7075-T73 Al, SPECTRUM B)

The most common case of a structural crack is a crack at a hole. Two experiments were performed on 7075-T73 specimens 0.5-inch thick. One specimen contained two holes of 0.2-inch diameter, each hole having a through-the-thickness crack at one side. The second specimen contained two holes of 0.5-inch diameter, each with a single corner crack. The basic spectrum was applied, but computations were based on Spectrum A, since it was shown adequate for previous cases.

Test data and computed crack-growth curves are shown in Figure 33. The curves result from semilinear analysis with the Bowie solution for a crack at a hole. Table 6 gives information on the baseline data used. The test data and the calculations appear to reflect the difference in K-history both between these and previous specimens.

The second case considered was a crack under a stringer reinforcement (Specimen Type c in Figure 6). The tests were performed at a limit load stress of 28.8 ksi. An attempt was made to derive the load transfer (skin to stringer) by strain gauge measurements on the stringers. For this purpose, 14 strain gauges were mounted on the stringers, one between each pair of fasteners. Unfortunately, the stringer contained such high bending stresses that the amount of load transfer could not be satisfactorily established. Nevertheless, the results were used to estimate the fastener loads and the reduction factor to the stress intensity caused by the fastener loads. This reduction factor was used in the crack-growth computations.

The calculated crack-growth curves and the experimental data are shown in Figure 34. The insert on Figure 34 shows the stress-intensity-reduction factor, β, as a function of crack size. The dashed curve shows what effect this reduction had on the calculated crack-growth life.

Since the four experimental curves are so close, the predicted curves are clearly outside the regime of experimental scatter. This conclusion does not necessarily mean that the computational scheme cannot cover this case of structural scatter; it more likely means that the stress-intensity formulation is unreliable. Thus, the computed crack-growth curve is not the best possible prediction for this situation. Such a prediction would require a formal stress-intensity analysis of the stiffened panel with one of the available procedures[2,8,10].

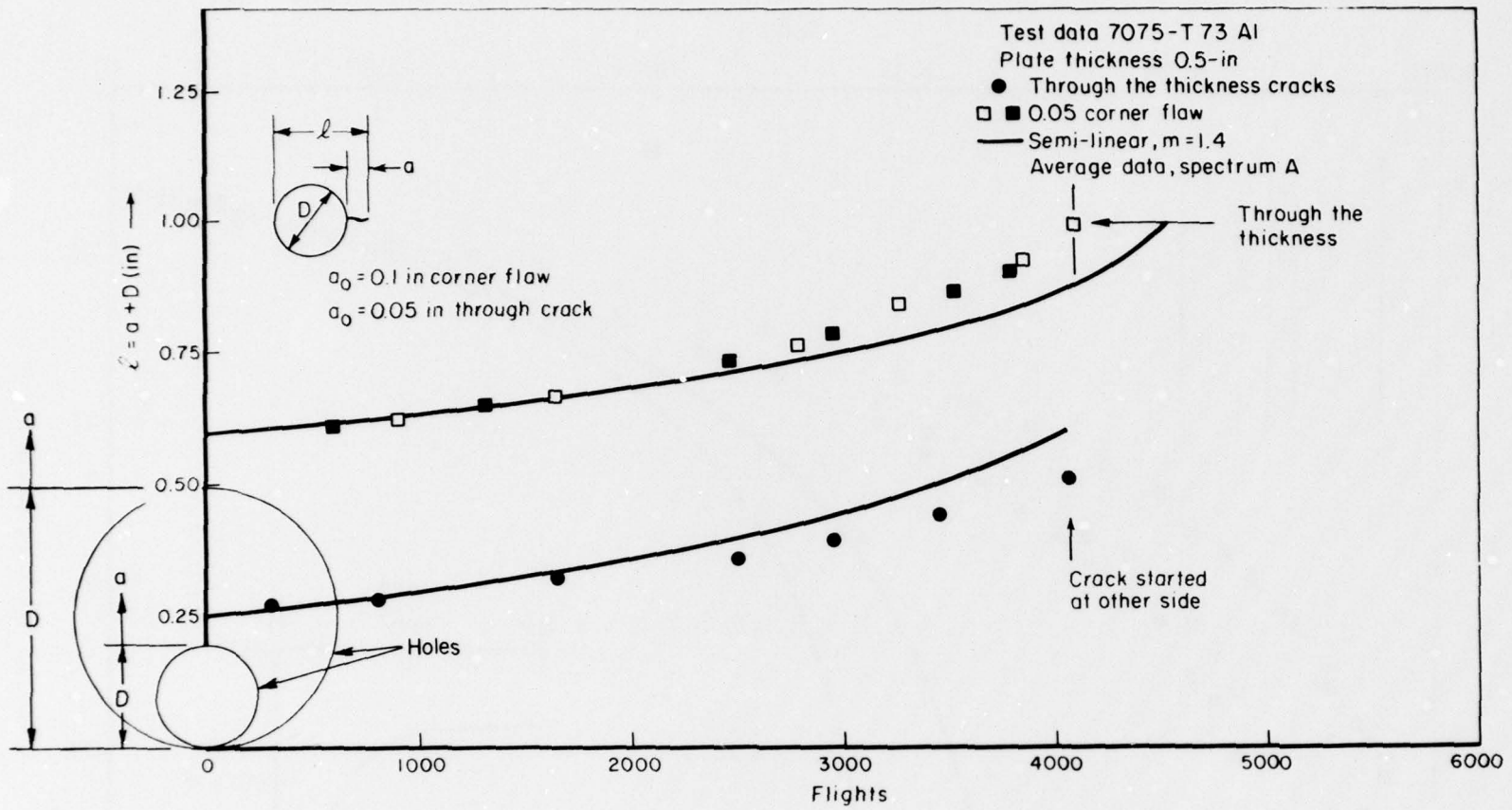

FIGURE 33. CRACKS AT HOLES IN 7075-T73 UNDER BASIC SPECTRUM

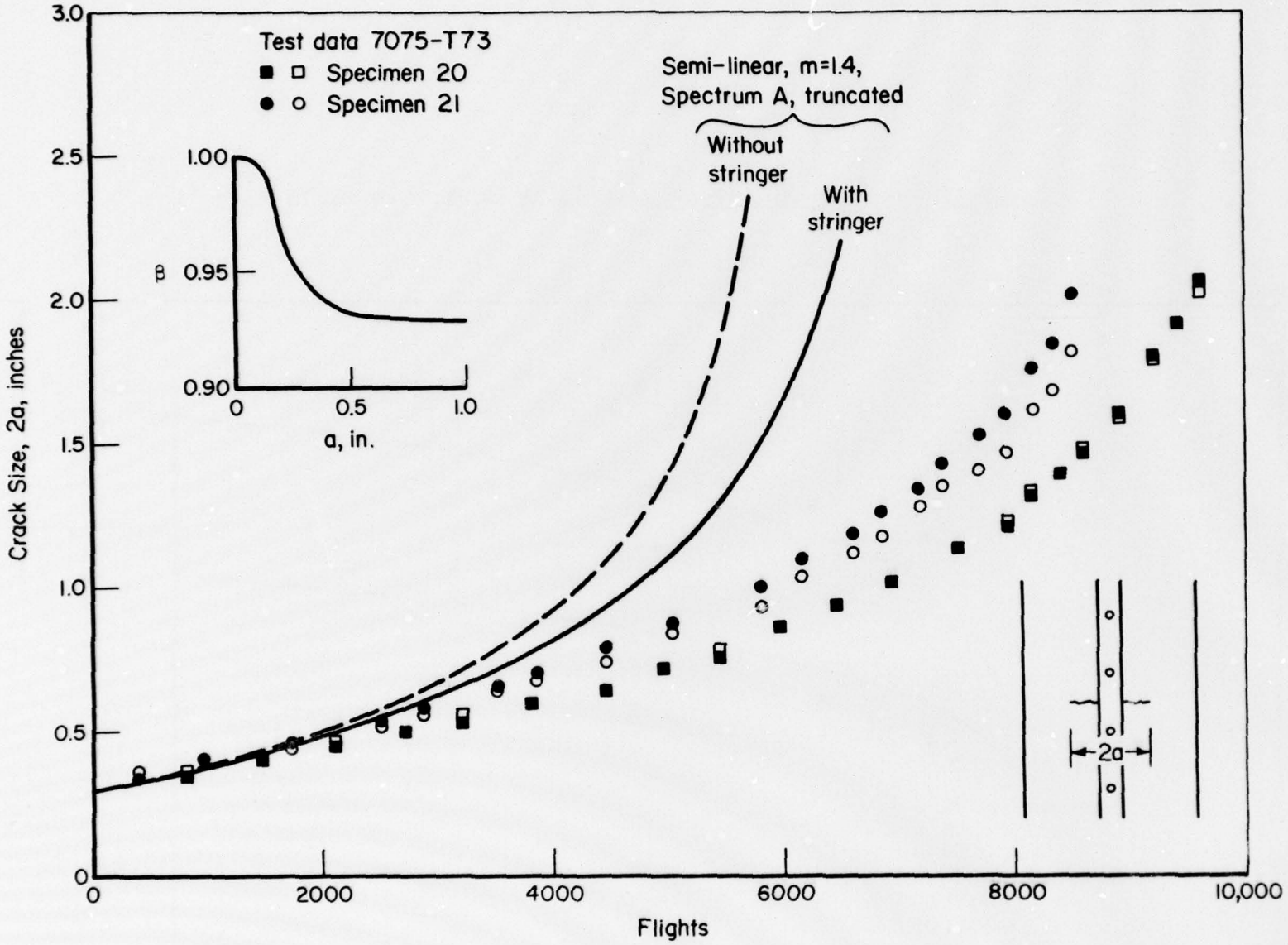

FIGURE 34. CRACK GROWTH IN STIFFENED PANELS

Therefore, on the basis of Figure 33, it is reasonable to conclude that a computational scheme can be developed for crack-growth prediction in all cases of structural cracking. Further, systematic analysis is recommended to prove the generality of the procedure. However, it is emphasized that even a perfect computational scheme cannot give reliable prediction if the stress-intensity formulations are inadequate. (Crack-growth rates depend on K to the 3rd or 4th power.)

7. THE ACCURACY OF CRACK-GROWTH PREDICTIONS

7.1 Scope

The purpose of this research program was to establish how and where to apply safety factors to crack-growth predictions. No attempt will be made to suggest the magnitude of such safety factors, since that is the responsibility of aircraft safety authorities. However, the results of this study do provide guidelines for determining safety factors.

The question of how and where to apply the safety factor will be addressed in Section 8 of this report. In order to deal with that problem, the accuracy of crack-growth predictions must be reviewed. The accuracy of predictions should not be judged on the basis of integration models alone since the reliability of prediction depends on four factors:

(1) Integration models and computational schemes

(2) Material behavior

(3) Stress-intensity factors

(4) Spectrum generation.

Since the first three items are closely related, they will be discussed as a group in Section 7.2. The last item will be discussed in Section 7.3. A summary of the discussion will be presented in Section 7.4.

7.2 Cracks

Using a well-adjusted crack-growth model, experimental data can be predicted within about 20 percent, regardless of material and spectrum. Other crack-growth models can probably be used also, since there appears to be a

constant factor between the rate predictions, independent of crack size (Figure 19).

Clearly, the discrepancies reflect both the inaccuracies in the computational model as well as the variations in material behavior. The scatter around the average baseline data is obvious from Figure 9. The variations in growth under spectrum loading (as particularly shown in Figures 23 and 32 are most likely caused by these same material variations. However, the test data were considered unique when the accuracy of the computed curves was examined. Thus, the variations in material behavior are included in the percent of deviation.

Generally speaking, the actual life will still be within 20 percent of the life predicted by a well-adjusted model, regardless of the size of the crack-growth increment. For a statistical treatment, the values of the standard deviation in Table 6 can be used. It would be a useful endeavor to bound the predicted lives from baseline data for various levels of probability in order to obtain more rigorous figures. However, 20 percent is adequate for the present discussion.

Modern stress analyses with either analytical or finite-element techniques provide very accurate stress-intensity factors. Although the accuracy may not be equally high at all crack sizes, it seems safe to assume that the calculated stress intensity will be within 10 percent. Though this percentage can never be fully verified, figures quoted in the literature for simple cases are often as low as 2 or 3 percent. Nevertheless, a detailed substantiation for more complex cases is recommended.

Assuming an average third-power dependence on K, the inaccuracies in the stress-intensity factor may cause deviations of $(1.1)^3 = 1.33$ in the computed crack-growth curves. If the anomalies due to the computational scheme and to material behavior (20 percent) would be of the same sign as those due to inaccuracies in K, the total deviation could be $1.2 \times 1.33 = 1.66$. Thus, the actual crack-growth life would be between 0.60 and 1.7 times the predicted life, regardless of material, spectrum, and crack-growth increment. In most cases, the prediction will be closer.

Naturally, these figures are approximate. A rigorous statistical analysis would be required to determine these bounds more precisely. However, these approximate numbers provide some insight to the adequacy of crack-growth predictions.

7.3 Spectra

Establishing a spectrum for a new airplane is a difficult task, involving much guesswork. Yet the spectrum shape is of paramount importance: a slight deviation in spectrum shape can easily cause a difference of a factor of 2 in crack-growth life, as can be seen in Figures 26 and 27.

The conversion of the load spectrum into a stress spectrum is also very critical. An inaccuracy in the estimated stress level at a given location can easily yield a difference of 50 percent in crack-growth life, as shown in Figures 30 and 31. (A third-power dependence on K would yield a 70 percent deviation; however, this disregards retardation effects.)

Thus, crack-growth predictions in the design stage could be a factor of $2.0 \times 1.5 = 3$ in error, due to inaccuracies in the stress spectrum. This proves the significance of in-flight measurement of the stress spectrum (rather than the load spectrum) as soon as test flying commences. It is reassuring that all crack-growth calculations can be repeated with the actual flight spectrum, and do not require additional tests. Hence, crack-growth information can be updated reliably both during test flying and later when service load information becomes available.

Only minor significance should be attached to the stress history (sequence) within one spectrum. It was shown that the Basic Spectrum and Spectrum A (actually two different stress histories with the same spectrum) produced the same crack-growth behavior. It was also shown that a spectrum can be represented with about 10 positive stress levels. Therefore, it seems more practical for computing and testing efficiency to select a spectrum approximation and load sequence as used here for Spectra A through D. Moreover, the flight-by-flight type of loading is more realistic, and is not overly sophisticated. Block sizes of 100 flights seem to be adequate.

The problem of the clipping level still needs to be addressed. Clipping is the reduction of the highest load level(s) to the next highest. For example, in Table 1, clipping level 1 means that level 2 would occur 3 times instead of 2 times; no cycles would be omitted. Clipping levels 1 and 2 means that level 3 would occur 10 times instead of 7 times, but levels 1 and 2 would not occur.

The effect of clipping on crack growth is demonstrated by Figure 35. These are computational results[10] for four completely different spectra, and test

Symbol		Spectrum	Linear Analysis (Flights)
a	▲ Willenborg △ Wheeler, 2.3	Fighter	270
b	● Willenborg ○ Wheeler, 2.3	Trainer	460
c	■ Willenborg □ Wheeler, 2.3	B-1 class bomber	140
d	▼ Willenborg ▽ Wheeler, 2.3	C-transport	1270

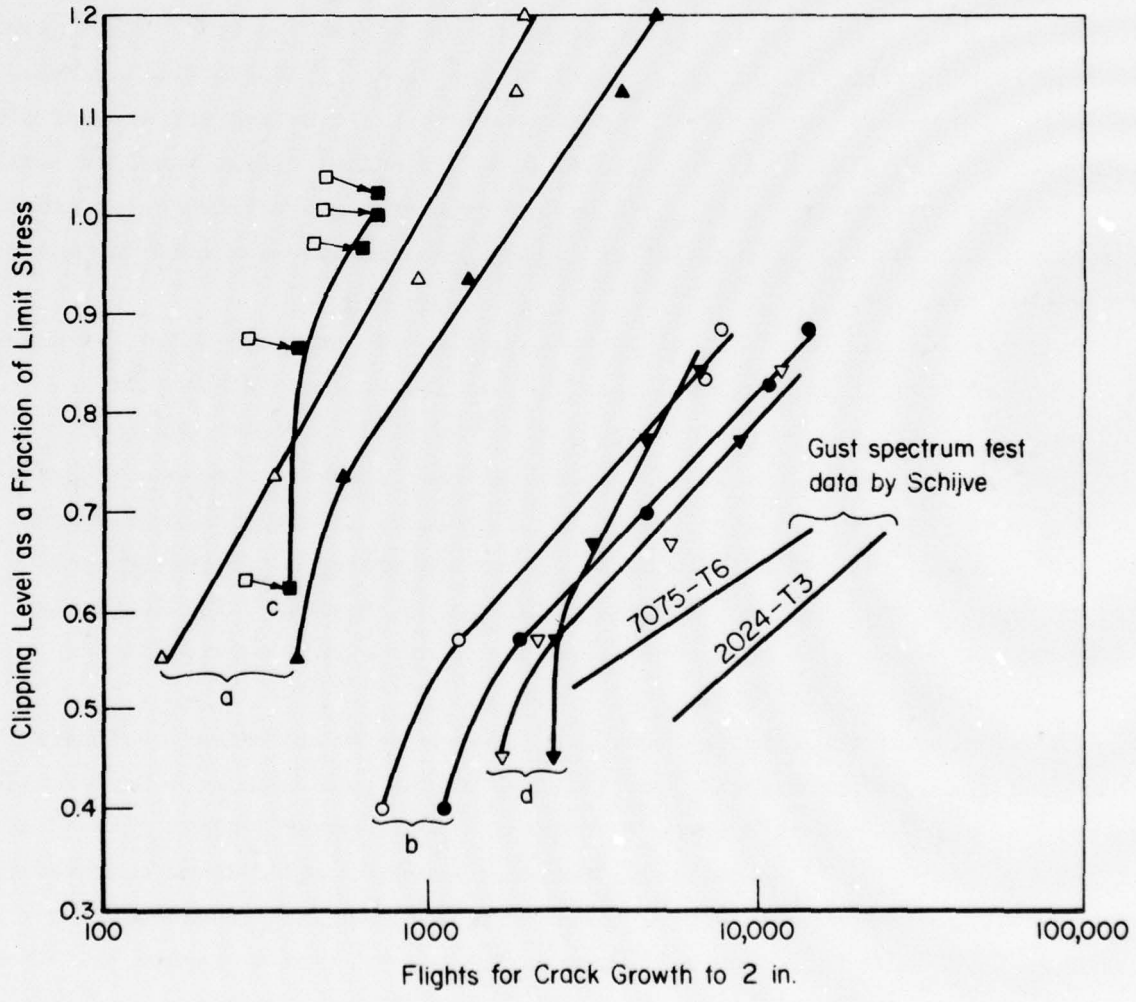

FIGURE 35. EFFECT OF CLIPPING FOR VARIOUS SPECTRA

data[12] for a gust spectrum. They show that the suggested clipping of the top levels of Spectrum A (1.04 and 0.92) could cause a reduction of almost 50 percent in crack-growth life (see fighter spectrum in Figure 35).

The argument is often heard that clipping is unrealistic and that all load levels should be included that actually occur in service. The latter part of this argument is crucial; if they indeed occur, they should be included. However, whether they will occur is questionable. The spectrum is only a conjecture or, at best, an interpretation of measured data. Slight inaccuracies of the spectrum are unimportant in the lower part, but are very significant in the upper part. The high load that is anticipated once in an aircraft life may or may not occur. The load expected to occur 10 times per aircraft life may be experienced 20 times by one aircraft and never by another. A pilot flying Mission Ia of Spectrum A may pull 7 g; he may also leave it at 6.5 g.

Clipping of the spectrum should be a factor for serious consideration in assessing the usefulness of crack-growth predictions. It is not difficult to show adequate life if high enough loads are included. Sensitivity studies of the type illustrated in Figure 35 should complement crack-growth predictions, so that possible deviations from the average can be evaluated. Semilinear analysis is a useful vehicle for such studies.

7.4 Summary

It was shown in the previous sections that the prediction of crack-growth per se can be expected to be within a deviation factor of 1.6. In the design stage, inaccuracies in the spectrum can cause discrepancies of at least the same magnitude and probably more. Thus, the actual crack-growth life in service can be anywhere from 0.4 to 2.5 times the predicted life in the design stage. (The numbers quoted give the order of magnitude only.) In the later stages, when accurate stress spectrum data have been collected from flight measurements, the crack-growth predictions can be updated. The actual crack-growth lives in service are expected to be within approximately 0.6 and 1.6 times the new predictions. Clipping sensitivity should then indicate whether more extreme deviations are likely.

8. SAFETY FACTOR IN DAMAGE-TOLERANCE ANALYSIS

Safety factors are required in a damage-tolerance analysis to account for possible variability due to unknowns, as discussed in the previous sections. A decision has to be made not only on the magnitude of these safety factors but also on how and when they should be applied. Various possibilities exist:

(a) Safety factor on fatigue stresses

(b) Safety factor on baseline data

(c) Safety factor on initial crack size

(d) Safety factor on fail-safe load

(e) Safety factor on final life

(f) Combinations of the above.

These possibilities will be discussed in the following paragraphs. The main criteria for judgment will be the relation with actual crack growth, the generality, and margin of safety.

A safety factor on fatigue stresses is very unattractive because of the complex nature of fatigue and fatigue-crack growth. Calculated crack-growth rates would have no straightforward relation with actual crack growth, and the calculated and actual retardation effects would be different. Thus, the margin of safety would be a variable, dependent upon geometry and spectrum.

A safety factor on baseline data would have similar drawbacks. In the simplest case, a constant factor, e.g., of 2, would be taken, independent of crack size. This means that a crack of a given size would grow twice as fast in the calculation than in reality. Since the plastic zone size at this crack length would not change, retardation would be effective over approximately half the number of cycles. This implies that retardation of a given cycle would also be wrong, so that it would be unclear how much retardation had changed exactly. Stresses of a given magnitude would also occur at different crack sizes than in actuality, i.e., at a different K-level. Thus, their associated growth rate would not simply be increased by a factor of 2, but the increase would depend on the entire previous history. As a consequence, the margin of safety would vary for different stress histories. The margin of safety would also change for cases with different K-crack length relations (e.g., a central crack with increasing K versus a crack at a loaded hole with decreasing, then increasing, K).

The situation would become even more complex if the factor on growth rate would change with different crack sizes. This would occur if upper bound data were taken instead of average data. The margin of safety would again depend upon history, crack geometry, and structural configuration. Moreover, it is difficult to give an unambiguous definition of upper bound data, as discussed in the following paragraphs.

In the plot of the da/dN - ΔK diagram of one constant amplitude test, a few outlying data points will be found. These may have been caused by erroneous measurements, but may also be real if the crack showed a somewhat faster growth locally. The data sets for the next tests will give a few more outlying points; thus causing the scatterband in the da/dN - ΔK plot.

Suppose the scatterband covers a factor of 2 in growth rate. This means that in each experiment there were a few anomalous places where crack growth was twice as fast as normal. These anomalies cannot be found in the total crack growth life (experience shows that the scatter in crack-growth life is far less than a factor of 2). Thus, using the scatterband to determine upper bound data is tacitly assuming anomalous behavior throughout the crack-growth life.

A last possibility would be to take a safety factor on K_c used in the Forman equation. This would affect the high growth rate region more than the low growth rate region (see Figure 36). Therefore, this practice would have the same shortcomings as discussed previously: It would result in a margin of safety depending upon crack configurations, growth increment, and stress history.

A safety factor on initial crack size seems an attractive possibility and needs to be explored. Figure 37 shows computed crack propagation curves for Spectrum A for various crack configurations in plates of different thicknesses. The curves were started at a 0.02-inch initial flaw. For reasons of safety, one might want to increase the initial crack size from 0.02 to 0.05 inch. Then the curves would start at 0.05 inch. How would this affect the margin of safety?

Let the margin of safety be defined as

$$MS = \frac{N_{02}}{N_{05}} - 1$$

where N_{02} is the crack growth life of a 0.02 inch initial flaw to failure and N_{05} is the growth life of a 0.05 inch initial flaw to failure. The ratios

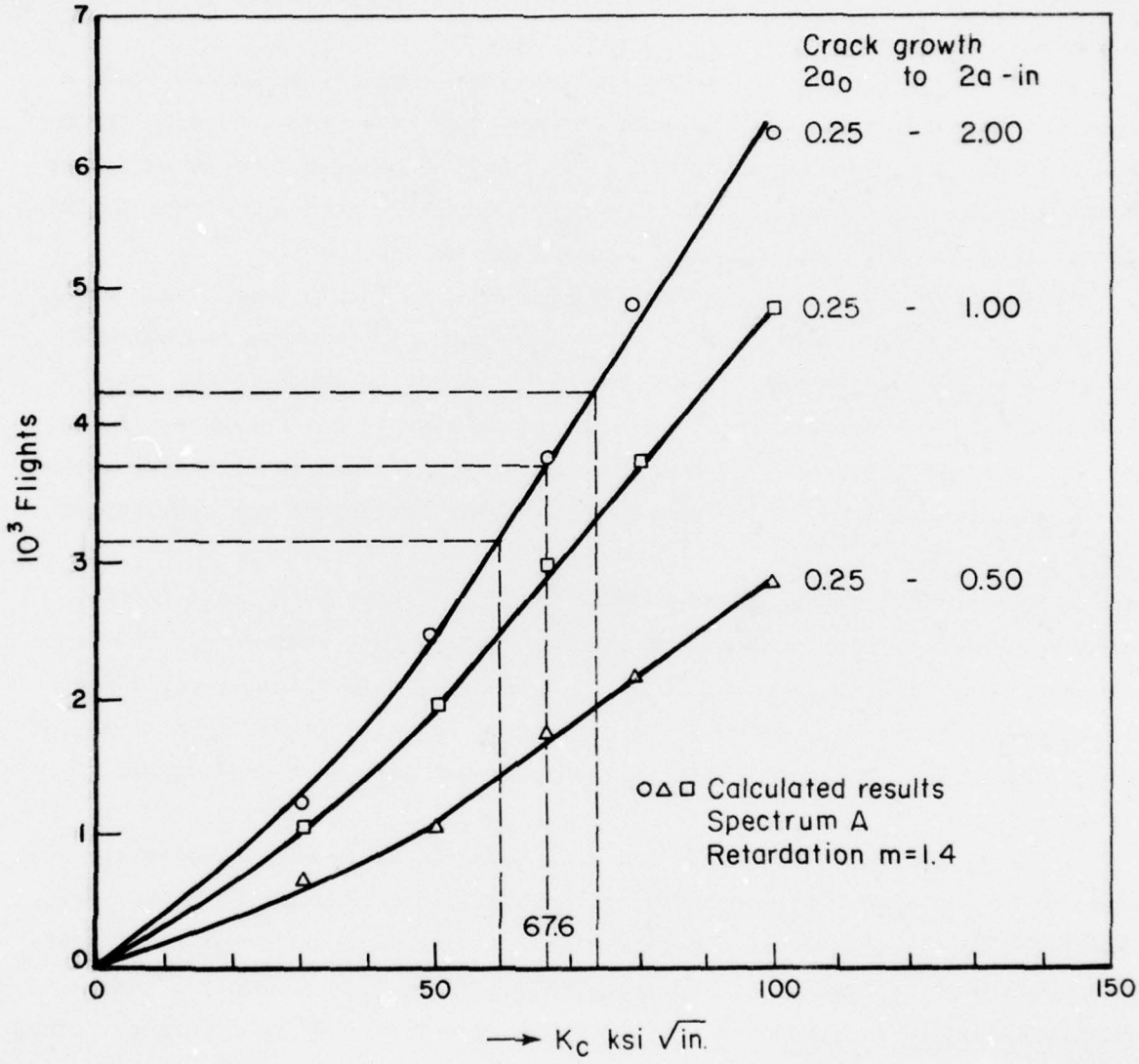

FIGURE 36. EFFECT OF K_C ON PREDICTED CRACK-GROWTH LIFE CALCULATED BY SEMILINEAR ANALYSIS USING FORMAN EQUATION

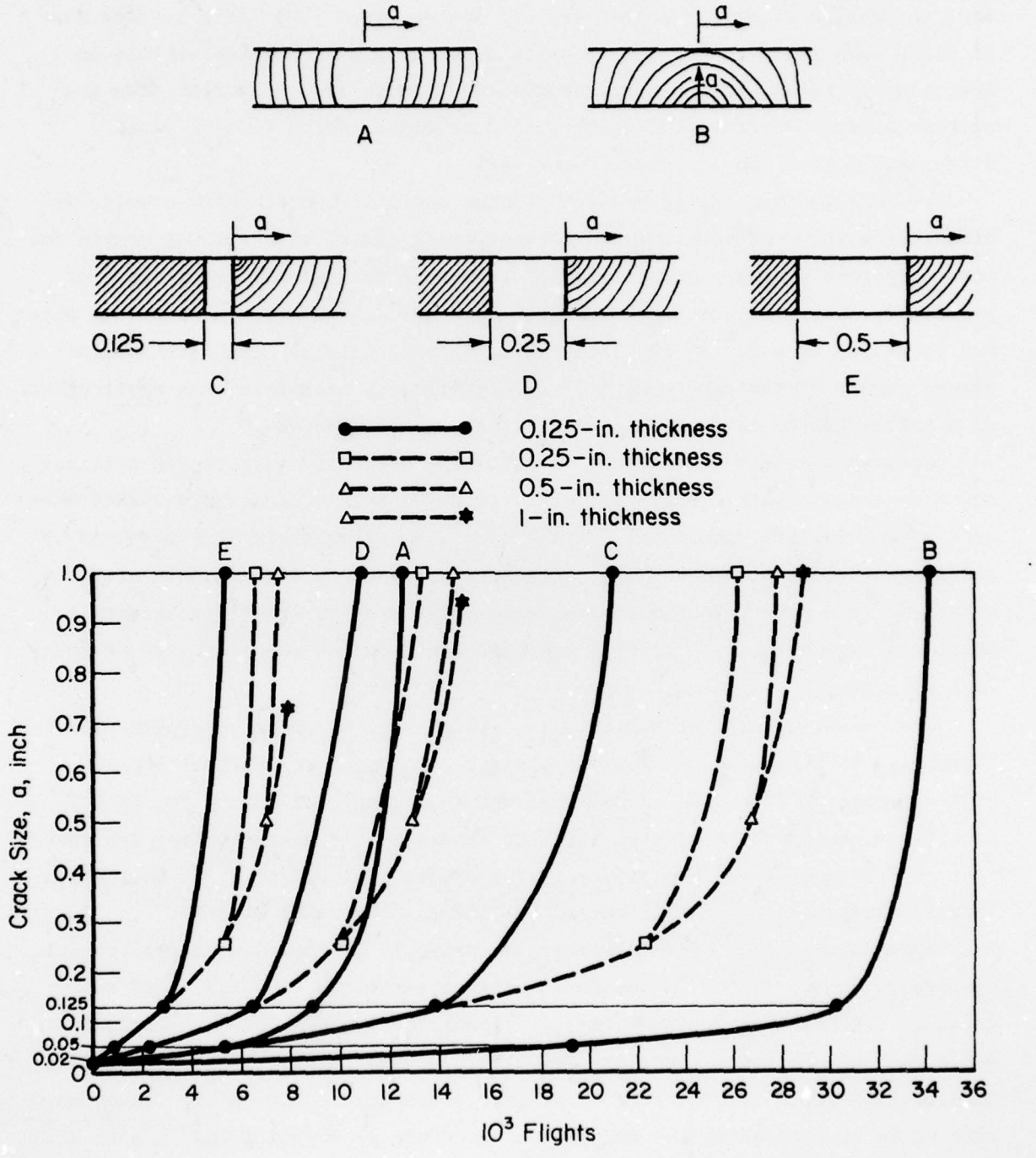

FIGURE 37. CRACK GROWTH FROM .02 AND .05 INCH INITIAL FLAW SIZES FOR VARIOUS CONFIGURATIONS, CALCULATED WITH SEMILINEAR ANALYSIS (SPECTRUM A)

N_{02}/N_{05} were derived from Figure 37 and are plotted in Figure 38. It appears that the margin of safety would vary all the way from 1.25 for a surface flaw in 0.125 inch plate to 0.1 for a corner crack at 0.5-inch diameter hole in 1-inch plate. These varying margins of safety result from different flaw geometries having a different K-crack size dependence, which in turn yield different initial growth rates (Figure 37).

It follows that taking a safety factor on initial crack size results in different margins of safety for different crack cases, with a lower margin for more dangerous cracks. An arbitrary increase of the initial crack size for particular structural configurations results in unknown margins of safety which may be as low as 0.1. By the same token, a fixed initial flaw size does not always result in the same margin of safety either. Therefore, the application of a safety factor to initial crack size should be rejected.

Setting a safety factor for the fail-safe load only affects the critical crack size at failure. Since all crack-growth curves turn sharply upward when approaching failure, the total crack-growth life is only slightly affected by a different fail-safe load. Thus, the margin of safety will be only slightly affected. The safety factor on fail-safe load is of no great consequence to total crack-growth life. It will be necessary from the point of view of residual strength.

The only remaining possibility is a safety factor on crack-growth life. Obviously, it is the most straightforward and most general possibility. A safety factor on life will always give the same margin of safety for life expectancy, independent of structural configuration, crack geometry, and spectrum. When combined with a safety factor on residual strength, it would give approximately the same margin of safety through all phases of life.

Another advantage of this safety factor would be the ease of application. Average crack-growth data — the least ambiguous — could be used. Best estimates of stresses and stress-intensity factors could be made. This report shows that crack-growth lives can be calculated reliably on this basis. (Test results illustrate the reliability of this procedure.) The safety factor on life would be applied at the end of the procedure by dividing the life at all crack sizes by the same factor; this would constitute the "safe" crack-growth curve. The "safety" would be quantifiable.

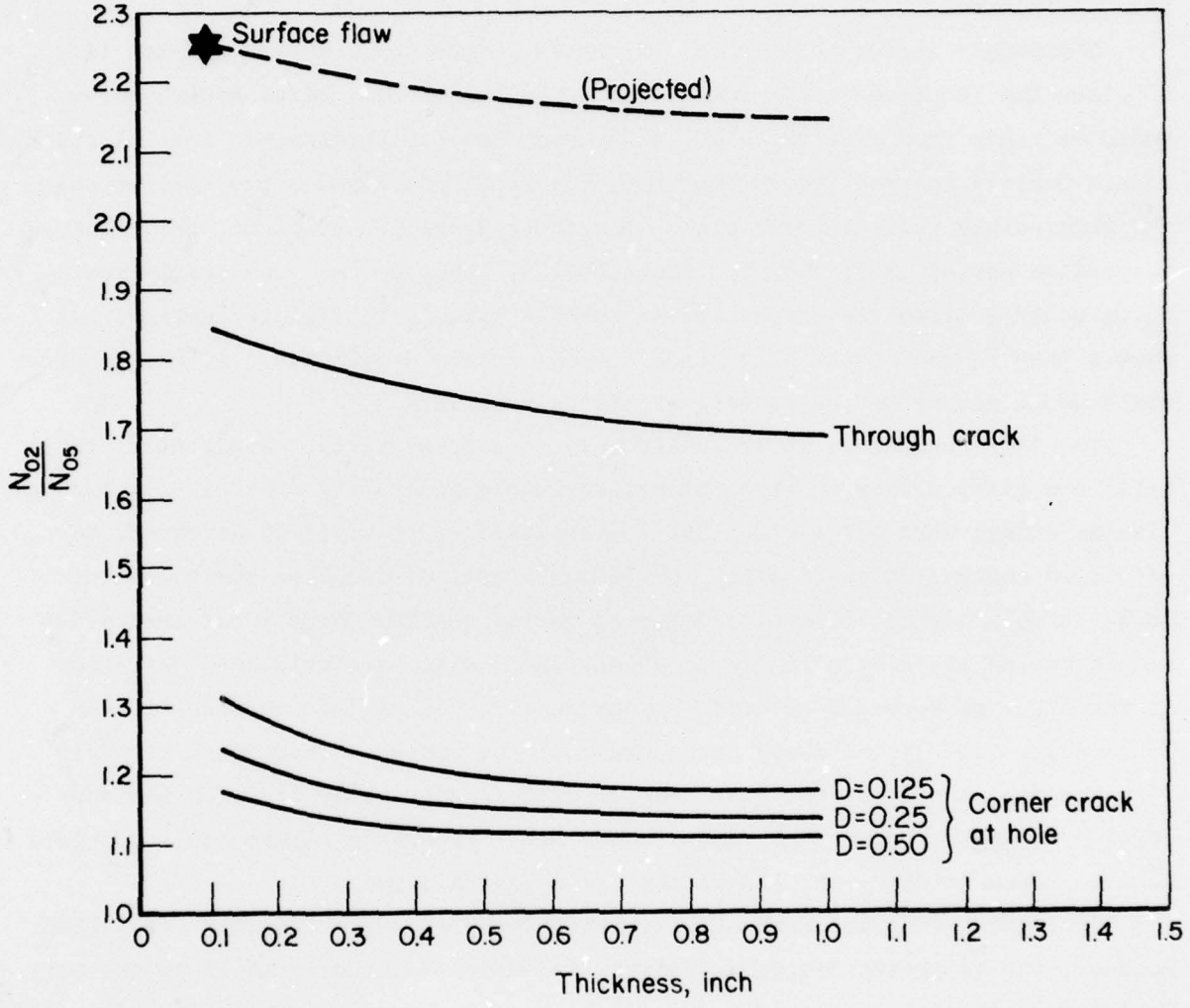

FIGURE 38. RATIO OF CRACK GROWTH LIVES FROM .02 and .05 INCH INITIAL FLAWS TO FAILURE FOR VARIOUS CONFIGURATIONS AS A FUNCTION OF THICKNESS

The possible application of this concept will be briefly considered. The critical location(s) of each component would be determined and the component considered cracked. The critical crack size for failure would be determined. Then, a crack-growth curve would be calculated from an arbitrary small crack size to failure.

The safety factor on life is designated j, and the required service life, L. Thus the required crack-growth life would be jL. The crack-growth curve would be taken from failure to jL, and would show the permissible initial crack size. Quality control should ensure that initial crack sizes are smaller than the permissible initial crack size. For an inspectable structure, the required inspection period is S; thus the required life would be jS. The crack-growth curve would provide the crack size at which a life jS to failure remains. It should then be shown that this crack size is indeed detectable. If the requirements would not be met, a redesign would be necessary.

The above procedure is presented only as a possibility. Admittedly, there still are difficulties in its application mainly in quality control. If the initial damage were not a crack but a sharp defect, it would be necessary to establish equivalent crack sizes for various types of defects. Furthermore, small defects may not always be detected during quality control (or cracks detected during inspections). In addition, there will be statistical variation in the sizes of detected defects. Consequently, the maximum permissible defects determined by the above procedure could be missed. Therefore, it would be necessary to project the distribution of detectable flaw sizes on the factored crack-growth curve. A "safe" upper limit of the detectable defect should then be taken as the lower end of the crack-growth curve.

Obviously, the procedure needs further detailed (more careful) evaluation. However, the foregoing discussion shows that other approaches would be far more ambiguous since the degree of safety would be an unknown variable, depending upon crack size, shape, and location.

9. CONCLUSIONS

(a) Available retardation models are a means for accurate prediction of crack propagation under flight-by-flight loading, provided the models are adjusted on the basis of experiments with similar

types of loading. In this respect, the Willenborg model is the least attractive because it is not adjustable except by adjusting baseline crack-growth data, which will cause inconsistencies in predictions if the model is applied to other crack configurations (different K-history).

(b) Crack growth depends strongly upon the shape of the spectrum. Therefore, crack-growth prediction should be updated when more reliable spectrum information becomes available.
Computed and experimental crack growth is only slightly dependent upon spectrum approximation and the number of stress levels, provided the loading is of the flight-by-flight type. Ten to 12 positive stress levels are sufficient. A block of 100 individual flights adequately represents a fighter history, both in experiments and computations, provided the crack increment per block is approximately 5 percent of the instantaneous crack size. (Larger increments are permissible at the end of the life.)

(c) The only satisfactory way to apply a safety factor to crack-growth predictions is to apply a factor to crack-growth life. A safety factor on initial crack size or on baseline crack-growth data is unacceptable because it results in different "degrees of safety", depending upon crack size, shape, and location. Moreover the "degree of safety" would be unknown.

10. RECOMMENDATIONS

This research program indicates that further study is needed to develop a fully satisfactory method of predicting fatigue-crack growth in service and determining the application of safety factors. Specifically, the following problems should be explored:

(a) Some statistics are now available on the variability of crack-growth predictions for materials with known properties and for cases with stress-intensity solutions. The next step would be a generalization to structural cracks of complex geometry in materials with variable properties. This step, already shown to be feasible, would likely lead to a quantitative evaluation of

the reliability of crack-growth computations to predict crack growth in service. The present program indicates how to apply safety factors; the next step would establish their magnitude.

(b) Some critical test cases could be designed to investigate the feasibility of the approach for safety factor application as proposed in Section 8 of this report. Such an investigation would test the paracticability of this approach, and would enable an assessment of the problems associated with flaw detectability. Simultaneously, these procedures should be applied to existing airplane systems that have shown satisfactory performance in order to substantiate or revise the safety factors developed under item (*a*).

(*c*) Statistics of flaw detectability and of equivalent crack sizes produced by various degrees of manufacturing quality should be established.

11. REFERENCES

1. Anon., "Damage Tolerance Design Data Handbook", MCIC-HB-01, 1972.

2. Broek, D., Elementary Engineering Fracture Mechanics, Noordhoff, 1974.

3. Wheeler, O. E., "Spectrum Loading and Crack Growth", Journal of Basic Engineering, 94 D, 1972, p 181.

4. Willenborg, J. D., et al, "A Crack Growth Retardation Model Using an Effective Stress Concept, AFFDL-TM-71-1 FBR, 1971.

5. Habibie, B. J., "Fatigue Crack Growth Prediction" (In German), Messerschmidt-Bolkow-Blohm, Report No. UH-03-71, 1971.

6. Hanel, J. J., "Crack Growth Prediction Under Variable Amplitude Loading on the Basis of a Dugdale Model" (In German), German Society for Materials Testing, 1973.

7. Bell, P. D., and Creager, M., "Crack Growth Analysis for Arbitrary Spectrum Loading", AFFDL-TR-74-129, 1975.

8. Various Authors, "Fracture Mechanics of Aircraft Structures", AGARDograph No. 176, 1974.

9. Gallagher, J. P., "A Generalized Development of Yield Zone Models", AFFDL-TM-FBR 74-28, 1974.

10. Broek, D., and Smith, S. H., "Damage Tolerance Design Guidelines", Forthcoming AFFDL publication.

11. Gallagher, J. P., and Hughes, T. F., "Influence of the Yield Strength on Overload Affected Fatigue-Crack-Growth Behavior in 4340 Steel", AFFDL-TR-74-27, 1974.

12. Schijve, J., et al, "Crack Propagation in Aluminum Alloy Sheet Materials Under Flight Simulation Loading", AFFDL-TR-69-50, 1970.

APPENDIX A

BASIC FIGHTER SPECTRUM AND FATIGUE-CRACK-GROWTH DATA

TABLE A-1. BASIC FIGHTER SPECTRUM

147785 in lbs of bending moment corresponds with a stress of 1 ksi for Ti-6Al-4V.
285893 in lbs of bending moment corresponds with a stress of 1 ksi for 7075-T73.

Level	Maximum Moment	Minimum Moment	Cycles, hours 20	200	1000	3000	6000
1	5147870	1595588	7	0	0	0	0
2	5147870	-184752	0	7	0	0	0
3	5147870	-492180	0	9	2	2	0
4	5147870	-923761	0	1	0	0	0
5	5147870	-1637577	0	0	1	2	1
6	5147870	-2351393	0	0	1	0	1
7	5147870	-3048412	0	0	0	0	1
8	5262752	-1109353	0	0	1	2	0
9	5262752	-837445	0	0	1	0	0
10	5262752	-2588379	0	0	0	2	0
11	5262752	-3355268	0	0	0	0	1
12	683900	1595588	3	2	1	1	1
13	6583900	-184752	0	3	1	0	1
14	6583900	-492180	0	4	2	0	0
15	6583900	-923761	0	0	2	1	0
16	6583900	-1637577	0	0	0	2	1
17	6583900	-2351393	0	0	0	1	1
18	6583900	-3048412	0	0	0	0	1
19	6819710	-1109353	0	0	0	2	1
20	6819710	-1837445	0	0	0	1	0
21	6819710	-2588379	0	0	0	1	0
22	6819710	-3355268	0	0	0	0	1
23	7893960	1595588	0	9	3	0	0
24	7893960	-184752	0	0	4	2	1
25	7893960	-492180	0	1	1	2	0
26	7893960	-923761	0	0	0	2	0
27	7893960	-1637577	0	0	0	1	0
28	7893960	-2351393	0	0	0	0	1
29	8302096	-1109353	0	0	0	0	1
30	8302096	-1837445	0	0	0	0	1
31	8302096	-2588379	0	0	0	0	1
32	8397832	1595588	0	2	2	2	0
33	8397832	-184752	0	0	1	0	1
34	8397832	-492180	0	0	1	2	0
35	8397832	-923761	0	0	0	0	1
36	8397832	-1637577	0	0	0	0	1
37	8649764	1595588	0	0	3	0	0
38	8649764	-184752	0	0	0	1	0
39	8649764	-492180	0	0	0	1	0
40	8817720	-492180	0	0	0	0	1
41	5348930	-391675	0	0	0	0	1
42	5939608	2809008	29	6	3	0	1
43	5939608	1063223	1	7	1	1	1
44	5939608	344738	0	1	4	0	0
45	5939608	111573	0	1	1	2	1

TABLE A-1. (Continued)

Level	Maximum Moment	Minimum Moment	Cycles, hours 20	200	1000	3000	6000
46	5939608	-229093	0	1	0	1	0
47	5939608	-465576	0	0	1	0	1
48	5939608	-492180	1	6	2	2	0
49	6313706	2809008	11	5	3	0	0
50	6313706	1063223	0	6	3	1	1
51	6313706	544738	0	0	3	2	0
52	6313706	111573	0	0	2	2	0
53	6313706	-229093	0	0	2	0	0
54	6313706	-465576	0	0	0	1	1
55	6313706	-492180	0	7	3	1	0
56	6563104	2809008	2	7	1	2	0
57	6563104	1063223	0	1	3	0	0
58	6563104	544738	0	0	0	2	1
59	6563104	111573	0	0	0	2	0
60	6563104	-229093	0	0	0	1	1
61	6563104	-492180	0	1	3	0	0
62	5272388	1507718	5	3	4	1	1
63	5272388		0	3	0	0	0
64	6844852	1507718	2	4	4	1	0
65	6844852		0	1	2	0	0
66	8324822	1507718	0	7	2	0	1
67	8324822		0	0	2	0	0
68	9249804	1507718	0	6	2	2	1
69	9249804		0	0	1	2	1
70	9675292	1507718	0	1	0	0	0
71	9675292		0	0	0	1	0
72	9962036	1507718	0	0	0	2	0
73	5396224	2849691	1	5	4	0	0
74	5396224	1152003	0	1	0	1	0
75	5396224	636633	0	0	0	2	0
76	5396224	212211	0	0	0	1	0
77	5396224		0	0	0	0	1
78	5772140	2849691	0	5	1	2	0
79	5772140	1152003	0	0	1	2	0
80	5772140	636633	0	0	0	0	1
81	5772140	212211	0	0	0	0	1
82	5772140		0	0	0	0	1
83	6063174	2849691	0	9	1	1	1
84	6063174	1152003	0	0	3	0	1
85	6063174	636633	0	0	0	1	0
86	6063174	212211	0	0	0	0	1
87	6063174		0	0	0	0	1
88	3554921	-673615	0	0	0	0	1
89	3554921	-1103927	0	0	0	0	1
90	4258626	-649026	0	0	1	1	0

TABLE A-1. (Continued)

Level	Maximum Moment	Minimum Moment	Cycles, hours				
			20	200	1000	3000	6000
91	4258626	-1200018	0	0	0	2	0
92	4258626	-1776247	0	0	0	1	0
93	4258626	-2317211	0	0	0	0	1
94	4551838	-405722	0	4	0	1	0
95	4551838	-1103927	0	0	2	1	0
96	4551838	-1739363	0	0	0	2	0
97	4551838	-2355388	0	0	0	0	1
98	4610478	1609623	3	3	0	2	1
99	4610478	97063	0	1	4	2	1
100	4610478	-501491	0	0	1	0	1
101	4610478	-1116221	0	0	0	2	0
102	4610478	-1714774	0	0	0	1	1
103	4610478	-2329505	0	0	0	0	1
104	5425804	-649026	0	0	0	2	0
105	5425804	-1200018	0	0	0	0	1
106	5425804	-1776247	0	0	0	1	0
107	5437128	-405722	0	3	2	2	0
108	5437128	-1103927	0	0	2	0	0
109	5437128	-1739363	0	0	0	1	1
110	5742874	1609623	1	5	1	1	1
111	5742874	97063	0	0	4	1	1
112	5742874	-501491	0	0	0	1	1
113	5742874	-1116221	0	0	0	1	0
114	5742874	-1714774	0	0	0	0	1
115	6100066	-405722	0	1	0	2	1
116	6100066	-1103927	0	0	0	2	0
117	6100066	-1739363	0	0	0	0	1
118	6557718	-649026	0	0	0	0	1
119	6557718	-1200018	0	0	0	0	1
120	6747474	-405722	0	0	1	2	0
121	6747474	-1103927	0	0	0	0	1
122	6859096	1609623	0	4	2	2	1
123	6859096	97063	0	0	1	1	1
124	6859096	-501491	0	0	0	0	1
125	7252526	-405722	0	0	0	2	0
126	7252526	-1103927	0	0	0	0	1
127	7744308	-649026	0	0	0	0	1
128	7744308	-1200018	0	0	0	0	1
129	8088558	609623	0	1	0	2	0
130	8088558	97063	0	0	0	1	0
131	9261724	-1128191	0	0	0	0	1
132	9261724	-1850014	0	0	0	0	1
133	9285664	1609623	0	1	0	0	0
134	9285664	97063	0	0	0	1	0
135	9746712	1609623	0	0	0	2	1

AD-A061 920 BATTELLE COLUMBUS LABS OHIO F/G 11/6
SPECTRUM LOADING FATIGUE-CRACK-GROWTH PREDICTIONS AND SAFETY-FA--ETC(U)
SEP 76 D BROEK, S H SMITH N62269-76-C-0093
UNCLASSIFIED BATT-G-6320 NADC-76383-30 NL

2 OF 2
AD A061920

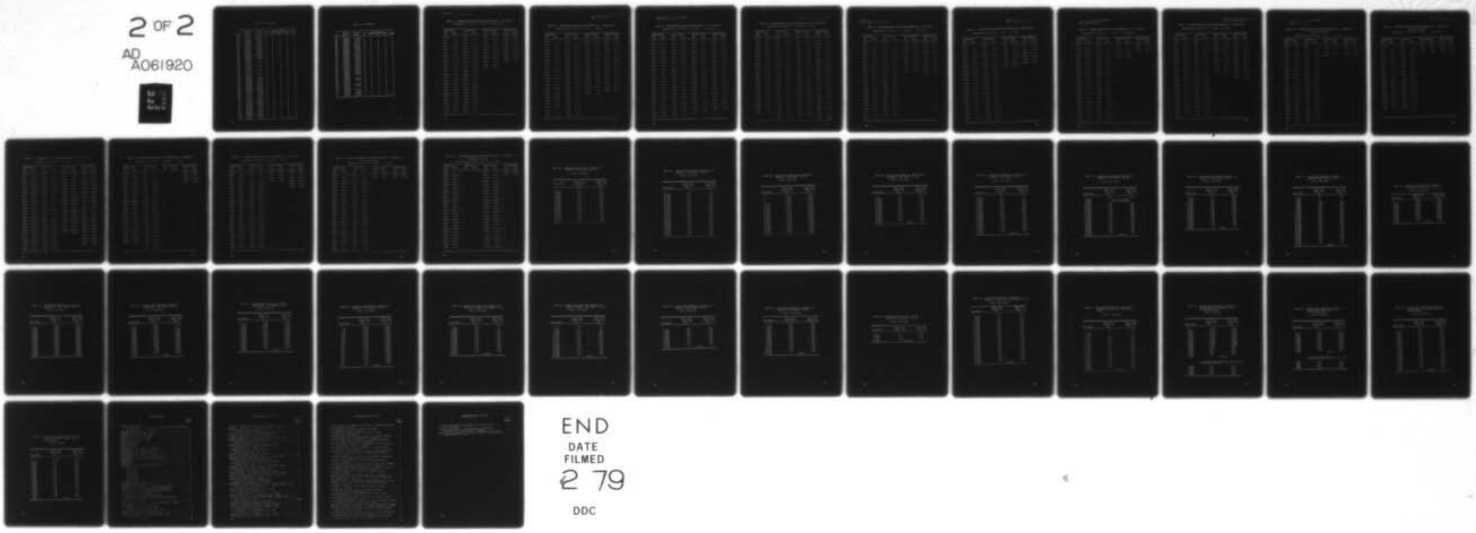

END
DATE FILMED
2 79
DDC

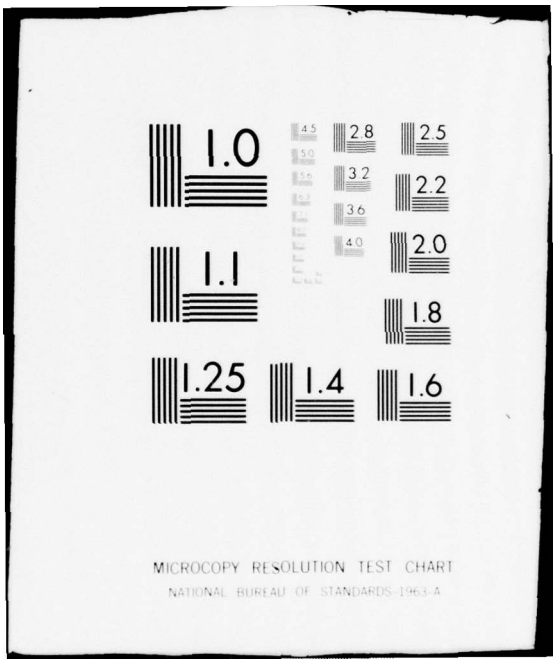
1.0
1.1
1.25
1.4
1.6
1.8
2.0
2.2
2.5
2.8
3.2
3.6
4.0
4.5
5.0
5.6
6.3
MICROCOPY RESOLUTION TEST CHART
NATIONAL BUREAU OF STANDARDS-1963-A

TABLE A-1. (Continued)

Level	Maximum Moment	Minimum Moment	Cycles, hours 20	200	1000	3000	6000
136	5491894	3027964	5	3	1	1	1
137	5491894	1312118	0	1	2	0	1
138	5491894	748085	0	0	0	2	1
139	5491894	219676	0	0	0	1	1
140	5491894	-274040	0	0	0	0	1
141	5943122	3027964	2	9	3	1	1
142	5943122	1312118	0	0	4	0	0
143	5943122	748085	0	0	0	1	1
144	5943122	219676	0	0	0	0	1
145	5943122	-274040	0	0	0	0	1
146	6239978	3027964	0	1	1	0	0
147	6239978	1312118	0	0	0	0	1
148	4270696	1397682	2	9	0	2	1
149	4270696		0	2	2	0	1
150	5435430	1397682	1	2	1	2	0
151	5435430		0	1	0	0	1
152	6561340	1397682	0	3	1	1	1
153	6561340		0	0	1	1	0
154	7764902	1397682	0	3	2	2	1
155	7764902		0	0	1	1	1
156	8914108	1397682	0	0	0	2	1
157	8914108		0	0	0	0	1
158	9706128	1397682	0	0	0	2	1
159	4561000	1755623	57	0	3	0	0
160	4561000	271488	12	3	2	2	0
161	4561000	-217190	0	5	0	0	0
162	4561000	-494271	2	6	2	2	0
163	4561000	-787315	0	2	1	1	0
164	4561000	-1339341	0	1	3	1	1
165	4561000	-1900417	0	0	1	2	1
166	5701250	1755623	26	3	2	0	0
167	5701250	271488	5	7	0	0	1
168	5701250	-217190	0	2	1	1	1
169	5701250	-494271	1	2	1	1	0
170	5701250	-787315	0	1	0	0	1
171	5701250	-1339341	0	0	4	0	0
172	5701250	-1900417	0	0	0	2	1
173	6823400	1755623	7	8	2	2	1
174	6823400	271488	1	7	0	0	0
175	6823400	-217190	0	0	3	1	1
176	6323400	-494271	0	3	3	0	1
177	6823400	-787315	0	0	1	1	1
178	6823400	-1339341	0	0	1	0	1
179	6823400	-1900417	0	0	0	1	0
180	7963650	1755623	1	9	4	2	0

TABLE A-1. (Continued)

Level	Maximum Moment	Minimum Moment	Cycles, hours 20	200	1000	3000	6000
181	7963650	271488	0	4	1	1	1
182	7963650	-217190	0	0	0	2	1
183	7963650	-494271	0	0	4	2	0
184	7963650	-787315	0	0	0	1	1
185	7963650	-1339341	0	0	0	1	0
186	9049604	1755623	0	4	3	1	0
187	9049604	271488	0	1	0	0	0
188	9049604	-217190	0	0	0	1	0
189	9049604	-494271	0	0	1	0	1
190	9049604	-787315	0	0	0	0	1
191	9909316	1755623	0	0	4	0	0
192	9909316	271488	0	0	0	2	1
193	9909316	-494271	0	0	0	0	1
194	4555072	188115	4	7	1	2	0
195	5428462	188115	4	0	4	2	0
196	6120438	188115	1	3	3	2	1
197	6718396	188115	0	3	3	1	0
198	7249150	188115	0	1	2	1	1
199	7605224	188115	0	0	0	2	1
200	3538669	1431800	5	7	0	0	0
201	3538669	337535	0	0	1	2	1
202	3538669		0	0	0	0	1
203	4289956	1431800	2	6	1	2	0
204	4289956	337535	0	0	0	2	1
205	4289956		0	0	0	0	1
206	4872476	1431800	1	4	2	0	1
207	4872476	337535	0	0	0	1	1
208	4872476		0	0	0	0	1
209	5444108	1431800	0	5	4	2	0
210	5444108	337535	0	0	0	0	1
211	5934076	1431800	0	1	2	0	0
212	6260722	1431800	0	0	1	2	0

TABLE A-2. CONSTANT-AMPLITUDE FATIGUE-CRACK-GROWTH DATA -- SPECIMEN AL-1

Maximum Stress = 15.0 ksi R = 0.15 t = 0.264 Inch

Upper Crack		Lower Crack		Upper Crack (Cont.)		Lower Crack (Cont.)	
A, Inch	N, Cycles	A, Inch	N, Cycles	A, Inch	N, Cycles	A, Inch	N, Cycles
0.119	.	0.115	.	1.140	39800.	0.995	40700.
0.133	5770.	0.153	12000.	1.210	40130.	1.025	40500.
0.143	8130.	0.172	15000.	1.270	40300.	1.050	40700.
0.163	12000.	0.197	18000.	1.335	40500.	1.095	40910.
0.190	15000.	0.218	20000.	1.430	40700.	1.115	41010.
0.221	18000.	0.240	22000.	1.585	40910.	1.125	41060.
0.239	20000.	0.259	23500.	1.680	41010.	1.125	41110.
0.272	22000.	0.286	25030.	1.735	41060.	1.130	41160.
0.294	23500.	0.303	26020.	1.810	41110.	1.145	41190.
0.322	25030.	0.317	27040.	1.915	41160.		
0.344	26020.	0.341	28020.	2.055	41190.		
0.368	27040.	0.370	29040.				
0.393	28020.	0.445	31010.				
0.419	29040.	0.495	32530.				
0.485	31010.	0.535	33710.				
0.550	32530.	0.595	34730.				
0.605	33710.	0.630	35700.				
0.661	34730.	0.675	36710.				
0.705	35700.	0.750	37710.				
0.770	36710.	0.805	38400.				
0.840	37710.	0.825	38700.				
0.925	38400.	0.865	39100.				
0.960	38700.	0.905	39500.				
1.015	39100.	0.935	39800.				
1.080	39500.	0.970	40100.				

TABLE A-3. CONSTANT-AMPLITUDE FATIGUE-CRACK-GROWTH DATA -- SPECIMEN AL-2

Maximum Stress = 12.75 ksi R = 0.0 t = 0.264

Upper Crack		Lower-Crack		Upper Crack (Cont.)		Lower Crack (Cont.)	
A, Inch	N, Cycles	A, Inch	N, Cycles	A, Inch	N, Cycles	A, Inch	N, Cycles
0.130	.	0.125	.	0.995	49000.	1.105	49600.
0.138	5960.	0.132	7710.	1.060	49600.	1.175	50200.
0.146	7710.	0.148	11020.	1.105	50200.	1.225	50610.
0.165	11020.	0.171	15010.	1.155	50610.	1.225	51010.
0.189	15010.	0.198	19020.	1.190	51010.	1.295	51310.
0.219	19020.	0.230	22000.	1.235	51310.	1.340	51600.
0.248	22000.	0.252	24030.	1.275	51600.	1.415	51900.
0.267	24030.	0.281	26170.	1.330	51900.	1.510	52100.
0.291	26170.	0.308	28020.	1.375	52100.	1.575	52250.
0.313	28020.	0.340	30030.	1.405	52250.	1.645	52350.
0.344	30030.	0.356	31030.	1.430	52350.	1.700	52400.
0.359	31030.	0.375	32120.	1.440	52400.	1.725	52450.
0.379	32120.	0.430	34500.	1.475	52480.	1.785	52550.
0.440	34500.	0.475	36500.	1.490	52550.	1.855	52600.
0.480	36500.	0.530	38510.	1.500	52600.	1.905	52650.
0.525	38510.	0.585	40010.	1.525	52650.	1.980	52680.
0.580	40010.	0.620	41000.	1.530	52680.	2.035	52710.
0.620	41000.	0.675	42500.	1.540	52710.		
0.670	42500.	0.735	44010.				
0.730	44010.	0.790	45010.				
0.770	45010.	0.825	46000.				
0.845	46000.	0.890	46800.				
0.865	46800.	0.935	47600.				
0.910	47600.	1.000	48400.				
0.960	48400.	1.050	49000.				

TABLE A-4. CONSTANT-AMPLITUDE FATIGUE-CRACK-GROWTH DATA -- SPECIMEN AL-3

Maximum Stress = 14.00 ksi R = 0.300 t = 0.251 Inch

Upper Crack		Lower Crack		Upper Crack (Cont.)		Lower Crack (Cont.)	
A, Inch	N, Cycles	A, Inch	N, Cycles	A, Inch	N, Cycles	A, Inch	N, Cycles
0.124	.	0.119	.	1.010	60000.	1.130	60500.
0.141	12400.	0.159	15400.	1.055	60500.	1.180	60900.
0.157	15400.	0.167	18400.	1.090	60900.	1.220	61200.
0.179	18400.	0.188	22400.	1.120	61200.	1.270	61500.
0.193	22400.	0.215	26400.	1.160	61500.	1.335	61800.
0.216	26400.	0.239	29400.	1.195	61800.	1.385	62050.
0.242	29400.	0.267	32400.	1.220	62050.	1.450	62300.
0.271	32400.	0.297	35000.	1.260	62300.	1.515	62500.
0.297	35000.	0.328	37500.	1.290	62500.	1.560	62650.
0.328	37500.	0.357	39500.	1.320	62650.	1.610	62800.
0.356	39500.	0.382	41000.	1.345	62800.	1.655	62900.
0.377	41000.	0.445	44000.	1.360	62900.	1.705	63000.
0.435	44000.	0.480	46000.	1.375	63000.	1.765	63100.
0.485	46000.	0.530	48000.	1.390	63100.	1.795	63170.
0.520	48000.	0.590	50000.	1.410	63170.	1.845	63240.
0.570	50000.	0.640	52000.	1.430	63240.	1.880	63290.
0.625	52000.	0.685	53500.	1.440	63290.	1.925	63340.
0.675	53500.	0.745	55000.	1.450	63340.	1.970	63380.
0.735	55000.	0.785	56000.	1.460	63380.	2.025	63440.
0.765	56000.	0.855	57000.	1.475	63440.	2.075	63480.
0.815	57000.	0.875	57700.	1.485	63480.	2.125	63510.
0.840	57700.	0.925	58400.	1.495	63510.	2.160	63530.
0.890	58400.	0.980	59000.	1.500	63530.	2.220	63550.
0.935	59000.	1.025	59500.	1.510	63550.		
0.970	59500.	1.065	61000.				

TABLE A-5. CONSTANT-AMPLITUDE FATIGUE-CRACK-GROWTH DATA -- SPECIMEN AL-4

Maximum Stress = 10.65 ksi R = 0.150 t = 0.251

Upper Crack		Lower Crack		Upper Crack (Cont.)		Lower Crack (Cont.)	
A, Inch	N, Cycles	A, Inch	N, Cycles	A, Inch	N, Cycles	A, Inch	N, Cycles
0.131	7500.	0.119	.	0.990	70300.	0.991	71100.
0.140	10500.	0.127	7500.	1.075	71900.	1.020	71800.
0.158	15500.	0.135	10500.	1.100	72500.	1.065	72500.
0.186	21500.	0.151	15500.	1.155	73200.	1.105	73200.
0.214	26500.	0.178	21500.	1.190	73800.	1.140	73800.
0.237	30500.	0.202	26500.	1.225	74400.	1.190	74400.
0.263	34500.	0.223	30500.	1.280	75000.	1.225	75000.
0.291	38000.	0.252	34500.	1.340	75600.	1.270	75600.
0.318	41000.	0.278	38000.	1.385	76100.	1.325	76100.
0.342	43500.	0.306	41000.	1.445	76600.	1.375	76600.
0.389	47500.	0.327	43500.	1.495	77000.	1.415	77000.
0.420	49500.	0.350	45500.	1.550	77400.	1.465	77400.
0.470	52500.	0.373	47500.	1.635	77900.	1.520	77700.
0.510	55000.	0.410	49500.	1.680	78100.	1.550	77900.
0.560	57000.	0.450	52500.	1.775	78300.	1.580	78100.
0.600	59000.	0.500	55000.	1.790	78500.	1.620	78300.
0.660	61000.	0.540	57000.	1.835	78650.	1.655	78500.
0.705	62500.	0.575	59000.	1.895	78700.	1.690	78650.
0.745	64000.	0.630	61000.	1.940	78800.	1.740	78700.
0.805	65600.	0.665	62500.	1.990	78900.	1.775	78800.
0.830	66500.	0.710	64000.	2.075	79040.	1.795	78900.
0.870	67500.	0.765	65500.	2.135	79110.	1.855	79040.
0.905	68500.	0.785	66500.	2.170	79160.	1.875	79110.
0.950	69500.	0.835	67500.	2.225	79210.	1.880	79160.
0.128	.	0.865	68500.	2.305	79280.	1.895	79210.
		0.915	69500.	2.385	79290.	1.930	79260.
		0.945	70300.			1.945	79290.

TABLE A-6. CONSTANT-AMPLITUDE FATIGUE-CRACK-GROWTH DATA -- SPECIMEN AL-5

Maximum Stress = 19.60 ksi R = 0.500 t = 0.251 Inch

Upper Crack		Lower Crack		Upper Crack (Cont.)		Lower Crack (Cont.)	
A, Inch	N, Cycles	A, Inch	N, Cycles	A, Inch	N, Cycles	A, Inch	N, Cycles
0.130	.	0.129	.	0.895	44700.	1.120	44950.
0.144	10000.	0.135	7000.	0.910	44800.	1.195	44700.
0.158	13000.	0.146	10000.	0.925	44900.	1.220	44900.
0.176	16000.	0.164	13000.	0.940	44900.	1.290	44900.
0.196	19000.	0.182	16000.	0.960	45070.	1.355	45000.
0.221	22000.	0.206	19000.	0.965	45140.	1.375	45070.
0.242	24500.	0.232	22000.	0.980	45210.	1.440	45140.
0.271	27000.	0.255	24500.	0.990	45280.	1.500	45210.
0.297	29000.	0.284	27000.	1.000	45330.	1.585	45280.
0.319	30500.	0.317	29000.	1.010	45360.	1.675	45330.
0.344	32000.	0.336	30500.			1.755	45360.
0.370	33500.	0.360	32000.				
0.425	35900.	0.389	33500.				
0.485	37900.	0.455	35900.				
0.530	39400.	0.520	37900.				
0.590	40700.	0.570	39400.				
0.630	41700.	0.635	40700.				
0.690	42500.	0.700	41700.				
0.720	43000.	0.765	42500.				
0.740	43300.	0.820	43000.				
0.770	43600.	0.865	43300.				
0.795	43900.	0.900	43600.				
0.825	44200.	0.955	43900.				
0.850	44400.	1.025	44200.				
0.865	44550.	1.085	44400.				

TABLE A-7. CONSTANT-AMPLITUDE FATIGUE-CRACK-GROWTH DATA -- SPECIMEN AL-6

Maximum Stress = 12.75 ksi R = 0.0 t = 0.479

Upper Crack		Lower Crack		Upper Crack (Cont.)		Lower Crack (Cont.)	
A, Inch	N, Cycles	A, Inch	N, Cycles	A, Inch	N, Cycles	A, Inch	N, Cycles
0.127	.	0.123	.	0.950	51000.	0.590	51600.
0.133	8000.	0.130	11000.	0.980	51600.	0.620	52200.
0.136	11000.	0.144	16000.	1.035	52200.	0.670	54000.
0.164	16000.	0.165	20000.	1.225	54000.	0.700	55000.
0.193	20000.	0.183	23000.	1.435	55000.	0.715	55700.
0.211	23000.	0.202	26000.	1.780	55700.	0.730	55800.
0.241	26000.	0.215	28000.	1.900	55800.	0.735	55870.
0.263	28000.	0.231	30000.	2.045	55870.		
0.289	30000.	0.242	31500.				
0.309	31500.	0.255	33000.				
0.331	33000.	0.271	34500.				
0.357	34500.	0.280	35000.				
0.374	35000.	0.330	37000.				
0.430	37000.	0.335	38700.				
0.465	38700.	0.355	40400.				
0.510	40400.	0.375	41900.				
0.540	41900.	0.390	43400.				
0.595	43400.	0.425	44700.				
0.645	44700.	0.440	44800.				
0.680	44800.	0.465	46900.				
0.720	46900.	0.490	47900.				
0.760	47900.	0.520	48700.				
0.815	48700.	0.535	49500.				
0.850	49500.	0.550	50700.				
0.905	50300.	0.575	51000.				

TABLE A-8. CONSTANT-AMPLITUDE FATIGUE-CRACK-GROWTH DATA -- SPECIMEN AL-7

Maximum Stress = 14.00 ksi R = 0.300 t = 0.480 Inch

Upper Crack		Lower Crack		Upper Crack (Cont.)		Lower Crack (Cont.)	
A, Inch	N, Cycles	A, Inch	N, Cycles	A, Inch	N, Cycles	A, Inch	N, Cycles
0.128	.	0.111	.	0.930	61600.	0.480	62800.
0.146	15000.	0.122	22000.	0.970	63200.	0.525	64400.
0.159	18000.	0.130	26000.	1.015	62800.	0.565	65800.
0.178	22000.	0.143	30000.	1.185	64400.		
0.199	26000.	0.154	33000.	1.455	65800.		
0.227	30000.	0.162	35500.				
0.259	33000.	0.173	38000.				
0.271	35500.	0.184	40000.				
0.297	38000.	0.194	42000.				
0.319	40000.	0.205	43500.				
0.344	42000.	0.215	45000.				
0.365	43500.	0.235	46500.				
0.388	45000.	0.245	48000.				
0.420	46500.	0.265	50000.				
0.450	48000.	0.295	52000.				
0.490	50400.	0.315	53600.				
0.535	52000.	0.330	54800.				
0.585	53600.	0.345	55800.				
0.625	54800.	0.360	56800.				
0.655	55800.	0.375	57800.				
0.690	56800.	0.395	58800.				
0.735	57800.	0.415	59800.				
0.780	58800.	0.430	60800.				
0.825	59800.	0.445	61600.				
0.880	60800.	0.465	62200.				

TABLE A-9. CONSTANT-AMPLITUDE FATIGUE-CRACK-GROWTH DATA -- SPECIMEN AL-8

Maximum Stress = 19.60 ksi R = 0.500 t = 0.481

Upper Crack		Lower Crack		Upper Crack (Cont.)		Lower Crack (Cont.)	
A, Inch	N, Cycles	A, Inch	N, Cycles	A, Inch	N, Cycles	A, Inch	N, Cycles
0.112	.	0.119	.	0.640	48300.	0.925	47900.
0.130	15000.	0.127	7000.	0.670	48700.	0.950	48100.
0.144	19000.	0.127	10100.	0.695	49100.	1.000	48700.
0.163	23000.	0.148	15000.	0.720	49200.	1.170	48700.
0.182	26000.	0.165	19000.	0.721	49250.	1.330	49100.
0.197	28000.	0.188	23000.	0.721	49270.	1.415	49200.
0.213	30000.	0.217	26000.	0.725	49290.	1.465	49250.
0.234	31900.	0.230	28000.	0.726	49330.	1.490	49270.
0.252	33400.	0.251	30000.	0.726	49370.	1.515	49290.
0.271	35000.	0.274	31800.	0.727	49430.	1.550	49330.
0.292	36400.	0.298	33400.	0.727	49490.	1.615	49370.
0.313	37600.	0.318	35000.			1.700	49430.
0.350	39400.	0.344	36400.			1.900	49490.
0.375	40900.	0.369	37600.				
0.415	42200.	0.415	39400.				
0.435	43200.	0.465	40900.				
0.465	44100.	0.500	42200.				
0.490	45000.	0.540	43200.				
0.515	45800.	0.580	44100.				
0.545	46500.	0.625	45000.				
0.570	47000.	0.670	45800.				
0.590	47300.	0.735	46500.				
0.605	47600.	0.795	47000.				
0.625	47900.	0.870	47300.				
0.630	48100.	0.960	47600.				

TABLE A-10. CONSTANT-AMPLITUDE FATIGUE-CRACK-GROWTH DATA -- SPECIMEN AL-9

Saltwater Environment

Maximum Stress = 12.75 ksi R = 0.0 t = 0.265

Upper Crack		Lower Crack		Upper Crack (Cont.)		Lower Crack (Cont.)	
A, Inch	N, Cycles	A, Inch	N, Cycles	A, Inch	N, Cycles	A, Inch	N, Cycles
0.129	.	0.133	.	0.895	17600.	0.954	17500.
0.146	5200.	0.164	5200.	0.924	17750.	0.990	17750.
0.181	7000.	0.197	7000.	0.941	17900.	0.996	17900.
0.204	8000.	0.219	8000.	0.963	18050.	1.017	18050.
0.239	9000.	0.256	9000.				
0.260	9500.	0.279	9500.				
0.280	9900.	0.300	9900.				
0.293	10300.	0.321	10300.				
0.309	10700.	0.339	10700.				
0.332	11100.	0.361	11100.				
0.351	11400.	0.380	11400.				
0.377	11900.	0.406	11900.				
0.419	12600.	0.453	12600.				
0.460	13200.	0.490	13200.				
0.505	13900.	0.520	13800.				
0.547	14400.	0.581	14400.				
0.588	15000.	0.632	15000.				
0.642	15500.	0.677	15500.				
0.674	15900.	0.717	15900.				
0.722	16300.	0.764	16300.				
0.759	16650.	0.813	16650.				
0.776	16950.	0.851	16950.				
0.854	17250.	0.899	17250.				
0.860	17550.	0.916	17450.				
0.872	17450.	0.931	17450.				

TABLE A-11. CONSTANT-AMPLITUDE FATIGUE-CRACK-GROWTH DATA -- SPECIMEN A10

Saltwater Environment

Maximum Stress = 12.75 ksi R = 0.0 t = 0.263 Inch

Upper Crack		Lower Crack		Upper Crack (Cont.)		Lower Crack (Cont.)	
A, Inch	N, Cycles	A, Inch	N, Cycles	A, Inch	N, Cycles	A, Inch	N, Cycles
0.135	.	0.133	.	0.942	23700.	0.832	23700.
0.218	10900.	0.210	10900.	0.968	24000.	0.869	24000.
0.226	10900.	0.217	10900.	1.004	24700.	0.896	24700.
0.240	11400.	0.229	11400.				
0.253	11900.	0.239	11900.				
0.288	13100.	0.273	13100.				
0.311	13900.	0.296	13900.				
0.337	14800.	0.321	14800.				
0.356	15200.	0.341	15200.				
0.383	15800.	0.363	15800.				
0.425	16800.	0.406	16800.				
0.470	17800.	0.446	17800.				
0.525	18800.	0.490	18800.				
0.567	19600.	0.534	19600.				
0.616	20300.	0.573	20300.				
0.660	20900.	0.614	20900.				
0.709	21500.	0.648	21500.				
0.756	22000.	0.692	22000.				
0.788	22500.	0.730	22500.				
0.838	23000.	0.769	23000.				
0.894	23400.	0.805	23400.				

TABLE A-12. CONSTANT-AMPLITUDE FATIGUE-CRACK-GROWTH DATA -- SPECIMEN T-1

Maximum Stress = 24.00 ksi R = 0.00 t = 0.216

Upper Crack		Lower Crack		Upper Crack (Cont.)		Lower Crack (Cont.)	
A, Inch	N, Cycles	A, Inch	N, Cycles	A, Inch	N, Cycles	A, Inch	N, Cycles
0.120	.	0.125	.	0.485	52600.	1.100	51600.
0.124	30000.	0.148	23000.	0.490	52800.	1.145	51900.
0.138	32000.	0.157	24000.	0.500	53000.	1.200	52200.
0.155	34000.	0.170	26000.	0.510	53200.	1.240	52400.
0.175	36000.	0.192	28000.	0.520	53400.	1.295	52600.
0.188	37500.	0.213	30000.	0.520	53550.	1.335	52800.
0.204	39000.	0.238	32000.	0.525	53700.	1.390	53000.
0.213	40000.	0.264	34000.	0.530	53800.	1.445	53200.
0.245	42000.	0.296	36000.	0.535	53900.	1.515	53400.
0.270	43500.	0.321	37500.	0.540	54000.	1.565	53550.
0.285	44700.	0.354	39000.	0.541	54070.	1.645	53700.
0.305	45900.	0.376	40000.	0.545	54120.	1.695	53800.
0.330	47100.	0.430	42000.	0.550	54170.	1.745	53900.
0.350	48000.	0.485	43500.	0.555	54220.	1.810	54000.
0.360	48500.	0.535	44700.	0.555	54270.	1.865	54070.
0.375	49000.	0.585	45900.	0.560	54300.	1.900	54120.
0.390	49500.	0.655	47100.	0.561	54320.	1.955	54170.
0.400	50000.	0.720	48000.	0.561	54340.	2.000	54220.
0.410	50400.	0.755	48500.	0.561	54350.	2.065	54270.
0.420	50800.	0.800	49000.	0.562	54360.	2.130	54300.
0.425	51200.	0.845	49500.			2.170	54320.
0.445	51600.	0.895	50000.			2.255	54340.
0.460	51900.	0.935	50400.			2.310	54350.
0.470	52200.	0.985	50800.			2.420	54360.
0.480	52400.	1.035	51200.				

TABLE A-13. CONSTANT-AMPLITUDE FATIGUE-CRACK-GROWTH DATA -- SPECIMEN T-2

Maximum Stress = 27.00 ksi R = 0.300 t = 0.216

Upper Crack		Lower Crack		Upper Crack (Cont.)		Lower Crack (Cont.)	
A, Inch	N, Cycles	A, Inch	N, Cycles	A, Inch	N, Cycles	A, Inch	N, Cycles
0.123	.	0.123	.			1.505	59000.
0.133	39000.	0.139	23000.			1.945	59800.
0.140	41000.	0.149	26000.			2.075	59900.
0.144	42500.	0.171	29000.			2.345	60000.
0.150	44000.	0.196	32000.				
0.152	45500.	0.220	34500.				
0.165	47500.	0.247	37000.				
0.175	49500.	0.271	39000.				
0.176	51000.	0.300	41000.				
0.180	52300.	0.323	42500.				
0.185	53300.	0.350	44000.				
0.186	54000.	0.383	45500.				
0.186	54700.	0.440	47500.				
0.190	55200.	0.505	49500.				
0.191	55700.	0.565	51000.				
0.191	56200.	0.625	52300.				
0.205	56500.	0.685	53300.				
0.210	56800.	0.735	54000.				
0.225	58000.	0.795	54700.				
0.226	59000.	0.840	55200.				
0.235	59900.	0.895	55700.				
0.236	59900.	0.960	56200.				
0.236	60000.	0.995	56500.				
		1.035	56800.				
		1.245	58000.				

TABLE A-14. CONSTANT-AMPLITUDE FATIGUE-CRACK-GROWTH DATA -- SPECIMEN T-3

Maximum Stress = 32.00 ksi R = 0.500 t = 0.216

Upper Crack		Lower Crack		Upper Crack (Cont.)		Lower Crack (Cont.)	
A, Inch	N, Cycles	A, Inch	N, Cycles	A, Inch	N, Cycles	A, Inch	N, Cycles
0.123	.	0.121	.	0.695	86400.	1.025	84000.
0.138	44000.	0.137	35000.	0.750	87400.	1.165	85200.
0.166	49100.	0.154	39000.	0.775	87900.	1.385	86400.
0.185	53000.	0.174	44000.	0.785	88000.	1.685	87400.
0.212	57000.	0.199	49000.			1.960	87900.
0.231	61000.	0.223	53000.			2.075	89000.
0.247	63000.	0.241	57000.				
0.261	65000.	0.281	61000.				
0.280	67000.	0.302	63000.				
0.301	69000.	0.323	65000.				
0.345	72000.	0.348	67000.				
0.375	74500.	0.377	69000.				
0.410	76500.	0.425	72000.				
0.440	78000.	0.485	74500.				
0.460	79000.	0.550	76500.				
0.475	80000.	0.605	78000.				
0.485	80700.	0.640	79000.				
0.510	81400.	0.695	80000.				
0.525	81900.	0.735	80700.				
0.540	82400.	0.780	81400.				
0.565	82900.	0.815	81900.				
0.566	83200.	0.865	82400.				
0.580	83600.	0.890	82900.				
0.595	84000.	0.930	83200.				
0.635	85200.	0.970	83600.				

TABLE A-15. CONSTANT-AMPLITUDE FATIGUE-CRACK-GROWTH DATA -- SPECIMEN T-4

Saltwater Environment

Maximum Stress = 24.00 R = 0.00 t = 0.219

Upper Crack		Lower Crack		Upper Crack (Cont.)		Lower Crack (Cont.)	
A, Inch	N, Cycles	A, Inch	N, Cycles	A, Inch	N, Cycles	A, Inch	N, Cycles
0.122	.	0.122	.	0.960	24010.	0.172	24010.
0.152	12800.	0.136	15000.	1.003	24140.	0.173	24140.
0.160	13500.	0.142	17000.				
0.208	14700.	0.144	17800.				
0.249	15300.	0.145	18600.				
0.257	15600.	0.148	19500.				
0.264	16000.	0.149	20300.				
0.283	16600.	0.149	20700.				
0.318	17200.	0.149	21000.				
0.329	17600.	0.158	21200.				
0.344	18000.	0.158	21400.				
0.380	18400.	0.159	21800.				
0.408	19000.	0.160	22100.				
0.452	19700.	0.161	22300.				
0.476	20300.	0.163	22500.				
0.511	20900.	0.164	22650.				
0.553	21500.	0.164	22800.				
0.591	22100.	0.168	22950.				
0.623	22700.	0.168	23100.				
0.672	23300.	0.168	23230.				
0.718	23800.	0.168	23360.				
0.758	24300.	0.171	23490.				
0.797	24800.	0.171	23620.				
0.857	25300.	0.172	23750.				
0.901	25700.	0.172	23880.				

TABLE A-16. CONSTANT-AMPLITUDE FATIGUE-CRACK-GROWTH DATA -- SPECIMEN T-5

Saltwater Environment

Maximum Stress = 24.00 R = 0.00 t = 0.216

Upper Crack		Lower Crack		Upper Crack (Cont.)		Lower Crack (Cont.)	
A, Inch	N, Cycles	A, Inch	N, Cycles	A, Inch	N, Cycles	A, Inch	N, Cycles
0.119	.			0.123	.	0.953	26100.
0.128	14700.			0.152	15000.	0.993	26450.
0.173	15300.			0.186	17000.		
0.179	15600.			0.205	17800.		
0.185	16000.			0.215	18600.		
0.229	16600.			0.245	19500.		
0.251	17200.			0.293	20300.		
0.272	17600.			0.319	20700.		
0.285	18000.			0.348	21000.		
0.310	18400.			0.367	21200.		
0.339	19000.			0.386	21400.		
0.370	19700.			0.435	21800.		
0.400	20300.			0.487	22100.		
0.428	20900.			0.521	22300.		
0.465	21500.			0.570	22500.		
0.496	22100.			0.593	22650.		
0.532	22700.			0.631	22800.		
0.575	23300.			0.663	22950.		
0.610	23800.			0.715	23100.		
0.646	24300.			0.747	23230.		
0.686	24800.			0.784	23360.		
0.724	25300.			0.815	23490.		
0.762	25900.			0.850	23620.		
0.800	26100.			0.887	23750.		
0.837	26430.			0.923	23880.		

TABLE A-17. FATIGUE CRACK GROWTH DATA, SPECIMEN AL-22
SPECTRUM B, LIMIT STRESS = 27.0 ksi

1 Block = 100 Flights

Block Number	Upper Crack Length, inch (2a)	Lower Crack Length, inch (2a)
0	0.27	0.26
21.4953	0.33	0.36
26.0502	0.36	0.44
30.9655	0.40	0.50
35.8903	0.49	0.60
39.2915	0.54	0.68
43.6583	0.62	0.74
46.8809	0.68	0.90
48.8903	0.76	0.98
52.0063	0.84	1.06
54.3448	0.89	1.18
56.1693	0.97	1.26
58.4420	1.04	1.36
60.0533	1.11	1.45
62.4232	1.20	1.64
63.7555	1.26	1.78
64.7712	1.34	1.88
65.1223	1.38	1.92

TABLE A-18. FATIGUE CRACK GROWTH DATA, SPECIMEN AL-18
SPECTRUM B, LIMIT STRESS = 30.0 ksi

1 Block = 100 Flights

Block Number	Upper Crack Length, inch (2a)	Lower Crack Length, inch (2a)
0	0.27	0.28
23.2069	0.47	0.51
24.5329	0.49	0.52
25.8401	0.53	0.54
26.7900	0.55	0.57
27.8997	0.56	0.60
28.8527	0.58	0.62
29.5360	0.60	0.66
31.3793	0.67	0.71
32.8777	0.71	0.76
34.5110	0.75	0.81
36.2602	0.82	0.87
37.7085	0.90	0.91
40.2226	0.98	1.02
41.9310	1.04	1.11
44.1191	1.14	1.24
46.4107	1.20	1.30
48.8088	1.31	1.44
50.4828	1.42	1.54
51.9060	1.45	1.66
53.2539	1.61	1.76
53.9028	1.61	1.83
54.8715	1.75	1.97
55.2226	1.77	2.01

TABLE A-19. FATIGUE CRACK GROWTH DATA, SPECIMEN AL-11
SPECTRUM B, LIMIT STRESS = 33.6 ksi

1 Block = 100 Flights

Block Number	Upper Crack Length, inch (2a)	Lower Crack Length, inch (2a)
0	0.2672	0.2724
7	0.3344	0.3254
8	0.3538	0.3463
12	0.4381	0.4145
14.4748	0.5066	0.4773
16.1321	0.5760	0.5358
17.2390	0.6165	0.5798
18.2327	0.6650	0.6245
19.0409	0.7094	0.6638
19.8365	0.7564	0.7151
21.0660	0.8607	0.7938
21.8616	0.9538	0.8757
22.5597	1.0280	0.9349
23.3302	1.1138	1.0024
23.9937	1.2994	1.1241
24.4686	1.3631	1.1828
24.7925	1.8145	1.3284
24.8365	1.8693	1.3466
24.9088	1.9244	1.3475
24.9591	1.9409	1.3675
25.0314	1.9615	1.3697

TABLE A-20. FATIGUE CRACK GROWTH DATA, SPECIMEN AL-19
SPECTRUM B, LIMIT STRESS = 37.0 ksi

1 Block = 100 Flights

Block Number	Upper Crack Length, inch (2a)	Lower Crack Length, inch (2a)
0	0.26	0.27
6.5987	0.32	0.36
7.6238	0.34	0.42
10.0627	0.38	0.48
12.7900	0.43	0.57
14.2038	0.50	0.67
14.9342	0.53	0.71
16.5705	0.60	0.85
17.5831	0.64	0.96
18.7367	0.72	1.14
19.4608	0.75	1.25
19.7022	0.78	1.41
19.7931	0.79	1.49
20.2508	0.82	1.61
20.5235	Failure	

TABLE A-21. FATIGUE CRACK GROWTH DATA, SPECIMEN Ti-11
SPECTRUM B, LIMIT STRESS = 55.0 ksi

1 Block = 100 Flights

Block Number	Upper Crack Length, inch (2a)	Lower Crack Length, inch (2a)
0	0.25	0.24
10.7806	--	--
14.2602	0.31	0.32
16.5235	0.33	0.35
20.5799	0.37	0.42
23.7022	0.45	0.51
26.9091	0.53	0.67
28.6332	0.60	0.75
29.5893	0.62	0.84
30.5611	0.80	0.93
31.9969	0.87	1.01
32.9060	0.95	1.12
33.8527	1.02	1.24
34.7116	1.14	1.33
35.4702	1.20	1.46
36.0094	1.27	1.51
36.8339	1.36	1.64
37.4514	1.46	1.78
37.9812	1.56	1.92
38.3605	1.58	2.02
40.9436	Failure	

TABLE A-22. FATIGUE CRACK GROWTH DATA, SPECIMEN Ti-8
SPECTRUM B, LIMIT STRESS = 60.0 ksi

1 Block = 100 Flights

Block Number	Upper Crack Length, inch (2a)	Lower Crack Length, inch (2a)
0	0.25	0.25
6.6426	Just barely started	
8.7398	Just barely started	
13.0533	0.38	0.38
14.3511	0.46	0.42
16.5204	0.55	0.54
18.5110	0.67	0.67
19.4608	0.74	0.74
20.4232	0.82	0.82
21.2821	0.92	0.92
22.0345	1.03	0.99
22.4232	1.07	1.06
23.3699	1.18	1.18
24.2006	1.33	1.32
24.8245	1.42	1.44
25.4232	1.48	1.52
26.1442	1.64	1.70
26.5799	1.82	1.86
26.9812	1.88	1.96
27.4107	1.90	2.06
29.0125	Failure	

TABLE A-23. FATIGUE CRACK GROWTH DATA, SPECIMEN Ti-9
SPECTRUM B, LIMIT STRESS = 65.0 ksi

1 Block = 100 Flights

Block Number	Upper Crack Length, inch (2a)	Lower Crack Length, inch (2a)
0	0.26	0.26
5.3699	--	0.29
7.6959	0.31	0.33
9.7931	0.32	0.39
11.5361	0.39	0.46
13.3542	0.46	0.54
14.9216	0.55	0.73
15.7586	0.70	0.83
16.5549	0.78	0.94
17.2915	0.84	1.02
18.1536	1.00	1.16
18.8213	1.08	1.28
19.7586	1.20	1.44
20.3824	1.30	1.54
21.0376	1.44	1.68
21.5925	1.54	1.84
22.1599	1.78	2.04
23.0219	Failure	

TABLE A-24. FATIGUE CRACK GROWTH DATA, SPECIMEN Ti-10
SPECTRUM B, LIMIT STRESS = 70.0 ksi

1 Block = 100 Flights

Block Number	Upper Crack Length, inch (2a)	Lower Crack Length, inch (2a)
0	0.25	0.25
2.7680	--	--
4.8433	--	--
6.0439	0.288	0.319
6.8809	0.300	0.33
7.6426	0.34	0.40
8.2696	0.35	0.45
8.8621	0.38	0.49
9.4796	0.40	0.52
10.0784	0.45	0.57
10.6803	0.50	0.63
11.2602	0.53	0.68
11.8809	0.62	0.80
12.3229	0.63	0.84
12.7712	0.69	0.91
13.1944	0.74	0.98
13.7085	0.79	1.09
14.2602	0.87	1.20
14.8213	0.99	1.38
15.2445	1.07	1.48
15.5455	1.14	1.66
15.8527	1.18	1.74
16.1348	1.24	1.82
16.3699	1.28	1.88
16.4922	1.32	1.97
16.7241	1.36	2.33
17.1223	Failure	

TABLE A-25. FATIGUE CRACK GROWTH DATA, SPECIMEN AL-12
SPECTRUM BASIC, LIMIT STRESS = 33.6 ksi

1 Block = 6000 Hours

Block Number	Upper Crack Length, inch (2a)	Lower Crack Length, inch (2a)
0	0.2845	0.2765
0.1810	0.3545	0.3419
0.2930	0.4264	0.3989
0.3588	0.4870	0.4608
0.4098	0.5559	0.5121
0.4337	0.5918	0.5353
0.4719	0.6516	0.5937
0.5260	0.7621	0.6853
0.5777	0.8912	0.8094
0.6141	1.0160	0.8977
0.6449	1.1622	0.9913
0.6643	Failure	

TABLE A-26. FATIGUE CRACK GROWTH DATA, SPECIMEN AL-14
SPECTRUM BASIC, LIMIT STRESS = 33.6 ksi

1 Block = 6000 Hours

Block Number	Upper Crack Length, inch (2a)	Lower Crack Length, inch (2a)
0	0.2613	0.2529
0.1363	0.3186	0.2937
0.1705	0.3456	0.3131
0.2291	0.3827	0.3434
0.2980	0.4415	0.3904
0.3333	0.4966	0.4322
0.3828	0.5421	0.4644
0.4280	0.6239	0.5313
0.4576	0.6580	0.5602
0.4927	0.7387	0.6046
0.4967	0.7797	0.6159
0.5071	0.8834	0.7000
0.5323	0.9721	0.7486
0.5649	1.1063	0.7983
0.5950	1.2920	0.8546
0.5962	1.3576	0.8769
0.6267	1.7542	0.9313

TABLE A-27. FATIGUE CRACK GROWTH DATA, SPECIMEN Ti-6
SPECTRUM BASIC, LIMIT STRESS = 65.0 ksi

1 Block = 6000 Hours

Block Number	Upper Crack Length, inch (2a)	Lower Crack Length, inch (2a)
0	0.2458	0.2679
0.1589	0.2811	--
0.1944	0.3191	0.3065
0.2291	0.3653	0.3324
0.2622	0.4107	0.3833
0.2953	0.4857	0.4371
0.3271	0.5534	0.4983
0.3333	0.6092	0.5509
0.3620	0.6986	0.6147
0.3927	0.7788	0.7032
0.4069	0.9582	0.7675
0.4256	0.9440	0.8328
0.4587	1.2142	1.0531
0.4924	1.4438	1.2556
0.4971	1.6792	1.4261
0.4980	1.7749	1.5764
0.5571	Failure	

TABLE A-28. FATIGUE CRACK GROWTH DATA, SPECIMEN Ti-7
SPECTRUM BASIC, LIMIT STRESS = 65.0 ksi

1 Block = 6000 Hours

Block Number	Upper Crack Length, inch (2a)	Lower Crack Length, inch (2a)
0	0.2540	0.2513
0.1676	0.2869	0.3053
0.1971	0.3120	0.3290
0.2329	0.3410	0.3789
0.2622	0.3854	0.4262
0.2978	0.4499	0.4994
0.3300	0.5375	0.6125
0.3589	0.5852	0.6681
0.3696	0.6418	0.7422
0.3951	0.7471	0.8559
0.4273	0.8866	1.0197
0.4602	1.0567	1.2767
0.4833	1.1190	1.3767
0.4931	1.2880	1.6227
0.4962	1.4554	1.9272
0.5216	Failure	

TABLE A-29. FATIGUE CRACK GROWTH DATA, SPECIMEN A1-15
SPECTRUM A, LIMIT STRESS = 33.6 ksi

1 Block = 100 Flights

Block Number	Upper Crack Length, inch (2a)		Lower Crack Length, inch (2a)
0	0.2701		0.2745
5.60	0.3128		0.3065
7.85	0.3267		0.3293
9.90	0.3486		0.3380
13.36	0.3961		0.3803
16.55	0.4534		0.4356
19.48	0.5208		0.5028
21.29	0.5795		0.5370
22.89	0.6227		0.5898
24.3	0.6761		0.6362
25.6	0.7287		0.6949
27.3	0.8061		0.7663
28.7	0.8830		0.8362
30.2	0.9785		0.9205
31.6	1.1073		1.0338
35.7	1.1953		1.1138
36.5	1.3340		1.2510
37.1	1.4477		1.3593
37.4	1.5170		1.4247
37.7	1.7024		1.5624
38.1	1.7874		1.6395
38.3	1.85	Failure	

TABLE A-30. FATIGUE CRACK GROWTH DATA, SPECIMEN A1-27
SPECTRUM A (COARSE), LIMIT STRESS = 33.6 ksi

1 Block = 6000 Hours

Block Number	Upper Crack Length, inch (2a)	Lower Crack Length, inch (2a)
0	0.24	0.25
7.0168	0.32	--
9.3866	0.35	0.31
12.3025	0.39	0.38
15.0924	0.43	0.40
16.8487	0.49	0.43
19.1008	0.58	0.52
20.8151	0.62	0.56
22.6807	0.70	0.64
24.3613	0.79	0.72
26.0336	0.91	0.80
27.1008	0.98	0.88
28.0336	1.10	0.94
29.1429	1.26	1.03
30.1176	1.46	1.14
30.4118	Failure	

TABLE A-31. FATIGUE CRACK GROWTH DATA, SPECIMEN Ti-13
SPECTRUM A (COARSE), LIMIT STRESS = 65.0 ksi

1 Block = 100 Flights

Block Number	Upper Crack Length, inch (2a)	Lower Crack Length, inch (2a)
0	0.27	0.25
2.1765	--	--
7.6975	0.31	0.31
9.3193	0.33	0.36
11.6218	0.37	0.40
13.8571	0.51	0.44
15.5126	0.64	0.62
17.1176	0.74	0.75
18.4706	0.92	0.91
19.6134	1.07	1.02
20.6634	1.22	1.18
21.6639	1.40	1.36
22.2353	1.60	1.48
22.4958	1.62	1.54
23.0504	1.78	1.68
23.5462	2.04	1.84
24.4118	Failure	

TABLE A-32. FATIGUE CRACK GROWTH DATA, SPECIMEN A1-24
SPECTRUM D, LIMIT STRESS = 33.6 ksi

1 Block = 100 Flights

Block Number	Upper Crack Length, inch (2a)	Lower Crack Length, inch (2a)
0	0.26	0.27
6.0061	0.38	0.44
6,8589	0.42	0.48
7.7423	0.44	0.52
8.8160	0.52	0.60
10.1350	0.64	0.78
10.5399	0.71	0.91
10.7546	0.72	0.97
11.0613	0.75	1.13
11.2699	0.78	1.31
11.4417	Failure	

TABLE A-33. FATIGUE CRACK GROWTH DATA, SPECIMEN Ti-12
SPECTRUM D, LIMIT STRESS = 65.0 ksi

1 Block = 100 Flights

Block Number	Upper Crack Length, inch	Lower Crack Length, inch
0	0.25	0.25
4.2577	0.35	0.31
5.2761	0.45	0.34
6.1779	0.53	0.42
6.9693	0.66	0.50
7.4601	0.80	0.56
7.8957	0.88	0.64
8.3252	0.94	0.71
8.8037	1.07	0.80
9.1840	1.24	0.90
9.3988	1.33	0.96
9.6135	1.48	0.98
9.7853	1.56	1.03
9.9571	1.68	1.10
10.1718	1.90	1.18
10.3681	2.34	1.26
10.5399	Failure	

TABLE A-34. FATIGUE CRACK GROWTH DATA, SPECIMEN A-7
SPECTRUM C, LIMIT STRESS = 33.6 ksi

1 Block = 100 Flights

Block Number	Upper Crack Length, inch	Lower Crack Length, inch
0	0.25	0.25
10.1744	0.32	0.31
12.0233	0.34	0.34
15.4767	0.38	0.37
18.4302	Grip Failure	

TABLE A-35. FATIGUE CRACK GROWTH DATA, SPECIMEN A1-26
SPECTRUM B (WITHOUT GAG), LIMIT STRESS = 33.6 ksi

1 Block = 100 Flights

Block Number	Upper Crack Length, inch (2a)	Lower Crack Length, inch (2a)
0	0.26	0.28
3.5240	--	--
5.4696	0.28	0.29
7.5112	0.33	0.33
10.0607	0.38	0.39
12.8594	0.42	0.44
15.0927	0.45	0.49
17.1342	0.52	0.54
18.8307	0.58	0.60
20.4345	0.63	0.66
21.8786	0.69	0.74
22.9712	0.75	0.79
24.2236	0.80	0.87
25.0927	0.86	0.91
26.1182	0.92	0.96
27.2109	0.98	1.04
28.3770	1.06	1.12
29.5048	1.14	1.20
30.6230	1.23	1.31
31.4824	1.32	1.39
32.1406	1.37	1.48
32.8435	1.46	1.57
33.4505	1.55	1.65
34.0543	1.62	1.79
34.6102	1.76	1.94
34.9105	1.86	2.14
35.5240	Failure	

TABLE A-36. FATIGUE CRACK GROWTH DATA, SPECIMEN Ti-14 SPECTRUM B (WITHOUT GAG), LIMIT STRESS = 65.0 ksi

1 Block = 100 Flights

Block Number	Upper Crack Length, inch (2a)	Lower Crack Length, inch (2a)
0	0.25	0.27
2.4696	--	--
5.2428	--	--
6.9776	0.30	0.32
8.6709	0.34	0.34
10.1917	0.36	0.42
11.7029	0.42	0.53
12.6901	0.50	0.60
13.6326	0.52	0.65
14.5942	0.60	0.78
15.3514	0.64	0.86
16.1917	0.72	0.96
16.8339	0.82	1.08
17.4249	0.88	1.16
18.1597	0.98	1.27
18.7923	1.06	1.38
19.3355	1.12	1.47
19.8914	1.24	1.62
20.3323	1.28	1.74
20.8019	1.40	1.86
21.4089	1.50	2.02
22.4217	Failure	

TABLE A-37. FATIGUE CRACK GROWTH DATA, SPECIMEN A1-17
SPECTRUM BASIC, LIMIT STRESS = 33.6 ksi
0.5 INCH DIAMETER HOLE

1 Block = 6000 Hours

Block Number	Upper Crack Length, inch (a)	Lower Crack Length, inch (a)
0.	0.2369	0.2506
0.1600	0.2554	0.2753
0.2118	0.2703	0.2815
0.2947	0.2781	0.3052
0.4367	0.3176	0.3505
0.5024	0.3466	0.3780
0.6487	0.3903	0.4251
0.7418	0.4416	0.4849
0.8384	0.5030	0.5449
0.9500	0.5566	0.6128
1.0024	0.68	0.74
1.0429	0.69	0.77
1.0729	0.74	0.84
1.1007	0.81	0.92
1.1291	0.86	1.05
1.1600	Failure	
	Second Crack Growth Data (other side of hole)	
1.0024	0.10	0.14
1.0429	0.11	0.18
1.0729	0.16	0.23
1.1007	0.24	0.35
1.1291	0.25	0.48

TABLE A-38. FATIGUE CRACK GROWTH DATA, SPECIMEN A1-29
SPECTRUM BASIC, LIMIT STRESS = 33 ksi
0.5 INCH DIAMETER HOLE

1 Block = 6000 Hours

Block Number	Upper Crack Length, inch (a)	Lower Crack Length, inch (a)
0	0.060	0.060
0.4471	0.120	0.110
0.5791	0.160	0.150
0.7616	0.260	0.230
0.8404	0.340	0.280
0.9360	0.420	0.360
0.9807	0.480	0.390
1.0060	0.620	0.500
1.0516	0.700	0.550
1.0842	0.780	0.630
1.0960	0.960	0.750
1.1267	Failure	
	Second Crack Growth Data (other side of hole)	
1.0060	0.060	0.050
1.0316	0.110	0.090
1.0842	0.210	0.210
1.0960	0.370	0.350

TABLE A-39. FATIGUE CRACK GROWTH DATA, SPECIMEN A1-20
SPECTRUM BASIC, LIMIT STRESS = 33.6 ksi
STIFFENED PANEL

1 Block = 6000 Hours

Block Number	Upper Crack Length, inch (2a)	Lower Crack Length, inch (2a)
0	0.31	0.31
0.1376	0.38	0.37
0.2358	0.41	0.41
0.3476	0.47	0.45
0.4511	0.50	0.50
0.5338	0.54	0.56
0.6404	0.60	0.60
0.7402	0.65	0.66
0.8240	0.72	0.71
0.8993	0.76	0.79
0.9962	0.87	0.87
1.0789	0.95	0.94
1.1584	1.01	1.02
1.2578	1.14	1.14
1.3218	1.22	1.23
1.3607	1.33	1.31
1.4000	1.39	1.40
1.4376	1.47	1.46
1.4916	1.58	1.56
1.5400	1.82	1.77
1.5649	1.91	1.90
1.6036	2.08	2.02
1.6947	Failure	

TABLE A-40. FATIGUE CRACK GROWTH DATA, SPECIMEN A1-21
SPECTRUM BASIC, LIMIT STRESS = 33.6 ksi
STIFFENED PANEL

1 Block = 6000 Hours

Block Number	Upper Crack Length, inch (2a)	Lower Crack Length, inch (2a)
0	0.2667	0.2685
0.0542	0.33	0.34
0.1627	0.39	0.41
0.2831	0.43	0.46
0.3709	0.51	0.52
0.4747	0.56	0.58
0.5749	0.62	0.64
0.6393	0.66	0.70
0.7438	0.73	0.79
0.8411	0.84	0.88
0.9740	0.93	1.00
1.0224	1.03	1.10
1.0969	1.11	1.19
1.1358	1.17	1.25
1.1951	1.27	1.34
1.2313	1.33	1.43
1.2796	1.39	1.52
1.3182	1.45	1.60
1.3613	1.61	1.77
1.3931	1.66	1.83
1.4293	1.82	2.02
1.4962	Failure	

DISTRIBUTION LIST

	No. of Copies
NAVAIRSYSCOM, AIR-50174 (2 for retention, 2 for AIR-530, 1 for AIR-530215, 1 for AIR-530221C, 2 for AIR-320B)	8
NAVAIRTESTCEN, Patuxent River, Maryland	1
NAVAVNSAFECEN, NAS, Norfolk, Virginia	1
CNAVANTRA, NAS, Corpus Christi, Texas	1
CNABATRA, NAS, Pensacola, Florida	1
CNARESTRA, NAS, Glenview, Illinois	1
CNATRA, NAS, Pensacola, Florida	1
NAVAIRSYSCOMREPLANT	1
NAVAIRSYSCOMREPCENT	1
NAVAIRSYSCOMREPAC	1
NAVAIREWORKFAC, NAS, Alameda, California	1
NAVAIREWORKFAC, NAS, Jacksonville, Florida	1
NAVAIREWORKFAC, NAS, Norfolk, Virginia	1
NAVAIREWORKFAC, NAS, Pensacola, Florida	1
NAVAIREWORKFAC, NAS, Quonset Point, Rhode Island	1
NAVAIREWORKFAC, NAS, San Diego, California	1
NAVAIREWORKFAC, NAS, Cherry Point, North Carolina	1
COMNAVAIRLANT	1
COMNAVAIRPAC	1
NWL, Dahlgren, Virginia (Attention Mr. Morton)	1
USAF Systems Command, WPAFB, Ohio 45433	
Attention FBR	1
Attention FB	1
Attention LLD	1
Attention SEFS	1
Attention FYA	1
Attention LAM	1
Attention FBA	1
Attention LPH	1
USA AMMRC, Watertown, Massachusetts	1
USA APG, Aberdeen, Maryland	1
USA AMRDL, Fort Eustis, Virginia (Attention Mr. Berrisford)	1
USA AVSCOM, St. Louis, Missouri (Attention AMSAV-GR)	1
Defense Research and Development Staff, British Embassy, Washington, D.C., via NAVAIR (AIR-5302)	1
Canadian Joint Staff, Navy Member, Washington, D.C., via NAVAIR (AIR-5302)	1
Technical Advisory, AFIAS-B, Directorate of Aerospace Safety, Norton AFB, California	1
DDC	12
NAVSEASYSCOM, Washington, D.C. 20362 (Attention Mr. C. Pohler, Code 035)	1
NAVSHIPRADCEN, Bethesda, Maryland 20034 (Attention Mr. A. B. Stavovy 730)	1
Bell Aerosystems Co., Buffalo, New York 14205	1
Bell Helicopter Co., Fort Worth, Texas 76101	1
Boeing Co., Airplane Div., Seattle, Washington 98124 (Attention Mr. T. Porter)	1

DISTRIBUTION LIST (continued)

	No. of Copies
Boeing Co., Airplane Div., Wichita, Kansas 67210	1
Boeing Co., Vertol Div., Philadelphia, Pennsylvania 19142	1
McDonnell Douglas Aircraft Corp., Aircraft Div., Long Beach, California 90801	1
General Dynamics/Convair, San Diego, California 92112	1
General Dynamics Corp., Fort Worth, Texas 76101	1
Goodyear Aerospace Corp., Akron, Ohio 44305	1
Grumman Aerospace Corp., Bethpage, Long Island, New York 11714	1
Aircraft-Missiles Div., Fairchild-Hiller Corp., Hagerstown, Maryland 21740	1
Kaman Aircraft Corp., Bloomfield, Connecticut 06002	1
Lockheed Aircraft Corp., Lockheed-California Co., Burbank, California 91503	1
Lockheed Aircraft Corp., Lockheed-Georgia Co., Marietta, Georgia 30061	1
LTV Aerospace Corp., Dallas, Texas 75222	1
Martin Co., Baltimore, Maryland 21203	1
McDonnell Douglas Aircraft Corp., St. Louis, Missouri 63166	1
Rockwell International, Columbus Aircraft Div., Columbus, Ohio 43216 (Attention Mr. O. Acker)	1
Rockwell International, Los Angeles, California 90053 (Attention Mr. G. Fitch)	1
Northrop Corp., Aircraft Div., Hawthorne, California 90250	1
Republic Aviation Div., Fairchild-Hiller Corp., Farmingdale, Long Island, New York 11735	1
Sikorsky Aircraft Co., Stratford, Connecticut 06497	1
Hdqtrs., R&T Div., AFSC, Bolling AFB, Washington, D.C. 22209	1
Office of Aerospace Research, Arlington, Virginia 22209	1
FAA (FS-120), Washington, D.C., 20553	1
Scientific and Technical Information Facility, College Park, Maryland 20740 (NASA Rep.)	2
Administrator, NASA, Washington, D.C. 20546	1
NASA-Langley Research Center, Materials Div., Hampton Virginia 23365 (Attention Mr. H. F. Hardrath)	1
National BuStds, Washington, D.C. 20234	1
Office of Naval Research, Washington, D.C. 20362 (Attention Dr. N. Perrone)	1
Director, Naval Research Lab, Washington, D.C. 20390	1
Midwest Research Institute, Kansas City, Missouri 64110	1
University of Illinois, Urbana, Illinois 61803 (Attention Prof. T. J. Dolan and Prof. J. Morrow)	1 each
University of Kansas, Lawrence, Kansas 66044	1
University of Michigan, Ann Arbor, Michigan 48105	1
University of Minnesota, Minneapolis, Minnesota 55455	1
Alcoa, Alcoa Labs, Alcoa Center, Pennsylvania 15069 (Attention Mr. J. G. Kaufman)	1
Lehigh University, Bethlehem, Pennsylvania 18015 (Attention Prof. G. C. Sih)	1
Belfour-Stulen, Inc., Traverse City, Michigan 49684	1
Cornell Aero. Lab, Buffalo, New York 14221	1

DISTRIBUTION LIST (continued)

	No. of Copies
Metals & Ceramics Information Center, Battelle, Columbus Laboratories Columbus, Ohio 43201	1
NASA, Lewis Research Center, Cleveland, Ohio 44153 (Attention Technical Library)	1
Naval Postgraduate School, Monterey, California 93940 (Attention Prof. Lindsey)	1
Battelle, Pacific Northwest Laboratories, P. O. Box 999, Richland, Washington 99352 (Attention Mr. W. E. Anderson)	1
School of Engineering, George Washington University, Washington, D.C. 20006 (Attention Prof. H. Liebowitz)	1
Dept. of Metallurgy, University of Connecticut, Storrs, Connecticut 06268 (Attention Prof. A. J. McEvily)	1
Dept. of Mech. Eng., Washington University, St. Louis, Missouri (Attention Prof. P. C. Paris)	1
Materials Dept., 6531 Boelter Hall, University of California at Los Angeles, Los Angeles, California 90024 (Attention Prof. A. S. Tetelman)	1
National Transportation Safety Board, 800 Independence, Washington, D.C. 20594 (Attention Mr. W. D. Cowan)	1
Federal Aircraft Establishment, Emmen, Switzerland (Attention Mr. J. Branger)	1
Civil Aviation Authority, Structures Section, Brabaron House, Redhill, Surrey RH11SQ, England (Attention Mr. M. B. Benoy)	1
Royal Aircraft Establishment, Structures Dept., Farnborough, Hants GU146TD, England (Attention Mr. W. T. Kirkby)	1
Aeronautical Research Labs, Melbourne, Australia (Attention Mr. J. Y. Mann)	1
DFVLR, 505 Pors Wahn, West Germany (Attention Dr. H. Nowack)	1
Pratt and Whitney Aircraft, P. O. Box 611, Middletown, Connecticut (Attention Mr. C. A. Rau)	1
IABG, 8012 Ottobrunn by Munich, West Germany (Attention Dr. W. Schutz)	1
Aeronautics Dept., Delft University, Delft, Holland (Attention Prof. J. Schijve)	1
National Aerospace Inst., NLR, Emmeloord, Holland (Attention Mr. J. B. deJonge)	1
Federal Aviation Administration, RLD, Schiphol, Holland (Attention Mr. H. N. Wolleswinkel)	1
Royal Aeronautical Society, 4 Hamilton Place, London, England (Attention Mr. E. R. Welbourne)	1
Service Technique Aeronautique, 4 Ave de la Porte d'Issy, Paris 15, France (Attention Mr. G. Bessonat)	1
British Aircraft Corporation, Commercial AC Div., Filton House, Bristol BS99 7AR, England (Attention Mr. N. F. Harpur)	1
Fokker-VFW Aircraft Co., Schiphol, Netherlands (Attention Mr. G. Fonk)	1
FAA, 800 Independence, Washington, D. C. 20594 (Attention Mr. D. Kemp)	1
University of Tennessee Space Inst., Tullahoma, Tennessee 37388 (Attention Prof. M. A. Wright)	1
Shell Oil Company, Civil Engineering Office, P. O. Box 2099, Houston, Texas 77001 (Attention Mr. P. W. Marshall)	1
David Taylor Naval Ship Research and Development Center, Bethesda, Maryland 20084 (Attention Mr. J. Corado)	1

DISTRIBUTION LIST (continued)

	No. of Copies
Air Force Flight Dynamics Lab, WPAFB, Ohio 45433 (Attention Mr. R. M. Engle)	1
VanderBilt University, P. O. Box 3245 Station B, Nashville, Tennessee 37235 (Attention Prof. P. Packman)	1
Dept. of Civil Aviation, P. O. Box 1733 P, Melbourne 3001, Australia (Attention Mr. M. R. Rice)	1